

---

[All ETDs from UAB](#)

[UAB Theses & Dissertations](#)

---

2011

## Evaluation of the Optical and Mechanical Properties of CAD-CAM Generated Yttria-Stabilized Zirconia Laminate Veneers

Tariq F. Alghazzawi  
*University of Alabama at Birmingham*

Follow this and additional works at: <https://digitalcommons.library.uab.edu/etd-collection>

---

### Recommended Citation

Alghazzawi, Tariq F., "Evaluation of the Optical and Mechanical Properties of CAD-CAM Generated Yttria-Stabilized Zirconia Laminate Veneers" (2011). *All ETDs from UAB*. 996.  
<https://digitalcommons.library.uab.edu/etd-collection/996>

This content has been accepted for inclusion by an authorized administrator of the UAB Digital Commons, and is provided as a free open access item. All inquiries regarding this item or the UAB Digital Commons should be directed to the [UAB Libraries Office of Scholarly Communication](#).

EVALUATION OF THE OPTICAL AND MECHANICAL PROPERTIES OF  
CAD/CAM GENERATED YTTRIA-STABILIZED ZIRCONIA LAMINATE  
VENEERS

by

TARIQ FADEL A. ALGHAZZAWI

GREGG M. JANOWSKI, COMMITTEE CHAIR  
GREGORY B. THOMPSON  
JACK E. LEMONS  
MILTON E. ESSIG  
PERNG-RU LIU  
ROBIN D. FOLEY

A DISSERTATION

Submitted to the graduate faculty of The University of Alabama at Birmingham,  
in partial fulfillment of the requirements for the degree of  
Doctor of Philosophy

BIRMINGHAM, ALABAMA

2011

Copyright by  
TARIQ FADEL A. ALGHAZZAWI  
2011

# EVALUATION OF THE OPTICAL AND MECHANICAL PROPERTIES OF CAD/CAM GENERATED YTTRIA-STABILIZED ZIRCONIA LAMINATE VENEERS

TARIQ FADEL A. ALGHAZZAWI

MATERIALS ENGINEERING

## ABSTRACT

The purpose of this investigation was to study three aspects which have been shown to limit clinical applications of yttria-stabilized zirconia (Y-TZP) for dental restorations. Mechanical property and structural changes due to low-temperature degradation (LTD) of Y-TZP led to increased surface roughness and monoclinic phase fractions, with a concomitant decrease in hardness and modulus. Yttria content and flexural strength were unchanged and phase transformation proceeded from the surface into the bulk of the material. The optical properties of Y-TZP, IPS e.max<sup>®</sup> CAD (IEC), and feldspathic porcelain (FP) laminate veneers showed that the underlying color of try-in pastes (TP) affected the color difference for different regions of IEC and FP veneers (cervical and body region). The IEC veneers were affected more by TP color than were FP veneers. The Y-TZP veneers were not affected by the color of the TP or the composite resin abutment (CRA) color. No effect of the color of the CRA was found for the overall color of all veneers except at the cervical region for FP veneers. However, there was an effect of different colors of TP on the color coordinates of the overall color for all the veneers. The mechanical properties of these three laminate veneers materials were studied for two designs, i.e., incisal overlapped preparation (IOP) and three-quarter preparation (TQP). No

effect of preparation design on the mean failure load of Y-TZP and IEC veneers was found and material type did not affect failure load for a given design except for IEC veneers which had a higher failure load than FP for the IOP design. The IOP design, Y-TZP and IEC veneers showed more failure by fracture of the CRA, while FP veneers fractured at the incisal region. The TQP design, Y-TZP veneers showed more failures by complete debonding, whereas the IEC and FP veneers showed more fractures of the CRA. The Y-TZP veneers showed the lowest number of fractures and highest complete debonding, while the FP veneers showed the highest number of fractures and lowest occurrence of complete debonding.

Keywords: Zirconia, Low-Temperature Degradation, Veneer, Color.

## ACKNOWLEDGMENTS

I am especially grateful to my advisor Dr. Gregg Janowski, who gave many hours of his precious time to assist and educate me. Because of his endless guidance, I complete this study with a good understanding of not only the dissertation's topic but also of many areas in Materials Science. For his guidance, I also learned how to design a research project and to write my research findings for publication. Without his support and help, this project would never have been finished.

I would like to thank Dr. Jack Lemons for continuous consultations and giving the benefit of his past 30 years of research in biomedical engineering; Dr. Perng-Ru Liu and Dr. Milton Essig for their consultations, experience in clinical research and CAD/CAM technology; Dr. Robin Foley for helping me in using the SEM, and finally Dr. Alfred Bartolucci for helping me in the conduction of the statistical analysis. Also, I would like to express deep gratitude to the Department of Materials Science and Engineering, University of Alabama at Birmingham, for affording me the chance to complete my PhD and providing a helpful environment with special thanks to Dr. Barry Andrews for leading the department. I would like to thank all of my colleagues and fellow students in the MSE department and the School of Dentistry.

Last, but certainly not least, I thank Dr. Leonard Mueninghoff and Dr. William Lacefield for their enthusiasm and encouragement. Their optimism and unwavering belief in my ability were great motivation to successfully complete this dissertation.

## TABLE OF CONTENTS

	<i>Page</i>
ABSTRACT.....	iii
ACKNOWLEDGMENTS .....	v
LIST OF TABLES.....	viii
LIST OF FIGURES .....	x
LIST OF TERMINOLOGY AND ABBREVIATIONS.....	xii
1. INTRODUCTION .....	1
1.1. Background of zirconia material.....	1
1.1.1. Discovery and mechanical properties .....	1
1.1.2. Medical and dental applications.....	1
1.1.3. Classification of zirconia .....	2
1.1.4. Manufacturing.....	2
1.1.5. Challenges.....	3
1.2. Literature review .....	4
1.2.1. Aging.....	4
1.2.2. Optical properties.....	7
1.2.3. Bonding to zirconia.....	8
1.3. Aims.....	11
1.3.1. Aim 1.....	11
1.3.2. Aim 2.....	11
1.3.3. Aim 3.....	11
2. MATERIALS AND METHODS.....	12
2.1. Materials and Sample Preparation .....	12
2.1.1. Low-Temperature Degradation Study .....	12
2.1.2. Optical Property Study.....	13
2.1.3. Mechanical Property Study.....	15
2.2. Testing Methods.....	16
2.2.1. Low-Temperature Degradation Study .....	16
2.2.2. Optical Property Study.....	18
2.2.3. Mechanical Property Study.....	20
2.3. Statistical Analysis.....	20
2.3.1. Low-Temperature Degradation Study .....	20

2.3.2. Optical Property Study.....	20
2.3.3. Mechanical Property Study.....	21
3. THE EFFECT OF LOW-TEMPERATURE DEGRADATION ON THE MECHANICAL PROPERTIES AND STRUCTURAL STABILITY OF DENTAL ZIRCONIA PREPARED BY SIMULATED DENTAL PRACTICE .....	32
4. EVALUATION OF THE OPTICAL PROPERTIES OF CAD-CAM GENERATED YTTRIA-STABILIZED ZIRCONIA AND GLASS-CERAMIC LAMINATE VENEERS.....	56
5. THE FAILURE LOAD OF CAD-CAM GENERATED ZIRCONIA AND GLASS-CERAMIC LAMINATE VENEERS WITH DIFFERENT PREPARATION DESIGNS .....	85
6. CONCLUSIONS.....	109
7. GENERAL REFERENCES.....	112
APPENDIX: DIFFERENT FAILURE MODES AFTER LOADING OF CEMENTED LAMINATE VENEERS ON COMPOSITE RESIN ABUTMENTS..	120



## LIST OF TABLES

<i>Table</i>	<i>Page</i>
<b>MATERIALS AND METHODS</b>	
1. Chemical composition of yttria-stabilized zirconia. ....	22
2. Material specifications of yttria-stabilized zirconia. ....	22
3. The procedure for sample preparation simulating dental practice. ....	23
4. The number of samples and data points within each sample for all characterization procedures and flexural strength. ....	23
5. The characteristics and the average thickness at each region of laminate veneer materials. ....	24
6. Interpretation of color change on the laminate veneers according to composite resin abutment color or try-in paste color. ....	25
7. The average veneer means thickness of laminate veneer materials for different preparation designs. ....	26
8. The mechanical properties for yttria-stabilized zirconia, IPS e.max <sup>®</sup> CAD, and feldspathic porcelain laminate veneers. ....	26
9. The Cementation procedures for yttria-stabilized zirconia, IPS e.max <sup>®</sup> CAD, and feldspathic porcelain laminate veneers. ....	27
<b>THE EFFECT OF LOW-TEMPERATURE DEGRADATION ON THE MECHANICAL PROPERTIES AND STRUCTURAL STABILITY OF DENTAL ZIRCONIA PREPARED BY SIMULATED DENTAL PRACTICE</b>	
1. Chemical composition of yttria-stabilized zirconia. ....	48
2. Material specifications of yttria-stabilized zirconia. ....	49
3. The procedure for sample preparation simulating dental practice. ....	50

4. The number of samples and data points within each sample for all characterization procedures and flexural strength. ....	51
5. The mean and standard deviations of the control and aged samples for all characterization procedures and flexural strength. ....	52

**EVALUATION OF THE OPTICAL PROPERTIES OF CAD-CAM GENERATED  
YTTRIA-STABILIZED ZIRCONIA AND GLASS-CERAMIC LAMINATE VENEERS**

1. The characteristics and the average thickness at each region of laminate veneer materials. ....	77
2. Interpretation of color change on the laminate veneers according to composite resin abutment color or try-in paste color. ....	78
3. The effect of color coordinates (L* a* b*) on increasing value of try-in paste (from yellow to opaque white) for the body region and composite resin abutment color (A <sub>2</sub> ) of different laminate veneer materials. ....	79
4. The effect of color coordinates (L* a* b*) on laminate veneer material for the body region and composite resin abutment color (A <sub>2</sub> ) with glycerin. ....	80

**THE FAILURE LOAD OF CAD-CAM GENERATED ZIRCONIA AND GLASS-  
CERAMIC LAMINATE VENEERS WITH DIFFERENT PREPARATION  
DESIGNS**

1. The average veneer means thickness of laminate veneer materials for different preparation designs. ....	105
2. The chemical composition and mechanical properties for yttria-stabilized zirconia, IPS e.max <sup>®</sup> CAD, and feldspathic porcelain laminate veneers. ....	106
3. The Cementation procedures for yttria-stabilized zirconia, IPS e.max <sup>®</sup> CAD, and feldspathic porcelain laminate veneers. ....	107
4. The location with number of failures at the bonded composite resin abutment-laminate veneer specimen, and mean failure load (N) of different preparation designs for different laminate veneer materials. ....	108

## LIST OF FIGURES

<i>Figure</i>	<i>Page</i>
<b>MATERIALS AND METHODS</b>	
1. Incisal overlapped preparation (IOP) design. ....	28
2. Three Quarter Preparation (TQP) design. ....	29
3. X-ray diffraction scan from 10-90°. The majority of the peaks match the tetragonal phase, card 04-005-4207, with a slight angular offset due to the Y <sub>2</sub> O <sub>3</sub> additions. Two monoclinic peaks are present at about 28.0 and 31.5°. One of the primary cards for the monoclinic phase is 04-004-4339. This scan indicates that zirconia is a random tetragonal polycrystal with some monoclinic also present. ....	30
4. Description of CIELAB System. ....	31
<b>THE EFFECT OF LOW-TEMPERATURE DEGRADATION ON THE MECHANICAL PROPERTIES AND STRUCTURAL STABILITY OF DENTAL ZIRCONIA PREPARED BY SIMULATED DENTAL PRACTICE</b>	
1. XRD analysis for the control (A) and aged (B) samples. Note a substantial increase of monoclinic phase (111) for the aged samples compared with the control. ...	53
2. The surface roughness values for control and aged samples. ....	54
3. The surface hardness and modulus of elasticity values for control and aged samples. ....	54
4. The fraction of monoclinic phase for different incident angles (14, 10, 8, 5, 3 degrees). The 3° incident angle had the highest monoclinic fraction while the 14° angle had the lowest monoclinic fraction. ....	55
<b>EVALUATION OF THE OPTICAL PROPERTIES OF CAD-CAM GENERATED YTTRIA-STABILIZED ZIRCONIA AND GLASS-CERAMIC LAMINATE VENEER</b>	
1. (a) Yttria-stabilized zirconia laminate veneers. (b) IPS e.max <sup>®</sup> CAD HT laminate veneers. (c) Feldspathic porcelain laminate veneers. The color change (ΔE) at the three veneer regions (cervical, body, incisal) with different composite resin	

abutments (A <sub>1</sub> , A <sub>2</sub> , A <sub>3</sub> ) and try-in paste colors (transparent, bleach XL, opaque, yellow) compared to the control color (composite resin abutment color (A <sub>2</sub> ) and glycerin). The perceptibility threshold ( $\Delta E$ ) is illustrated by a horizontal dotted line at 3.7.....	81
2. The effect of laminate veneer thickness from cervical region to incisal region on the color difference for yttria-stabilized zirconia, IPS e. max <sup>®</sup> CAD HT, and feldspathic porcelain materials. ....	84

## LIST OF TERMINOLOGY AND ABBREVIATIONS

a*	It is a color coordinate which is used to measure the chroma along the red-green axis.
AFM	Atomic force microscopy.
b*	It is a color coordinate which is used to measure the chroma along the yellow-blue axis.
Body region	The region of the tooth which is between cervical and incisal regions considered a duplicate morphology in size and shape of all upper or lower tooth in the mouth.
CAD/CAM	Computer Assisted Design/Computer Assisted Machining, which is a technology used to fabricate restoration by machining it from a ceramic block.
Cast	A model which is made of gypsum stone. It is considered a duplicate morphology in size and shape of all upper or lower teeth in the mouth.
CEJ	It is an a cemento-enamel junction which is the demarcation line between enamel which covers the clinical crown of the tooth, and the cementum which covers the root of the tooth.
Cementation	It is a procedure which is used to attach or lute the crown, fixed partial denture or laminate veneer to the natural tooth.
CEREC 3D	A third generation type of CAD/CAM system (Sirona Dental Systems, Bensheim, Germany).
Cervical region	Inferior 1/3 of the tooth height in proximity to the gum (gingival) tissue.
Chroma	It is the relative concentration, or strength, or saturation, or intensity of a hue.

CIE Lab color system	This system is based on the three attributes of color, hue, value, and chroma and which embraces the concept of standard observers and standard illuminants. It uses 3 basic coordinates, L, a, and b (A specific shade is defined by its location within the system by these coordinates).
Coping	The interior layer of the crown (substructure) which provides support for the veneering porcelain. This layer replaces missing dentin layer in natural teeth.
Core	The interior layer of the crown (substructure) which provides a support for the veneering porcelain. This layer replaces missing dentin layer in natural teeth.
CRA	Composite resin abutment.
CTE	Co-efficient of thermal expansion.
Delta E	It is a color difference which is used to describe whether the changes in the overall shade are perceivable to the human observer based on CIELAB color parameters ( $L^*$ $a^*$ $b^*$ ).
Dentin	The interior layer of the tooth beneath the enamel.
Diamond bur	Diamond chips attached to a linear metal shank which reduces the tooth when rotated.
Diastema	An open space between teeth, frequently noted as a space in the oral cavity between two incisor teeth.
Die	It is the section of a model which is made of stone and is considered a duplicate replica in size and shape of one tooth in the mouth.
Distal	The surface of a tooth away from the midline.
EDS	Energy dispersive spectroscopy.
Enamel	The exterior layer of the tooth which is composed of hydroxyapatite crystals.
Extrinsic staining	A procedure which is used to improve the color of the dental restoration by application of colored stains on its external surface.
FB	Feldspathic porcelain.

Finishing line	The junction or interface between the prepared and unprepared tooth surfaces.
Framework	The interior layer of the fixed partial denture (substructure) which provides support for the veneering porcelain. This layer replaces missing natural tooth and dentin layers of the adjacent natural teeth.
Glass ionomer cement	It is a type of luting cement which contains fluoro-alumina silicate particles.
Glazing	It is a procedure intended for application of a very thin layer in order to seal the surface cracks and strengthen the dental restoration.
HIP	Hot isostatic pressure.
Hue	The quality by which one color family is distinguished from another (e.g. red from yellow).
IEC	IPS e.max <sup>®</sup> CAD.
Impression	It is a material which is used to replicate the morphology of the teeth and adjacent tissues-a negative replica in which a gypsum material will be poured to form a positive replica.
In-Ceram Alumina	A pure alumina material.
In-Ceram Zirconia	It is alumina material reinforced with zirconia particles fabricated by glass infiltration technique.
Incisal region	Superior 1/3 of the tooth height in proximity to the cutting/incising edge.
Intrinsic staining	It is a procedure which used to improve the color of the dental restoration by application of colored stains on its internal surface.
IOP	Incisal overlapped preparation.
IPS Empress <sup>®</sup> I	A brand name of a type of glass ceramic which consist of leucite crystals.
IPS e.max <sup>®</sup> CAD	A brand name of a type of glass ceramic which consist of lithium disilicate crystals.
L*	It is a color coordinate which is used to measure the value along lightness-darkness axis.

Laminate veneer	A shell-like artificial layer which covers the front surface of the teeth. This layer replaces missing enamel of natural teeth.
LEDs	Light emitting diodes.
Lingual	The surface of the tooth adjacent to the tongue.
LTD	Low-temperature degradation is a spontaneous $t-m$ transformation occurring over time at low temperatures, when the $t-m$ transformation is not triggered by the local stress produced at the tip of an advancing crack.
Luting cement	It is the material which is used to attach or lute the crown or fixed partial denture to the natural tooth.
Mandibular	Referring to the mandible (jaw bone) in the skull.
Master cast	It is the original and referenced of a model which is made of stone.
Master die	It is the original and referenced model which is made of stone, and it is considered a duplicate morphology in size and shape of one tooth in the mouth.
Maxillary	Referring to the maxilla in the skull.
Mesial	The surface of a tooth closest to the midline.
Occlusal scheme	The type of occlusion in which the teeth interdigitate together.
Panavia 21 Ex or TC	A type of resin cement.
Paradigm MZ 100	It is a type of composite resin.
Parafunctional	Abnormally directed forces applied on the teeth more than normal biting forces.
PFM	A type of crown consisting of metal substructure with an external veneer of porcelain bonded to the metal substructure in order to provide an esthetic restoration.
ProCAD	A type of glass-ceramics.
Proximal	Referring to the mesial or distal surfaces of the tooth.
Ra	The arithmetic average of the profile ordinates within the measured section.



Resin cement	A type of luting cement with high modulus of elasticity.
Restoration	It can be crown, fixed partial denture or laminate veneer.
RMS	The root mean square value of the profile ordinates within the measured section.
SEM	Scanning electron microscopy.
Shade	Color.
Standard preparation	The removal of the labial or anterior front surface of a tooth while also involving the incisal cutting edge of the tooth.
Substrate color	The color of the die which simulates the dentin.
TDS	TurboDent system.
Three-quarter veneer preparation	A tooth preparation normally involving the removal of the mesial, distal, labial, and incisal surfaces of a tooth.
Tooth preparation	A procedure to remove one or more external surfaces of a tooth to create a geometric design in order to place a restoration. Normally, involves removal of enamel, while exposing the underneath dentin.
TQP	Three quarter preparation.
Try-in paste	A water soluble material which is used to verify the color of the luting cement before attaching or luting the crown or laminate veneer to the natural tooth. It has an identical color of luting cement after photo-polymerization.
TZP	Tetragonal zirconia polycrystals.
Value	The amount of brightness or darkness in a hue. The quality of grayness in comparison with white (high value) and black (low value).
Variolink <sup>®</sup> II	Brand name of dual-cured resin cement with both light and chemical activation.
Veneering porcelain	The exterior layer of the crown, and it is fired to gives the core translucency and esthetics like natural tooth.
Vita Mark II	A feldspathic ceramic material.

Working die	A positive replica of a prepared tooth on which a restoration is fabricated.
XRD	X-ray diffraction.
Y-TZP	Zirconia material stabilized by yttria.

## 1. INTRODUCTION

### *1.1. Background of zirconia material*

#### *1.1.1. Discovery and mechanical properties*

Zirconium oxide ( $ZrO_2$ ) or zirconia is a metal oxide that was identified as a reaction product of heating the gem zircon by the German chemist Martin Heinrich Klaproth in 1789.<sup>1</sup> Zirconia is polymorphic in nature, meaning that it displays a different equilibrium (stable) crystal structure at different temperatures with no change in chemistry. It exists in three crystalline forms: monoclinic (room temperature to 1170 °C), tetragonal (1170 °C–2370 °C) and cubic (2370 °C–up to melting point).<sup>2</sup>

Stabilizing oxides, such as magnesia, ceria, yttria, and calcia, are added to zirconia in order to retain the tetragonal phase in a metastable condition at room temperature, thereby enabling a phenomenon called transformation toughening to occur. Zirconia has been shown to transform to the more stable monoclinic phase when it interacts with a crack. The 4% volume increase acts to close the crack and influence propagation. This transformation-toughening process gives zirconia its enhanced mechanical properties and makes it relatively unique among ceramic materials. Studies have shown that zirconia has a fracture toughness of 9 to 10  $MPa/m^{(1/2)}$  and flexural strength of 900 to 1200  $MPa$ .<sup>2</sup>

#### *1.1.2. Medical and dental applications*

Zirconia was introduced as a biomaterial because of its enhanced mechanical properties along with its biological and chemical inertness which enhanced biocompatibility.<sup>3</sup> The biomedical application of zirconia started in the 1960s,<sup>4</sup> focusing on ortho-

pedics for total hip replacements.<sup>5,6</sup> Additionally, dental applications were introduced because of the white color and mechanical properties, plus to replace the metallic sub-structure of dental restorations such as implant abutments,<sup>7,8</sup> single crowns,<sup>9,10</sup> fixed partial dentures,<sup>11,12</sup> orthodontic brackets,<sup>13</sup> and endodontic posts/dowels.<sup>14-16</sup>

### *1.1.3. Classification of zirconia*

Zirconia has been classified according to the type of material which surrounds the zirconia grains to facilitate tetragonal-to-monoclinic transformation. This includes: (i) partially stabilized zirconia (PSZ) [tetragonal zirconia grains (t-zirconia grains) which are embedded in a cubic zirconia matrix such as Mg-PSZ and Ca-PSZ]; (ii) zirconia toughened alumina (ZTA) (t-zirconia grains are immersed in a high elastic modulus matrix such as In-Ceram zirconia)<sup>17</sup>; and (iii) tetragonal zirconia polycrystals (TZP) which consists of 100% t-zirconia grains such as Y-TZP and Ce-TZP.

### *1.1.4. Manufacturing*

CAD/CAM technology has had a positive influence on zirconia which is widely available for applications in dentistry. This technology enables the machining of pre-made zirconia blocks into copings and frameworks. The technique is that a master die is scanned, and the restoration is designed on the computer screen using sophisticated software. Zirconia has been machined by two different processes: (i) soft-machining of the framework from pre-sintered blocks (green state) prepared using cold isostatic pressure (CIP) into a larger size than the scanned die and sintered 20-30% to full density at a certain time and temperature in order to compensate for enlargement; and (ii) hard-machining which involves machining the framework from fully densely sintered zirconia blocks. The soft milling procedure has been shown to be easier and less time consuming,

but the compensation for the enlargement of the framework by sintering may increase marginal discrepancy. Hard milling, although it introduces cracks and is highly time consuming, produces much stronger frameworks and an improved fit at the margin because there is no sintering shrinkage.<sup>18,19</sup>

#### *1.1.5. Challenges*

Bonding of fixation cement to zirconia is a challenge. The key to a strong attachment between zirconia and cement is sufficient surface roughness of the zirconia surface. Hydrofluoric acid has not been used to increase the surface roughness in part because there is no glass in zirconia. Abrasion with alumina particles ( $\text{Al}_2\text{O}_3$ ) increases surface roughness, but it causes surface cracks plus it reduces the flexural strength.<sup>20</sup> The  $\text{Al}_2\text{O}_3$  particles can be modified by coating the particles with glass forming silica modified alumina particles. The process of sandblasting the intaglio surface of zirconia restorations with silica modified alumina particles is called a tribochemical silica coating. This glassy coating enhances chemical bonding with a silane coupling agent and utilization of resin cement, but the bond strength is not as strong as bonding of the resin cement to traditional porcelain.<sup>21,22</sup> Further advances in the materials chemistry led to new primers and luting cements which can bond to the zirconia surface, including phosphate-modified resin cements or phosphoric acid primers that produce adhesion like a silane coupling agent. However, bond strength has been shown to be suboptimal. The currently available approaches for adhesive bonding of zirconia are not sufficient for most clinical applications, and there is no long-term data to support their use.

The opacity of zirconia limits transmission of light, so zirconia must be covered by veneering to optimize esthetics. In this regard, liners have been used to mask the zir-

conia frameworks, but these materials have been shown to have low bond strength to the veneering ceramic and could be one of the factors for chipping of the veneering porcelain.<sup>23</sup>

The transformation toughening associated with the tetragonal-to-monoclinic transformation is desirable in the presence of a crack because the excess volume caused by tetragonal-to-monoclinic transformation reduces crack propagation. This transformation also occurs in the presence of hydrothermal stress, such as environments with water, blood, and synovial fluids. In this case, the tetragonal to monoclinic transformation is considered unfavorable because the excess volume is not compensated by crack space and causes micro- and macrocracking which thereby reduces mechanical properties. This phenomenon is called low-temperature degradation (LTD) or aging. Furthermore, the presence of pre-existing cracks can make LTD worse because the cracks act as inlets for the water to leak inside the microstructure and causing more transformation. Several factors were investigated to reduce LTD, such as increasing grain size, temperature, vapor, surface defects of the material, type, percentage and distribution of stabilizing oxides, and processing techniques.<sup>24,25</sup> Still, these have been ineffective, while the most successful method to reduce LTD for dental zirconia is by covering with veneering ceramic.

## *1.2. Literature review*

### *1.2.1. Aging*

Haraguchi et al.<sup>26</sup> first reported two cases of surface degradation (roughening and micro-cracking) associated with the tetragonal-to-monoclinic transformation. The monoclinic content was 20% and 30% for the femoral heads, respectively, after 3 and 6 years *in vivo*. The transformation was associated with an increase in surface roughness

(Ra) from 6 to 120 nm. The micrographs showed that small surface domes were present on the pole of the heads, and these domes were most likely monoclinic spots.

Roy et al.<sup>27</sup> investigated the dissolution of Mg-TZP and Y-TZP for femoral heads by aging through autoclaving at 134 °C and 207 kPa steam in stages up to 49 h. The aged Y-TZP specimens had significantly higher monoclinic phase concentration (34.7% vs. 5.60%) and surface roughness (Ra = 11.9 nm vs. 4.89 nm). However, there was no statistically significant differences in monoclinic phase concentration (7.75% vs. 6.73%), and roughness (Ra = 6.08 nm vs. 5.78 nm) between the aged and nonaged Mg-PSZ specimens. Furthermore, images from the nonaged group showed that the surface of Y-TZP specimens were relatively featureless. The Y-TZP specimens exhibited a rough “orange peel” like appearance while there were no differences in surface morphology between the aged and nonaged Mg-PSZ. Some have proposed that the increase in volume associated with transformation of Y-TZP pushed individual grains out of the surface, causing the microscopically observed “orange peel” effect and increased the surfaces roughness. The surface of Mg-PSZ heads did not exhibit an “orange peel” texture after artificial aging, and neither the mean peak height nor the peak spacing of Mg-PSZ were significantly influenced by the LTD process. The results of this study are in agreement with another study in which phase transformation, roughness, and hardness of Mg-PSZ did not vary after 8.9 years *in vivo*, suggesting that the surface of Mg-PSZ is not affected by aging and thereby the wear of adjacent bearing surfaces is not influenced.<sup>28</sup>

Kosmac et al.<sup>29</sup> reported that aging of Y-TZP at 37 °C for 24 h in artificial saliva resulted in a detectable amount of monoclinic zirconia. A higher amount of transformation was found with accelerated aging at 134 °C for 2 h. While aging for 24 h at this tem-

perature, the amount of monoclinic phase exceeded 25%. The flexural strength was 15% lower as compared with sintered ceramics when immersed in artificial saliva for 24 h at 37 °C. Chevalier et al.<sup>30</sup> reported a less significant strength reduction when the as-sintered specimens were subjected to accelerated aging prior to testing in artificial saliva. There was no effect on the strength under monotonic fatigue loading when the transformation on the surface of the specimens was 25% after accelerated aging in artificial saliva. At least in the short-term, the observations were that the resultant residual surface compressive stresses suppressed the water-assisted stress-corrosion process.

Lilley<sup>31</sup> reported that decreasing grain size and increasing yttria concentration both lead to reduced tetragonal to monoclinic transformation. Papanagiotou et al.<sup>32</sup> reported that after aging treatment, the yttria concentration decreased from 6.76 to 4.83 wt%. This decrease in yttria percentage suggests that aging has an effect on the concentration of this stabilizing oxide, which seems to be reduced under this specific LTD treatment. A decreased percentage of yttria has important effects on the solubility of the material by making the tetragonal zirconia grains more vulnerable to monoclinic transformation under temperature and environmental conditions even less severe than the experimental condition studied.

Ardlin<sup>33</sup> studied the chemical stability and the effect of aging (4% acetic acid at 80 °C for 168 h) on flexural strength, and crystalline structures of two shades, P0 (white) and P17 (yellow), of Denzir<sup>TM</sup> Y-TZP blocs used for dental restorations. Forty specimens with 20 specimens for each shade were ground and polished, and ten specimens of each shade were exposed to low-temperature aging. The surfaces of the specimens were evaluated by SEM, X-ray diffractometry, and roughness. The chemical solubility in 4% acet-



ic acid was assessed by weight loss. SEM was used to evaluate the surfaces of Y-TZP and dental feldspathic samples immersed in 8% SnF. The two shades of the specimens, which had a high flexural strength, were not affected by aging and exhibited high chemical stability in the tested solutions.

### *1.2.2. Optical properties*

Aboushelib et al.<sup>23</sup> reported that the application of veneer ceramic over the zirconia framework masked the opacity of zirconia. A liner material or deep chroma dentin was needed to reproduce the required color. The author concluded that the use of pre-colored zirconia frameworks did not offer any direct advantage over the standard natural zirconia. Moreover, Hjerpe et al.<sup>34</sup> reported a decrease in the strength of zirconia that had been color shaded with zirconia coloring liquids.

Very little data are available on the shade reproduction with veneering ceramic systems for zirconia cores.<sup>35,36</sup> The differences between veneering ceramics for zirconia cores and veneering ceramics for PFM, alumina, glass infiltrated and PFM restorations are mainly related to CTE. A reasonable position states that most of the factors influencing the color of the more widely investigated ceramic systems may affect veneering ceramics for zirconia cores as well.<sup>37-39</sup> Celik et al.<sup>40</sup> reported that the color of the all-ceramic zirconia core with different veneering porcelain shades is influenced by repeated firings. The results of the Celik study were confirmed by Ozturk et al.<sup>41</sup> who reported that there was significant changes in L\*a\*b\* color data as the number of firings increased. The L\*a\*b\* were affected by ceramic composition (DC-Zirkon or IPS e.max Press), number of firings (3, 5, 7, 9) and ceramic thickness (0.5, 1, 1.5 mm). As the ceramic thickness increased, the value of L\* reduced for both ceramic materials, and there was a

change in color coordinates for IPS e.max Press ( $a^*$  and  $b^*$  are increased), and DC-Zirkon ( $a^*$  increased but not  $b^*$ ) specimens.

With respect to layering, Lee et al.<sup>37</sup> reported that the brand of core material may influence the final color of sample as much as veneering. Ho-Jung et al.<sup>36</sup> reported that the effect of veneer ceramic on a zirconia substrate (Lava), specific to the color changes of the layered ceramics, varied by brand, shade, and dentin porcelain thickness. The authors concluded that the final appearance of zirconia core ceramic restorations can be manipulated by varying the dentin porcelain thickness.

Few data are available on the translucency of different zirconia core materials at the clinical thickness as required for restorations. Heffernan et al.<sup>39</sup> reported that the opacity (contrast ratio) of a 0.5 mm thick In-Ceram Zirconia core was 1.00 (completely opaque). Chen et al.<sup>42</sup> also reported an opacity value of 1.00 for Cercon Base Zirconia with a 0.5 mm thickness. This brand of zirconia was shown to be highly opaque by Baldissera et al.<sup>43</sup> who reported translucency values for different zirconia materials with the direct transmission method and light transmission instead of the contrast ratio. In this study, Lava frames of 0.3 and 0.5 mm thickness resulted in the most translucent material among those tested. The authors reported that all of the evaluated materials may be considered translucent to a certain degree, although the quantity of transmitted light was not remarkable when compared to the value of the positive control.

### *1.2.3. Bonding to zirconia*

Resin-based composite luting cements are recommended as the best materials for cementation of all-ceramic restorations.<sup>44</sup> These types of cements have compositions and characteristics similar to conventional composites and consist of inorganic fillers embed-

ded in an organic matrix (e.g., Bis-GMA, TEGDMA, UDMA). The sealing of the marginal region at the restoration-tooth interface and retention of a restoration have been shown to be dependent on the ability of the luting cement to attach along the intaglio surface of the restoration.<sup>45</sup> Studies have shown that zirconia is difficult for enhanced micromechanical retention using hydrofluoric acid to enhance attachment strength to cement. Kern and Wegner<sup>46</sup> reported on the long-term bond strength of phosphate monomer-containing resin-based composite cements to zirconia. They compared the tensile bond strength to zirconia using different bonding systems: Panavia Ex, Panavia 21 Ex, Bis-GMA alone, Bis-GMA after silanization, Bis-GMA after tribochemical silica coating and silanization, Bis-GMA after acrylization, and chemical-cured polyacid-modified resin composite cement. After 150 days of post placement, the conclusion was that Panavia Ex and Panavia 21 Ex were the only luting cements that exhibited higher magnitude bond strengths (Panavia:  $49.7 \pm 8.1$ MPa; Panavia 21:  $46.0 \pm 7.4$ MPa) without a significant loss in bond strength after artificial aging. Wegner and Kern investigated tensile bond strength over 2 years of resin cements to zirconia, and it was confirmed that the functional phosphate ester group of MDP formed a water-resistant chemical bond with the zirconia surface.<sup>47</sup> However, Derand and Derand<sup>48</sup> found that Panavia Ex did not form a strong bond to zirconia and Superbond C & B (4 META/TBB/PMMA) had a significantly greater bond strength. Similarly, Lee et al.<sup>49</sup> and Ernst et al.<sup>50</sup> reported that Superbond C & B produced a greater bond strength than Panavia F. The increase in the bond strength was explained by bonding of the anhydride group in 4-META to the zirconia surface and the tribochemical coating.

Other factors that could affect bond strength are the thickness of the luting cement, composition of the zirconia (zirconia brand), and type of resin cement. Even though Superbond C & B had a greater bond strength when tested in shear compared to MDP-containing resin cements, research over the years has focused on improving the bond strength of MDP resin cements to  $ZrO_2$ .<sup>51-60</sup> The improvement of the bond strength was explained by chemical structure of MDP resin cement that are hydrolytically stable, and, therefore, do not decrease in bond strength over time. The addition of MDP-containing bonding/silane coupling agent to enhance bonding of MDP resin cements has produced positive results. It was shown that particle air-abrasion or tribochemical coating, followed by the application of MDP-containing bonding/silane coupling agent, resulted in increased bond strength compared to MDP-containing cements.<sup>51,54,65,66</sup> It is known that acidic monomers rapidly hydrolyze silane coupling agents, producing the siloxane bonds necessary for chemical bonding.<sup>67</sup> It is thought that the acidic nature of MDP enhances the siloxane bonding produced by silane coupling agents and results in improved retention of resin cements to  $ZrO_2$ .<sup>66</sup> Other phosphate monomer-containing cements like RelyX Unicem, a universal self-adhesive resin cement, and non-phosphate monomer-containing cements like RelyX ARC and Bifix QM(VOCO GmbH, Cuxhaven, Germany), Bis-GMA resin cements, and Multilink Automix (Ivoclar Vivadent, Amherst, NY, USA), a phosphonic acid based cement, have exhibited statistically comparable bond strength to MDP-containing resin cements in laboratory studies.<sup>51,54,55,57-60,64</sup> Although these resin cements have shown good mechanical retention, MDP-containing resin cement continues to be the popular choice for luting  $ZrO_2$  prosthetics in clinical applications due to its low incidence of retention loss leading to failure.<sup>65-69</sup>

### *1.3. Aims*

#### *1.3.1. Aim 1*

- The influence of dental preparation on the phases (tetragonal vs. monoclinic) of zirconia intended for restorations.
- The effect of aging treatment on the flexural strength, nanoindentation, hardness, Young's modulus, surface roughness, and structural stability of yttria-stabilized zirconia (Y-TZP).
- The depth distribution of the transformation determined.

#### *1.3.2. Aim 2*

- Investigate the effect of try-in paste, composite resin abutment colors, and different veneer regions on the optical properties of feldspathic porcelain, CAD/CAM generated yttria-stabilized zirconia, and IPS e.max<sup>®</sup> CAD laminate veneers.

#### *1.3.3. Aim 3*

- Compare the failure load without thermocycling process of yttria stabilized zirconia, and IPS e.max<sup>®</sup> CAD veneers with feldspathic porcelain veneers supported by composite resin dies (elastic modulus is close to tooth dentin).
- Evaluate the effect of incisal overlapped preparation and three-quarter preparations relative to the failure load of different laminate veneer materials.
- Determine the failure mode of all laminate veneers.

## 2. MATERIALS AND METHODS

This section on Materials and Methods will follow the tradition organization of describing the materials and their preparation, followed by experimental methods and testing protocols. In the cases where the approaches for the three specific aims differ, there are separate subsections for each.

### *2.1. Materials and Sample Preparation*

#### *2.1.1. Low-Temperature Degradation Study*

Sixty-four zirconia disc-shaped samples (diameter 11.78 mm, thickness 1.35 mm) were fabricated by the TurboDent system (Pou-Yuen Technology Co., Ltd. No. 6, Fugong Rd., Fusing Township, Changhua County 506, Taiwan). The discs were oversized to compensate for 20.8% shrinkage during sintering. The chemical composition and material specifications of zirconia<sup>70</sup> are listed in Tables 1 and 2.

The samples were prepared to simulate dental practice as illustrated in Table 3 for the fabrication of a zirconia restoration. The samples were finished using the Exact-Micro-Grinding System (Model number 300-310, Germany) with 35  $\mu\text{m}$  diamond lapping film (Allied High Tech Products, Inc., Rancho Dominguez CA) at standard speed and pressure without water. The samples were colored with A<sub>1</sub> dyeing liquid according to the manufacturer's instructions. The dyed discs were then sintered to full density as recommended by the manufacturer (the TurboDent system requires a 7.5 hour firing cycle at maximum temperature of 1530 °C to include heating and cooling). The samples were

further ground with 35  $\mu\text{m}$  continuous diamond lapping film, and then were polished with 0.5  $\mu\text{m}$  diamond lapping film. Each disc was then fired at a temperature of 910 °C to simulate the porcelain application process; however, for this study, the veneering porcelain was not applied.

The samples were divided into two equal groups - the control group and the accelerated aging group, with thirty-two samples for each group. Four samples were used for XRD, surface roughness, hardness, modulus, and elemental analysis, and 28 samples for flexural strength for each group (control and aged samples). Multiple measurements were made in each sample for surface roughness, hardness, modulus, and elemental analysis as illustrated in Table 4.

#### *2.1.2. Optical Property Study*

The zirconia laminate veneers were constructed from the same zirconia material used from low-temperature degradation study.

A maxillary left lateral incisor (Model #R861, Columbia Dentoform Corporation, Long Island City, NY) was used for the veneer preparations and an index was fabricated prior to preparation to standardize the thickness of the laminate veneers. The incisal overlapped preparation (IOP) was defined as 0.5-mm facial reduction, and 1.5-mm incisal edge reduction (Figure 1). An impression of the prepared tooth with adjacent teeth was made with polyvinyl-siloxane impression material (Aquasil Ultra digit<sup>TM</sup> XLV Regular Set; Aquasil Monophase, DENSPLY International, York, PA). Type IV die stone (Jade Stone, Whip Mix Corp, Louisville, KY) was used to pour the impression in order to fabricate the master cast.

The master die was scanned and a restoration site designed using the TurboDent system (TDS) CAD/CAM technology (Pou-Yuen Technology Co., Ltd. No. 6, Fugong Rd., Fusing Township, Changhua County 506, Taiwan). A total of 30 composite resin abutments were machined using Paradigm MZ 100 blocks (3M ESPE, St. Paul, MN) with three different colors: A<sub>1</sub> (light color), A<sub>2</sub> (medium color), A<sub>3</sub> (dark color). Ten composite resin abutments were fabricated for each color.

Ten (10) yttria-stabilized zirconia (Y-TZP) laminate veneers were fabricated using the TDS technique as described: an optical impression of the master die was taken with a laser scanner, and a restoration designed, and milled from partially sintered zirconia blocks, colored, sintered to have an overall 0.3 mm thickness. The Y-TZP was covered with the appropriate veneer porcelain (VITA VM9) according to the manufacturer's instructions.

Ten (10) glass-ceramic laminate veneers were machine from IPS e.max<sup>®</sup> CAD HT blocks (Ivoclar Vivadent Inc, Amherst, N.Y) using CEREC 3D CAD/CAM technology (Sirona Dental Systems LLC, Charlotte, NC). The CEREC powder (IPS Contrast Spray; Ivoclar Vivadent AG, Amherst, NY) was sprayed with opaquing powder to obtain a uniform layer, with an optimal thickness of 32 μm to visualize both the internal line angles of the preparation and define the cavosurface margin.<sup>71</sup> An optical impression of the sprayed master die was made with a laser scanner and then designed according to the manufacturer's instructions with the veneers being milled from partially crystallized blocks, and then fully crystallized according to the manufacturer's instructions. Another ten (10) glass-ceramic laminate veneers were fabricated manually using feldspathic por-



celain (Noritake Super Ex 3, Noritake Kizai Co., LTD., Nagoya, Japan) using conventional refractory techniques.

Each veneer was measured at pre-designated regions using a precision caliper with an accuracy of 0.001 mm. The average thickness, composition, and grain size for each laminate veneer material are provided in Table 5.

### *2.1.3. Mechanical Property Study*

Using the IOP of the maxillary left lateral incisor on the dentoform from the previous experiment, the preparation was further extended to break both the mesial and distal contacts (Figure 2) to have a three-quarter preparation (TQP). A second impression was taken with the adjacent teeth after completing the TQP and then poured with type IV die stone in order to fabricate the 2<sup>nd</sup> master cast.

In addition to the 30 laminate veneers and 30 composite resin abutments fabricated from the previous experiment for IOP, another set of 30 composite resin abutments, 30 laminate veneers (10 yttria-stabilized zirconia, 10 IPS e.max<sup>®</sup> CAD HT, and 10 feldspathic porcelain laminate veneers) were fabricated for TQP with identical conditions as the previous experiment. All the veneers were measured using an accurate caliper after fabrication for TQP design as in Table 7. The modulus of elasticity and flexural strength of all laminate veneer materials are given in Table 8.

All the composite resin abutments were fixed in a buccal-lingual inclination angle of 135° between the long axis of the abutment and the horizontal plane of the abutment holder using a surveyor and fixed in place by self-curing acrylic resin (Ortho-Jet, Lang) in the abutment holders. The abutments were embedded 2 mm below the cemento-enamel junction (CEJ) to simulate the clinical bone level, cleaned with 35% phosphoric acid (Ul-

tra-Etch, Ultradent Products, Inc., South Jordan, UT) for 30 s, rinsed, and dried. Subsequently, the laminate veneers were cemented on the composite resin abutments to fabricate the test specimens (Table 9). Feldspathic porcelain and IPS e.max<sup>®</sup> CAD laminate veneers were bonded with the same procedure and luting agent (Variolink II; Ivoclar Vivadent, Amherst, NY) except for the etching time of hydrofluoric acid (60 s for feldspathic porcelain veneers and 20 s for e.max<sup>®</sup> CAD veneers). Yttria-stabilized zirconia laminate veneers do not have glass in their microstructure, so RelyX<sup>™</sup> Unicem 2 with tribochemical silica-coating was selected for bonding the yttria-stabilized zirconia material as recommended in the literature.<sup>72</sup>

## *2.2. Testing Methods*

### *2.2.1. Low-Temperature Degradation Study*

The accelerated aging group was given an aging treatment (100 °C, 7 days in boiling artificial saliva<sup>73</sup>) in order to simulate low-temperature degradation in the oral environment.

Surface roughness was determined using a DI3100 microscope (Digital Instruments, Inc.) in contact mode with oxide-sharpened silicon nitride probes and an average scanning speed of 50 μm/s without any additional surface preparation. Average roughness (Ra) (the arithmetic average of the profile ordinates within the measured section) and root mean square roughness (RMS) (the root mean square value of the profile ordinates within the measured section) were measured.<sup>74</sup>

The phase distribution was analyzed on an x-ray diffractometer (Siemens D500 Bruker AXS, Madison, Wis). Initial scan was conducted from 10-90° to demonstrate that zirconia is a random polycrystal which validates the phase analysis method (Figure 3).

These experiments were conducted primarily with Bragg-Brentano geometry between 27-32 ° (2θ), with Kα radiation. Scans were performed at 40 kV, 30 mA, step size of 0.005°/step, and a scan time of 8 sec/step. The tetragonal-to-monoclinic transformation was detected on the top surface of the samples. The relative amount ( $X_M$ ) of the transformed monoclinic zirconia in the specimens was calculated from the integral intensities of the monoclinic ( $\bar{1}11$ ), (111) and the tetragonal (101) peaks. This characterization was based on the equation proposed by Garvie & Nicholson<sup>75</sup>:

$$X_m = \frac{I_{111}^m + I_{\bar{1}11}^m}{I_{111}^m + I_{\bar{1}11}^m + I_{101}^t}$$

The monoclinic fractions were calculated as a function of different x-ray incidence angles (14, 10, 8, 5, 3 degrees) in order to determine the depth distribution of tetragonal-to-monoclinic transformation from the surface into the depth of the material after the aging process.

Nanoindentation and Young's modulus measurements were made on the surface of the zirconia samples using a nanoindenter<sup>®</sup> XP/G200 (Oak Ridge, TN) system calibrated by using Corning 7980. A Berkovich diamond indenter with 120 ° for each facet was used for all the measurements. The loading/unloading rate was 0.3 mN/s. A 10 s hold time at a maximum load and 10 s at 10% of maximum load during unloading was used to minimize thermal drift. The 5 x 5 matrix was taken for each sample using 500 nm as maximum penetration depth with 35 nm apart distance, and the Poisson ratio was 0.25. The data was processed using vendor software to produce load-displacement curves, and the mechanical properties were calculated using Testworks<sup>®</sup> software.

Scanning electron micrographs (Philips 515 Scanning Electron Microscope; Philips Electronics, Eindhoven, Netherlands) of the samples were obtained with an accele-

rating voltage of 30 kV. The samples were coated with carbon for elemental analysis with energy dispersive spectroscopy (EDS) in order to quantify material composition (yttrium, zirconium, oxygen, aluminum, and hafnium) for the control and aged samples.

Fifty-six samples were subjected to a biaxial flexural strength test (piston-on-three balls) according to the ISO standard 6872 for dental ceramics<sup>76</sup> using a universal testing machine (Instron, Satec Systems Inc., Model: Apex T5000, Grove PA). Each specimen was placed with the treated surface under tension on three, 3.18 mm diameter hardened steel balls positioned 120° apart on a support circle with a diameter of 10 mm. A thin plastic sheet (0.05 mm thick) was placed between the punch and the specimen to facilitate an even load distribution. The samples were loaded with a flat piston with a diameter of 1.5 mm at the center of the specimen at a crosshead speed of 0.5 mm/min until failure occurred. The fracture load was recorded (N) and the biaxial flexural strength for each specimen was calculated.

### *2.2.2. Optical Property Study*

Four (4) different colors of try-in pastes: bleach XL, opaque white, transparent, and yellow were utilized for the assessment of the optical effects of the luting cement (Variolink<sup>®</sup> II, Ivoclar Vivadent, Schaan, Liechtstein) on the visual appearance and favorable color coordinates of all the laminate veneers.

A spectrophotometer (Crystaleye, Model CE 100-DC/US, Ver.1.3.1.0 Olympus, Japan) was used in this study to measure CIELAB color coordinates: L\* from white (+100) to black (0), a\* from red (+90) to green (-70), b\* from yellow (+100) to blue (-80) as indicated in Figure 4.<sup>77</sup> This device uses seven light emitting diodes (LEDs) as an illumination source with 45/0° geometry. The image-capture time was 0.2 s. The spectral

data were acquired from the captured image of the laminate veneers. The reflectance magnitudes were measured from 400 to 700 nm wavelength with 1 nm intervals for pixel regions.

Color coordinates were measured in the incisal, body, and cervical regions of all laminate veneers with different combinations of laminate veneer material, composite resin abutment color, and try-in paste color along with three repeated readings for each combination. The color changes ( $\Delta E$ ) were calculated between the control laminate veneers [using composite resin abutment color ( $A_2$ ) with glycerin] and the experimental laminate veneers (using a combination of three composite resin abutment colors and four try-in paste colors) in the three tooth regions using the following equations:<sup>78</sup>

$$\Delta L = L_{\text{control}} - L_{\text{experiment}}$$

$$\Delta a = a_{\text{control}} - a_{\text{experiment}}$$

$$\Delta b = b_{\text{control}} - b_{\text{experiment}}$$

$$\Delta E = [(\Delta L)^2 + (\Delta a)^2 + (\Delta b)^2]^{1/2}$$

and  $\Delta E = 3.7$  was considered as the perceptibility threshold.<sup>79</sup>

The effect on the colors from the composite resin abutment and try-in paste on the color of the laminate veneer were interpreted in four different cases as shown in Table 6. Case (1): the color of veneers was not changed by the composite resin abutment color nor by the try-in paste color. Case (2): the color of the laminate veneers was changed by the try-in paste color only. Case (3): the color of the veneers was changed by both the composite resin abutment and the try-in paste colors. Case (4): the color of veneers was changed by the composite resin abutment color, but the change was improved by the try-in paste color.

### *2.2.3. Mechanical Property Study*

Each specimen was mounted in the universal testing machine (Instron, model Apex T5000, Satec Systems Inc., Grove, PA). A polymeric material (0.2 mm thick) was placed between the flat punch (diameter of 4 mm) and the center of the incisal edge of the cemented laminate veneers to facilitate more even load distribution. The specimens were loaded at a crosshead speed of 0.5 mm/min until a sudden drop of the load was recorded.

## *2.3. Statistical Analysis*

### *2.3.1. Low-Temperature Degradation Study*

The measurements of the tested spots for each group were averaged for the control and aged sample sets. The t-test was used between the control and aged samples.<sup>80</sup>

### *2.3.2. Optical Property Study*

The mean and standard deviation ( $\pm$ SD) of  $\Delta E$  for each veneer material was calculated and averaged for the combinations of the composite resin abutment and try-in paste colors at each veneer region. Comparisons between tooth regions were made using repeated measures of the analysis of variance (RM ANOVA).<sup>81</sup> When the RM ANOVA was significant, the Neuman-Keuls test was used to determine which comparisons were significantly different.<sup>82</sup>

The color coordinates were measured and averaged for each try-in paste color (except transparent) for all laminate veneer materials at the body region of the composite resin abutment color ( $A_2$ ). Color coordinates were measured for the composite resin abutment color ( $A_2$ ) with glycerin at the body region of all laminate veneer materials in order to compare the color coordinates for each veneer material. The effects of try-in paste color and laminate veneer material on color coordinates were assessed using

ANOVA. When the ANOVA was significant, Tukey's HSD test was used to determine which comparisons were significantly different. A  $p$ -value of  $<0.05$  was considered significant.<sup>82</sup>

### *2.3.3. Mechanical Property Study*

The failure loads of 10 samples were averaged for each veneer material/preparation design, and mean and standard deviations calculated. The t-test was used to compare the failure load between the two preparation designs (IOP and TQP) for each veneer material, and one-way ANOVA was used to compare the failure load between the three veneer materials. If the ANOVA test was significant ( $p < 0.05$ ), Tukey's HSD test was used to determine if veneer materials were significantly different.<sup>80</sup>

Table 1. Chemical composition of yttria-stabilized zirconia.

Chemical component	Mol %
Zirconium dioxide (ZrO <sub>2</sub> )	92.642
Yttrium oxide (Y <sub>2</sub> O <sub>3</sub> )	5.3
Hafnium oxide (HfO <sub>2</sub> )	1.78
Aluminum oxide (Al <sub>2</sub> O <sub>3</sub> )	0.253
Others	0.025

Table 2. Material specifications of yttria-stabilized zirconia.

Specification	Value
Density ( $\rho$ )	6.05 g/cm <sup>3</sup>
Thermal expansion coefficient (TEC)	10 X 10 <sup>-6</sup> K <sup>-1</sup>
Flexural strength	1200 MPa
Fracture toughness (K <sub>IC</sub> )	8 MN/m <sup>(1/2)</sup>
Modulus of elasticity (E)	210 GPa
Grain size	0.35 $\mu$ m
Vickers hardness (HV 10)	1200 Hv
Melting point	2680 °C
Shrinkage after sintering	20.8%



Table 3. The procedure for sample preparation simulating dental practice.

	Actual dental procedure	Sample preparation
Finishing	Universal silicone wheel (30-40 $\mu\text{m}$ )	35 $\mu\text{m}$ diamond lapping film using Exact-Micro-Grinding System
Color infiltration	Different colors of dyeing liquids	Dyed by A <sub>1</sub> color
Sintering	7.5 hour firing cycle at maximum temperature of 1530 °C to include heating and cooling stages	7.5 hour firing cycle at maximum temperature of 1530 °C to include heating and cooling stages
Grinding	Fine-diamond bur (30-40 $\mu\text{m}$ )	35 $\mu\text{m}$ diamond lapping film using Exact-Micro-Grinding System
Polishing	Rubber polishers (10 $\mu\text{m}$ ) with diamond polishing paste (1 $\mu\text{m}$ )	0.5 $\mu\text{m}$ diamond lapping film using Exact-Micro-Grinding System
Heat treatment without veneering porcelain application (800-900 °C)	910 °C in a porcelain processing oven	910 °C in a porcelain processing oven

Table 4. The number of samples and data points within each sample for all characterization procedures and flexural strength.

		Number of samples for each group (control and aged)	Number of data points within each sample
Surface	Ra (nm)	4	16
Roughness	RMS (nm)	4	16
Amount of Monoclinic (%)		4	1
Hardness (GPa)		4	97
Young's Modulus (GPa)		4	97
	Zr	4	12
Elemental	O	4	12
Analysis	Y	4	12
(wt %)	H <sub>f</sub>	4	12
	Al	4	12
Flexural Strength (MPa)		28	1

Table 5. The characteristics and the average thickness at each region of laminate veneer materials.

	Average veneer mean thickness in mm ( $\pm$ SD)			Composition	Grain size
	Cervical region	Body region	Incisal region		
Ytria-stabilized zirconia	0.87 $\pm$ 0.06	0.88 $\pm$ 0.09	0.94 $\pm$ 0.08	ZrO <sub>2</sub> (92.6 mol%), Y <sub>2</sub> O <sub>3</sub> (5.3 mol%), HfO <sub>2</sub> (1.78 mol%), Al <sub>2</sub> O <sub>3</sub> (0.25 mol%), others (0.025 mol%)	0.35 $\mu$ m
IPS e.max <sup>®</sup> CAD HT	0.84 $\pm$ 0.08	0.95 $\pm$ 0.07	0.76 $\pm$ 0.05	SiO <sub>2</sub> (57-80 wt%), Li <sub>2</sub> O (11-19 wt%), K <sub>2</sub> O (0-13 wt%), P <sub>2</sub> O <sub>5</sub> (0-11 wt%), ZrO <sub>2</sub> (0-8 wt%), ZnO (0-8 wt%), other and coloring oxides (0-12 wt%)	Platelet-shaped crystals is in the range of 0.2 to 1.0 $\mu$ m
Feldspathic porcelain	0.45 $\pm$ 0.05	0.54 $\pm$ 0.08	0.63 $\pm$ 0.09	SiO <sub>2</sub> (64.5%), Al <sub>2</sub> O <sub>3</sub> (14.4%), CaO (<1%), MgO (<1%), K <sub>2</sub> O (8.7%), Na <sub>2</sub> O (9.2%), Li <sub>2</sub> O (<1%)	26.4 $\mu$ m

Table 6. Interpretation of color change on the laminate veneers according to composite resin abutment color or try-in paste color.

Case	Color of try-in paste	$\Delta E$	The effect of color change on the laminate veneer
1	Transparent Yellow or bleach XL or opaque white	$\Delta E < 3.7$ $\Delta E < 3.7$	The color of laminate veneers was neither changed by composite resin abutment color nor by try-in paste color
2	Transparent Yellow or bleach XL or opaque white	$\Delta E < 3.7$ $\Delta E > 3.7$	The color of laminate veneers was changed by yellow or bleach XL or opaque white try-in paste colors (the higher value of $\Delta E$ , the higher color change)
3	Transparent Yellow or bleach XL or opaque white	$\Delta E > 3.7$ $\Delta E > 3.7$	The color of laminate veneers was changed by both composite resin abutment color and any color of yellow or bleach XL or opaque white try-in paste colors (the higher value of $\Delta E$ , the higher the color change)
4	Transparent Yellow or bleach XL or opaque white	$\Delta E > 3.7$ $\Delta E < 3.7$	The color of laminate veneers was changed by composite resin abutment color (the higher value of $\Delta E$ , the higher color change), but its change was decreased by any color of yellow or bleach XL or opaque white try-in paste colors (the lower value of $\Delta E$ , the better the improvement of color change)

Table 7. The average veneer means thickness of laminate veneer materials for different preparation designs.

Veneer material	Average veneer mean thickness in mm ( $\pm$ SD)	
	IOP (n= 10 per each design)	TQP (n= 10 per each design)
Yttria-stabilized zirconia	0.90 ( $\pm$ 0.08)	1.10 ( $\pm$ 0.14)
IPS e.max <sup>®</sup> CAD	0.85 ( $\pm$ 0.10)	0.84 ( $\pm$ 0.10)
Feldspathic porcelain	0.54 ( $\pm$ 0.11)	0.85 ( $\pm$ 0.20)

Table 8. The mechanical properties for yttria-stabilized zirconia, IPS e.max<sup>®</sup> CAD, and feldspathic porcelain laminate veneers.

	Modulus of elasticity (GPa)	Flexural Strength (MPa)
Yttria-stabilized zirconia	210	1200
IPS e.max <sup>®</sup> CAD	95	360
Feldspathic porcelain	82	111

Table 9. The Cementation procedures for yttria-stabilized zirconia, IPS e.max<sup>®</sup> CAD, and feldspathic porcelain laminate veneers.

Step number	Step-by-step procedure	Feldspathic porcelain and IPS e.max <sup>®</sup> CAD	Yttria-stabilized zirconia
1	Surface treatment for the intaglio surface	Etching with 5% hydrofluoric (acid ceramic etching gel; Ivoclar Vivadent, Amherst, NY) for 60 seconds in case of feldspathic porcelain veneers and 20 seconds for IPS e.max <sup>®</sup> CAD veneers, then rinsed with water, dried with air	Tribochemical silica-coating using sandblaster unit (Renfert, basic classic, 2945-4025, Hilzingen/Germany) filled with CoJet-Sand (30- $\mu$ m silica-modified Al <sub>2</sub> O <sub>3</sub> particles, CoJet <sup>™</sup> system; 3M ESPE, St. Paul, Minn): perpendicular to the surface from a distance of approximately 10 mm for a period of 15 s at 2.8 bar pressure, then air blasted
2	Apply silane coupling agent	VersaLink Porcelain Bonding for 5 minutes (Sultan-Healthcare, Hackensack, NJ)	ESPE-Sil for 5 minutes (3M ESPE)
3	Luting cement	Variolink II with light cure bleach base (Variolink II; Ivoclar Vivadent, Amherst, NY)	A self-adhesive universal resin cement (RelyX <sup>™</sup> Unicem 2, 3M ESPE)
4	Cure* for initial fixation from facial side	5 seconds	2 seconds
5	Cure* for final fixation from facial, mesial, distal and palatal sides	40 seconds	20 seconds
6	Finishing	Hand instruments (#15c scalpel, #371716, Bard- Parker; Becton Dickinson, Franklin Lakes, NJ), and Dialite Ultra Polishers (Brasseler USA <sup>®</sup> Dental Rotary Instruments, Savannah, GA.)	
7	Polishing	The margins were polished with a diamond polishing paste (Henry Schein Inc., Melville, NY) and a rubber cup (#9631.204.030; Komet Dental, Rock Hill, SC).	

\* The laminate veneers were light polymerized with at least a 600 mW/cm<sup>2</sup> light intensity (Demetron<sup>®</sup> LC<sup>™</sup> Kerr Corporation, Orange, CA).



Figure 1. Incisal overlapped preparation (IOP) design.



Figure 2. Three Quarter Preparation (TQP) design.

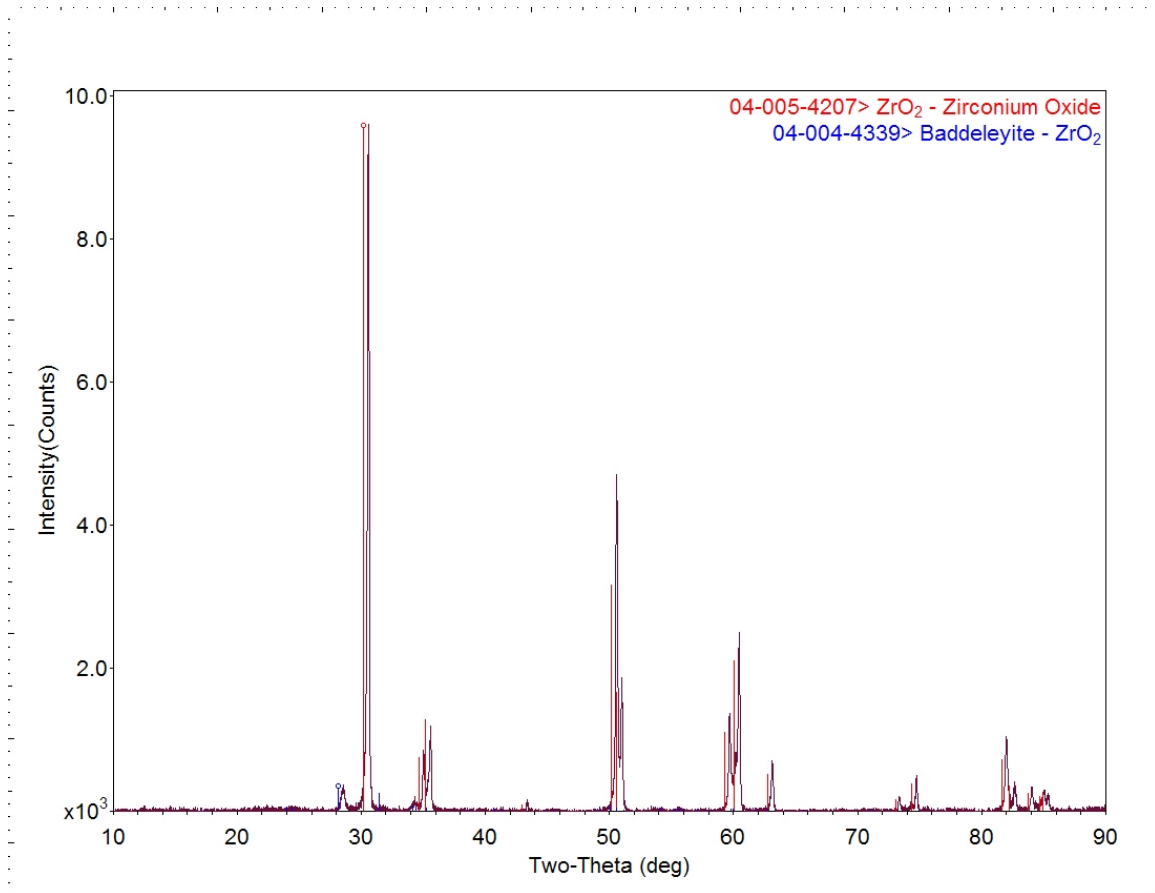


Figure 3. X-ray diffraction scan from 10-90°. The majority of the peaks match the tetragonal phase, card 04-005-4207, with a slight angular offset due to the Y<sub>2</sub>O<sub>3</sub> additions. Two monoclinic peaks are present at about 28.0 and 31.5°. One of the primary cards for the monoclinic phase is 04-004-4339. This scan indicates that zirconia is a random tetragonal polycrystal with some monoclinic also present.



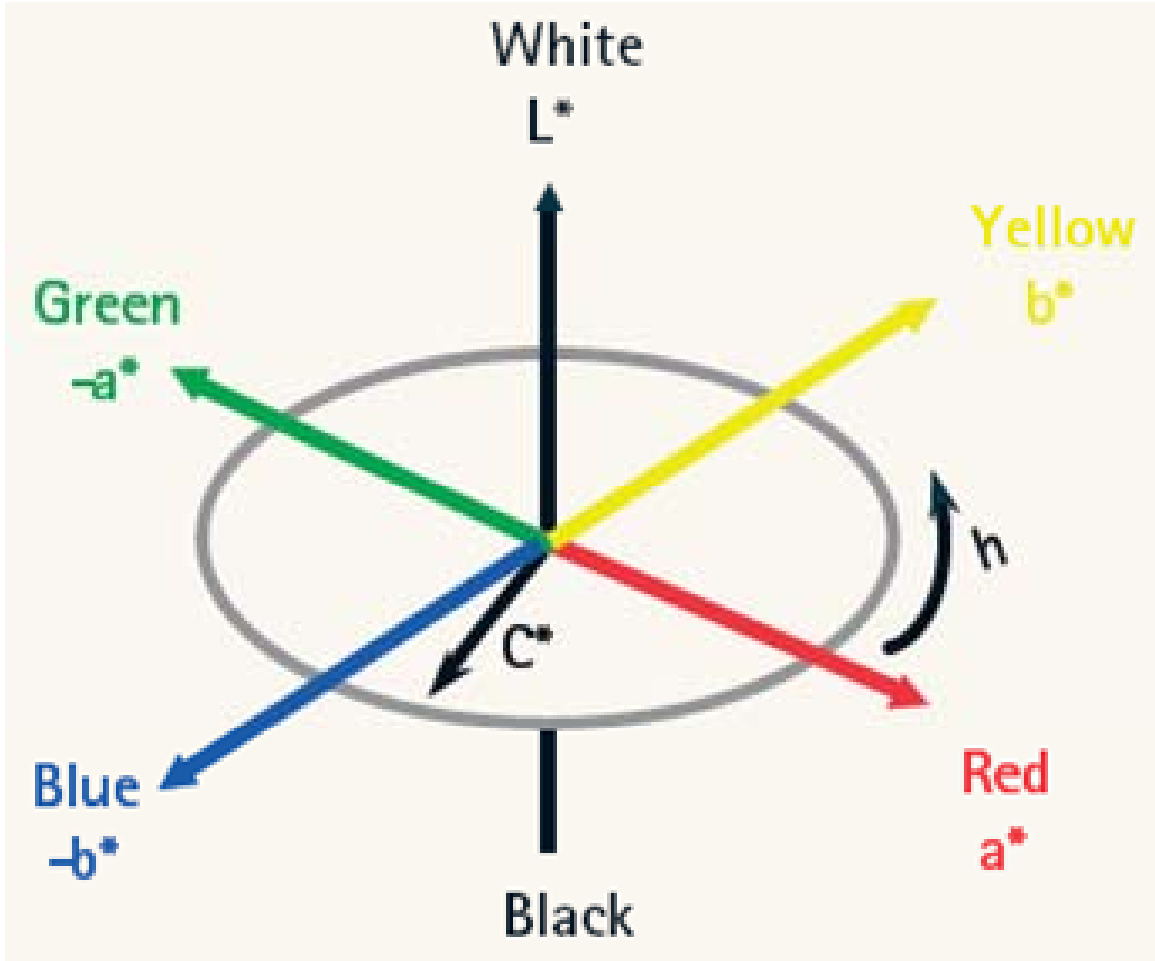


Figure 3. Description of CIELAB System.

3. THE EFFECT OF LOW-TEMPERATURE DEGRADATION ON THE  
MECHANICAL PROPERTIES AND STRUCTURAL STABILITY OF DENTAL  
ZIRCONIA PREPARED BY SIMULATED DENTAL PRACTICE

TARIQ F. ALGHAZZAWI, JACK E. LEMONS, PERNG-RU LIU, MILTON E. ESSIG,  
GREGG M. JANOWSKI

*Submitted to Journal of Prosthodontics*

Format adapted for dissertation

## Abstract

Statement of problem. It is critical to determine if low-temperature degradation (LTD) of zirconia occurs using dental procedures in conditions that simulate extended use in the oral environment.

Objectives. The purpose of this study is to investigate the effect of LTD on the flexural strength, nanoindentation hardness, Young's modulus, surface roughness, and structural stability of yttria-stabilized zirconia.

Methods. Sixty-four zirconia samples were prepared to simulate dental practice. The samples were divided into the control group and the accelerated aging group. The simulated group followed the same procedure as the control group except for the aging treatment. Atomic force microscopy was used to measure surface roughness. The degree of tetragonal-to-monoclinic transformation was determined using x-ray diffraction. Nanoindentation hardness and modulus measurements were carried out on the surface of the zirconia samples using a nanoindenter<sup>®</sup> XP/G200 system. The yttria level for non-aged and aged samples was measured using energy dispersive spectroscopy. Flexural strength was determined using the piston-on-three-ball test. The t-test was used to determine statistical significance.

Results. Means and standard deviations were calculated using all observations for each condition. The *p* value comparing non-aged and aged values comes from a group t test. The LTD treatment results in increased surface roughness (from 12.23 to 21.56 nm for Ra and 15.06 to 27.45 nm for RMS) and monoclinic phase fractions (from 2 to 21%), with a concomitant decrease in hardness (from 16.56 to 15.14 GPa) and modulus (from 275.68

to 256.56 GPa). Yttria content (from 4.43 to 4.46%) and flexural strength (from 586.86 to 578.31 MPa) were unchanged.

Conclusion. The LTD treatment induced the tetragonal-to-monoclinic transformation with surface roughening in zirconia prepared using dental procedures.

Clinical Implications. Tetragonal-to-monoclinic transformation will increase surface roughness which might prevent the use of zirconia dental restorations without protective veneering porcelain.

### Introduction

Zirconia is a polymorphic material that exists in three different crystal structures: monoclinic, tetragonal, and cubic. Pure zirconia is monoclinic from room temperature to 1170 °C.<sup>1</sup> Above that temperature, it transforms into the tetragonal phase. At a temperature of 2370 °C, zirconia transforms into a cubic phase. The tetragonal phase may be stabilized by adding small amounts of metallic oxides, such as Y<sub>2</sub>O<sub>3</sub>, MgO, CeO, or CaO, but it is, in fact, metastable at room temperature. Processes such as grinding and sandblasting can trigger the tetragonal-to-monoclinic phase transformation. This transformation is accompanied by a 3–4% volume expansion that induces compressive stresses, thereby closing the crack tip and preventing further propagation. This characteristic, known as transformation toughening, leads to the increased fracture strength and fracture toughness of Y-TZP ceramics compared with other dental ceramics.<sup>1,2</sup>

Zirconia is inert and has high-temperature applications; yet it was surprising that Kobayashi et al. reported that the material can transform at approximately 250 °C.<sup>3</sup> This low-temperature transformation can have serious implications for clinical applications of zirconia-based materials. For example, more than 600,000 zirconia femoral heads were

implanted worldwide, mainly in the United States and Europe. The zirconia manufacturers assumed that the problem of transformation was irrelevant until 2001, when several hundred hip prosthesis failures were reported at times that wore shorter than anticipated.<sup>4</sup>

Transformation toughening caused by tetragonal-to-monoclinic transformation is desirable in the presence of a crack because the excess volume caused by tetragonal-to-monoclinic transformation reduces crack propagation. This transformation also occurs in the presence of hydrothermal stress such as water, blood, and synovial fluids over a long period of time. This is considered unfavorable because the excess volume is not compensated by crack space and causes micro- and macrocracking, reducing the mechanical properties. This phenomena is called low-temperature degradation (LTD) or aging. The following features for LTD have been established:<sup>4</sup> (1) the tetragonal-to-monoclinic transformation starts on the surface and progresses into the material; (2) reduction in grain size and/or increase in concentration of stabilizer reduces transformation rate; and (3) degradation is time dependent and proceeds more rapidly at temperatures between 200 °C and 300 °C. LTD is responsible for grain push-out,<sup>5,6</sup> increased surface roughening,<sup>7,8</sup> increased wear, decreased hardness,<sup>9</sup> and loss of strength (20% decrease in the fracture strength),<sup>10-12</sup> which may lead to performance deterioration.<sup>13</sup>

Dental restorations function in an aggressive environment with saliva, pH changes and cyclic loading. Coping/framework has dual protection against aging through veneering porcelain on the external surface and luting cement on the internal surface. However, it has been shown recently<sup>14</sup> that common luting cements absorb water via dentinal tubules, thereby exposing the zirconia coping to moisture, which, in turn, may lead to aging problems over a shorter period of time than anticipated.

It is critical to determine if LTD of zirconia prepared using dental practice procedures occurs in conditions that simulate extended use in the oral environment. The surface finish of the restoration is critical, and the fabrication with CAD/CAM technology and veneering of the ZrO<sub>2</sub>-framework is a multi-step process with the potential for operator variability. These surface treatments may affect the long-term stability and the aging sensitivity of zirconia and the success of the restoration. Both the aging environment and fabrication details for the dental zirconia restoration are very different from those of zirconia femoral heads. Thus, there is a need for basic material studies of zirconia for dental applications.

The objectives of this study were to investigate (1) the influence of dental preparation on the phases (tetragonal vs. monoclinic) of zirconia intended for restorations (2) the effect of aging treatment on the flexural strength, nanoindentation, hardness, Young's modulus, surface roughness, and structural stability of yttria-stabilized zirconia (Y-TZP), (3) determine the depth distribution of the transformation. The hypotheses were (1) dental preparation would not affect the phases of dental zirconia, and (2) the aging treatment would decrease the tetragonal phase stability of the dental zirconia which leads to more yttria loss, more tetragonal-to-monoclinic transformation, increased surface roughness, lower hardness, lower modulus of elasticity, and the flexural strength would not be affected.

### Materials and Methods

Sixty-four zirconia disc-shaped samples (diameter 11.78 mm, thickness 1.35 mm) were fabricated by the TurboDent system (Pou-Yuen Technology Co., Ltd. No. 6, Fugong Rd., Fusing Township, Changhua County 506, Taiwan). The discs were oversized

to compensate for 20.8% shrinkage during sintering. The chemical composition and material specifications of zirconia<sup>15</sup> are listed in Tables 1 and 2.

The samples were prepared to simulate dental practice as illustrated in Table 3 for the fabrication of a zirconia restoration. The samples were finished using the Exact-Micro-Grinding System (Model number 300-310, Germany) with 35  $\mu\text{m}$  diamond lapping film (Allied High Tech Products, Inc., Rancho Dominguez CA) at standard speed and pressure without water. The samples were colored with A<sub>1</sub> dyeing liquid according to the manufacturer's instructions. The dyed discs were then sintered to full density as recommended by the manufacturer (the TurboDent system requires a 7.5 hour firing cycle at maximum temperature of 1530 °C to include heating and cooling). The samples were further ground with 35  $\mu\text{m}$  continuous diamond lapping film, and then were polished with 0.5  $\mu\text{m}$  diamond lapping film. Each disc was then fired at a temperature of 910 °C to simulate the porcelain application process; however, for this study, the veneering porcelain was not applied.

The samples were divided into two equal groups - the control group and the accelerated aging group, with thirty-two samples for each group. Four samples were used for XRD, surface roughness, hardness, modulus, and elemental analysis, and twenty eight samples for flexural strength for each group (control and aged samples). Multiple measurements were made in each sample for surface roughness, hardness, modulus, and elemental analysis as illustrated in Table 4. The accelerated aging group was given an aging treatment (100 °C, 7 days in boiling artificial saliva<sup>16</sup>) in order to simulate low-temperature degradation in the oral environment.

### *Atomic force microscopy (AFM)*

Surface roughness was determined using a DI3100 microscope (Digital Instruments, Inc.) in contact mode with oxide-sharpened silicon nitride probes and an average scanning speed of 50  $\mu\text{m/s}$  without any additional surface preparation. Average roughness (Ra) (the arithmetic average of the profile ordinates within the measured section) and root mean square roughness (RMS) (the root mean square value of the profile ordinates within the measured section) were measured.<sup>17</sup>

### *X-ray diffraction (XRD)*

The phase distribution was analyzed on an x-ray diffractometer (Siemens D500 Bruker AXS, Madison, Wis). These experiments were conducted primarily with Bragg-Brentano geometry, between 27-32  $^{\circ}$  (2 $\theta$ ), with  $K\alpha$  radiation. Scans were performed at 40 kV, 30 mA, step size of 0.005 $^{\circ}$ /step, and a scan time of 8 sec/step. The tetragonal-to-monoclinic transformation was detected on the top surface of the samples. The relative amount ( $X_M$ ) of the transformed monoclinic zirconia in the specimens was calculated from the integral intensities of the monoclinic ( $\bar{1}11$ ), (111) and the tetragonal (101) peaks. This characterization was based on the equation proposed by Garvie & Nicholson<sup>18</sup>:

$$X_m = \frac{I_{111}^m + I_{\bar{1}11}^m}{I_{111}^m + I_{111}^m + I_{101}^t}$$

The monoclinic fractions were calculated as a function of different x-ray incidence angles (14, 10, 8, 5, 3 degrees) in order to determine the depth distribution of tetragonal-to-monoclinic transformation from the surface into the depth of the material after the aging process.



### *Nanoindentation hardness and Young's modulus*

Nanoindentation and Young's modulus measurements were made on the surface of the zirconia samples using a nanoindenter<sup>®</sup> XP/G200 (Oak Ridge, TN) system calibrated by using Corning 7980. A Berkovich diamond indenter with 120° for each facet was used for all the measurements. The loading/unloading rate was 0.3 mN/s. A 10 s hold time at a maximum load and 10 s at 10% of maximum load during unloading was used to minimize thermal drift. The 5 x 5 matrix was taken for each sample using 500 nm as maximum penetration depth with 35 nm apart distance, and the Poisson ratio was 0.25. The data was processed using vendor software to produce load-displacement curves, and the mechanical properties were calculated using Testworks<sup>®</sup> software.

### *Scanning electron microscopy (SEM)*

Scanning electron micrographs (Philips 515 Scanning Electron Microscope; Philips Electronics, Eindhoven, Netherlands) of the samples were obtained with an accelerating voltage of 30 kV. The samples were coated with carbon for elemental analysis with energy dispersive spectroscopy (EDS) in order to quantify material composition (yttrium, zirconium, oxygen, aluminum, and hafnium) for the control and aged samples.

### *Biaxial flexural strength*

Fifty six samples were subjected to a biaxial flexural strength test (piston-on-three balls) according to the ISO standard 6872 for dental ceramics<sup>19</sup> using a universal testing machine (Instron, Satec Systems Inc., Model: Apex T5000, Grove PA). Each specimen was placed with the treated surface under tension on three, 3.18 mm diameter hardened steel balls positioned 120° apart on a support circle with a diameter of 10 mm. A thin plastic sheet (0.05 mm thick) was placed between the punch and the specimen to

facilitate an even load distribution. The samples were loaded with a flat piston with a diameter of 1.5 mm at the center of the specimen at a crosshead speed of 0.5 mm/min until failure occurred. The fracture load was recorded (N) and the biaxial flexural strength for each specimen was calculated.

### *Statistical Analysis*

The measurements of the tested spots for each group were averaged for the control and aged sample sets. The t-test was used between the control and aged samples.

### Results

Qualitative results are shown in Table 5. Means and standard deviations were calculated using all observations for the two conditions. The *p* value comparing control and aged values comes from a group t test.

Elemental analysis using EDS of the control samples indicated high concentrations of zirconium (Zr), oxygen (O), and small concentrations of yttrium (Y), hafnium (Hf), and aluminum (Al). The aged samples indicated very similar concentrations without any significant reduction in the concentration of yttrium (4.43 % for control samples and 4.46 % for aged samples) or zirconium (80.73 % for control sample and 80.68 % for aged samples).

The aging treatment resulted in an increase in both the monoclinic fraction and surface roughness. The XRD analysis performed on control samples indicated a small monoclinic fraction (2%). However, the aged samples showed a substantial amount of monoclinic fraction (21%) as shown in Figure 1. The surface roughness was measured and the results are shown in Figure 2. There was a significant increase in the surface

roughness (Ra: 12.23 to 21.56 nm and RMS: 15.06 to 27.45 nm) between control and aged samples.

The hardness and modulus were measured, and the results are shown in Figures 3. There was a significant decrease in the hardness (from 16.56 to 15.14 GPa) and modulus (from 275.68 to 256.56 GPa) between control and aged samples. The flexural strength was not affected between control samples (586.86 MPa) and aged samples (578.31 MPa).

The distribution of the tetragonal to monoclinic phase fraction within the surface can also be measured with XRD. A low incident angle will limit the x-ray penetration depth and will yield data more reflective of the material closest to the surface. Figure 4 shows that as the x-ray incidence angle increased from 3 degrees to 14 degrees, the fraction of monoclinic phase was decreased (3 degree: 39.3 %, 5 degree: 31.5%, 8 degree: 27.2%, 10 degree: 23.6%, 14 degree: 20.7%). This confirms that the tetragonal-to-monoclinic transformation is decreasing from the surface into the depth of the material where the surface has a larger fraction of monoclinic phase (39.3% at 3 degrees) than the deeper area (20.7% at 14 degrees).

## Discussion

Zirconia copings/frameworks are usually fabricated using partially sintered Y-TZP blocks, and then are subjected to different surface treatments. In our study, a minimal fraction of monoclinic phase (2%) was detected for the control samples, as these samples were exposed to various processing treatments that included final heat treatment to a temperature of 910 °C used in porcelain fabrication. This finding is in agreement with several authors who reported that heat treatments in the temperature range 900–1000 °C

induce the reverse transformation from monoclinic to tetragonal after aging, grinding or sand-blasting of Y-TZP.<sup>20,21</sup>

There is no universally accepted mechanism that explains the origins of the tetragonal-to-monoclinic transformation in the presence of moisture, but there are three mechanisms proposed in the literature. The first is that water ( $H_2O$ ) reacts with yttria ( $Y_2O_3$ ) to form yttrium hydroxide ( $Y(OH)_3$ ), which depletes the stabilizing oxide sufficiently to cause transformation to the monoclinic phase.<sup>22</sup> The second mechanism is water attack of the Zr–O bond which leads to stress accumulation due to movement of –OH into the crystal structure. This motion generates lattice defects which act as nucleating agents for subsequent transformation from the tetragonal-to-monoclinic phase.<sup>23</sup> Finally,  $O_2$ - (not OH-) from water dissociation fills oxygen vacancies.<sup>24</sup> Panagiotou et al.<sup>25</sup> reported that LTD resulted in a loss of yttria (from 6.76 to 4.83 wt%) when Vita In-Ceram YZ was aged in boiled water for 7 days, which supports the first mechanism. In our study, there was a significant amount of tetragonal-to-monoclinic transformation, but the yttria and zirconia content were unchanged within the sensitivity of EDS. (The same experimental method was used by Panagiotou et al.). This apparently contradictory result may be due to the different compositions of zirconia that were used. Thus, the data lends indirect support to the mechanisms of either attack of the Zr-O bonds or the  $O_2$ - filling oxygen vacancies.

The strength after LTD is affected by the thickness of the transformed layer on the surface (which is related to the amount of monoclinic phase observed),<sup>26</sup> and the extension of the cracks. In the present study, there was no significant difference in flexural strength among the samples ( $P = 0.678$ ). Furthermore, the flexural strength was not af-

ected by the amount of the monoclinic transformed (from 2 to 21%) after accelerated aging in artificial saliva because tetragonal-to-monoclinic transformation occurred in the external surface only with shallower depth, and the internal flaws were not critical enough to affect the flexural strength. This finding is in agreement with another study.<sup>25</sup> The values for flexural strength ( $586.86 \pm 71.47$  MPa for control samples and  $578.31 \pm 75.25$  MPa for aged samples) in this study were much lower compared with other studies.<sup>25,27</sup> Lower values could be due to less-ideal sample dimensions (thick samples with smaller diameter) were used in this study to calculate the flexural strength, but it is within the minimal accepted flexural strength (500 MPa) as recommended by ISO13356;2008.<sup>19</sup>

The phase transformation of artificially aged Y-TZP discs illustrated in the current study increased the surface roughness, and this is comparable to previous studies<sup>8,12</sup> because the volume expansion (3-5 %) associated with the tetragonal-to-monoclinic transformation leads to grain pushout and surface uplift which imparted the surface roughening. Although the roughness of Y-TZP significantly increased with aging, a roughness of  $R_a = 0.021 \mu\text{m}$  and  $RMS = 0.027 \mu\text{m}$  is still considered to be very smooth compared with acceptable surface roughness for bacterial colonization ( $0.2 \mu\text{m}$ )<sup>28</sup> and within the range of roughness of  $0.25$  to  $0.5 \mu\text{m}$  to be undetected by a patient's tongue.<sup>29</sup>

Santos et al.<sup>8</sup> confirmed that there was a drop in hardness (nanoindentation testing) with the zirconia femoral head (from 18 to 11 GPa) caused by an extensive monoclinic transformations (from 0 to 78%). In the present study, there was a decrease in hardness (from 16.56 to 15.14 GPa) and modulus (from 275.68 to 256.56 GPa). This happened due to the induced micro-cracks from transformation after artificial aging.<sup>24</sup>

## Conclusions

Within the limitation of this study, the following can be concluded:

1. Dental preparation procedures do not induce the tetragonal-to-monoclinic transformation without aging.
2. The LTD treatment induced the tetragonal-to-monoclinic transformation (21%) in dental zirconia with surface roughening from 12 to 22 nm (Ra) ( $p = 0.017$ ).
3. The hardness (17 to 15 GPa,  $p = < 0.001$ ) and modulus (276 to 257 GPa,  $p = < 0.001$ ) were reduced by LTD.
4. The transformation proceeds from the surface into the bulk of the material.
5. In vivo studies need to be conducted to evaluate clinical significance.

## Acknowledgement

This project was supported by the American College of Prosthodontists Education Foundation (ACPEF) Research Fellowship Award on November 28, 2008.

## References

1. Piconi C, Maccauro G. Zirconia as a ceramic biomaterial. *Biomaterials* 1999;20:1–25.
2. Pittayachawan P, McDonald A, Petrie A, Knowles JC. The biaxial flexural strength and fatigue property of Lava Y-TZP dental ceramic. *Dent Mater* 2007;23:1018–1029.
3. Kobayashi K, Kuwajima H, Masaki T. Phase change and mechanical properties of  $ZrO_2$ - $Y_2O_3$  solid electrolyte after ageing. *Solid State Ion* 1980;3:489-93.
4. Denry IL, Holloway JA. Microstructural and crystallographic surface changes after grinding zirconia-based dental ceramics. *J Biomed Mater Res B: Appl Biomater* 2006;76:440-8.
5. Deville S, Gremillard L, Chevalier J, Fantozzi G. A critical comparison of methods for the determination of aging sensitivity in biomedical grade yttria-stabilized zirconia. *J Biomed Mater Res Part B: Appl Biomater* 2005;72:239-245.
6. Chevalier J. What future for zirconia as a biomaterial?. *Biomaterials* 2006;27:535-543.
7. Hernigou P, Bahrami T. Zirconia and alumina ceramics in comparison with stainless-steel heads. Polyethylene wear after a minimum ten-year follow-up. *J Bone Joint Surg Br* 2003;85:504-509.
8. Santos EM, Vohra S, Catledge SA, Cook M, McClenny MD, Lemons J, Moore KD. Examination of surface and material properties of explanted zirconia femoral heads. *J Arthroplast* 2004;19(Suppl 2):30–34.
9. Catledge SA, Cook M, Vohra YK, Santos EM, McClenny MD, Moore KD. Surface crystalline phases and nanoindentation hardness of explanted zirconia femoral heads. *J Mater Sci Mater Med* 2003;14:863-867.
10. Fleming GJP, Jandu HS, Nolan L, Shaini FJ. The influence of alumina abrasion and cement lute on the strength of a porcelain laminate veneering material. *J Dent* 2004;32:67-74.
11. Addison O, Fleming GJ, Marquis, PM. The effect of thermocycling on the strength of porcelain laminate veneer materials. *Dent Mater* 2003;19:291-297.
12. Tanaka K, Tamura J, Kawanabe K, Nawa M, Uchida M, Kokubo T, Nakamura T. Phase stability after aging and its influence on pin-on-disk wear properties of Ce-TZP/ $Al_2O_3$  nanocomposite and conventional Y-TZP. *J Biomed Mater Res A* 2003;67:200-207.

13. Guo X. On the degradation of zirconia ceramics during low-temperature annealing in water or water vapor. *J Physics Chem Solids* 1999;60:539-46.
14. Jevnikar, P., Sersa, I., Sepe, A., Jarh, O. and Funduk, N., Effect of surface coating on water migration into resin-modified glass ionomer cements: a magnetic resonance micro-imaging study. *Magn. Reson. Med.* 2000;44:686-691.
15. Personal communication from Pou-Yuen Technology Co., Ltd. No. 6, Fugong Rd., Fusing Township, Changhua County 506, Taiwan.
16. Personal communication from Firoz Rahemtulla, PhD. The University of Alabama at Birmingham, School of Dentistry Department of Prosthodontics.
17. BS EN ISO 4287: 2000 Geometrical product specification (GPS). Surface texture: profile method-terms, definitions and surface texture parameters.
18. Garvie RC, Nicholson PS. Phase analysis in zirconia systems. *J Am Ceram Soc* 1972;55:303-5.
19. International Standard ISO 6872:2008 Dental ceramics. International Organization for Standardization, Geneva, Switzerland.
20. Kosmac T, Oblak C, Marion L. The effects of dental grinding and sandblasting on ageing and fatigue behavior of dental zirconia (Y-TZP) ceramics. *J Eur Ceram Soc* 2008;28:1085-1090.
21. Wanga H, Abousheliba MN, Feilzera AJ. Strength influencing variables on CAD/CAM zirconia frameworks. *Dent Mater* 2008;24:633-638.
22. Lange FF, Dunlpo GL, Davis BI. Degradation during ageing of transformation toughened  $ZrO_2$ - $Y_2O_3$  materials at 250 °C. *J Am Ceram Soc* 1986;69:237-40.
23. Yoshimura M, Noma T, Kawabata K, Somiya S. Role of water on the degradation process of Y-TZP. *J Mater Sci Lett* 1987;6:465-7.
24. Chevalier J, Gremillard L, Virkar AV, Clarke DR. The tetragonal-monoclinic transformation in zirconia: lessons learned and future trends. *J Am Ceram Soc* 2009;92:1901-20.
25. Papanagiotou HP, Morgano SM, Giordano RA, Pober R. In vitro evaluation of low-temperature aging effects and finishing procedures on the flexural strength and structural stability of Y-TZP dental ceramics. *J Prosthet Dent* 2006;96:154-64.
26. Ban S, Sato H, Suehiro Y, Nakanishi H, Nawa M. Biaxial Flexure Strength and Low Temperature Degradation of Ce-TZP/ $Al_2O_3$  Nanocomposite and Y-TZP as



Dental Restoratives. *J Biomed Mater Res Part B: Appl Biomater* 2008;87:492-498.

27. Curtis AR, Wright AJ, Fleming GJP. The influence of surface modification techniques on the performance of a Y-TZP dental ceramic. *J Dent* 2005;1-12.
28. Bollen C, Lambrechts P, Quirynen M. Comparison of surface roughness of oral hard materials to the threshold surface roughness for bacterial plaque retention. *Dent Mater* 1997;13:258-269.
29. Jones CS, Billington RW, Pearson GJ. The in vivo perception of roughness of restorations. *Br Dent J* 2004;196:42-45.

Table 1. Chemical composition of yttria-stabilized zirconia.

Chemical component	Mol %
Zirconium dioxide ( $ZrO_2$ )	92.642
Yttrium oxide ( $Y_2O_3$ )	5.3
Hafnium oxide ( $HfO_2$ )	1.78
Aluminum oxide ( $Al_2O_3$ )	0.253
Others	0.025

Table 2. Material specifications of yttria-stabilized zirconia.

Specification	Value
Density ( $\rho$ )	6.05 g/cm <sup>3</sup>
Thermal expansion coefficient (TEC)	10 X 10 <sup>-6</sup> K <sup>-1</sup>
Flexural strength	1200 MPa
Fracture toughness ( $K_{IC}$ )	8 MN/m <sup>(1/2)</sup>
Modulus of elasticity (E)	210 GPa
Grain size	0.35 $\mu$ m
Vickers hardness (HV 10)	1200 Hv
Melting point	2680 °C
Shrinkage after sintering	20.8%

Table 3. The procedure for sample preparation simulating dental practice.

	Actual dental procedure	Sample preparation
Finishing	Universal silicone wheel (30-40 $\mu\text{m}$ )	35 $\mu\text{m}$ diamond lapping film using Exact-Micro-Grinding System
Color infiltration	Different colors of dyeing liquids	Dyed by A <sub>1</sub> color
Sintering	7.5 hour firing cycle at maximum temperature of 1530 °C to include heating and cooling stages	7.5 hour firing cycle at maximum temperature of 1530 °C to include heating and cooling stages
Grinding	Fine-diamond bur (30-40 $\mu\text{m}$ )	35 $\mu\text{m}$ diamond lapping film using Exact-Micro-Grinding System
Polishing	Rubber polishers (10 $\mu\text{m}$ ) with diamond polishing paste (1 $\mu\text{m}$ )	0.5 $\mu\text{m}$ diamond lapping film using Exact-Micro-Grinding System
Heat treatment without veneering porcelain application (800-900 °C)	910 °C in porcelain processing oven	910 °C in porcelain processing oven

Table 4. The number of samples and data points within each sample for all characterization procedures and flexural strength.

		Number of samples for each group (control and aged)	Number of data points within each sample
Surface	Ra (nm)	4	16
Roughness	RMS (nm)	4	16
Amount of Monoclinic (%)		4	1
Hardness (GPa)		4	97
Young's Modulus (GPa)		4	97
Zr		4	12
Elemental	O	4	12
Analysis	Y	4	12
(wt %)	H <sub>f</sub>	4	12
	Al	4	12
Flexural Strength (MPa)		28	1

Table 5. The mean and standard deviations of the control and aged samples for all characterization procedures and flexural strength.

		Mean $\pm$ SD (control samples)	Mean $\pm$ SD (aged samples)	<i>p</i> -value
Surface Roughness	Ra (nm)	12.23 $\pm$ 6.16	21.56 $\pm$ 13.39	0.017
	RMS (nm)	15.06 $\pm$ 7.23	27.45 $\pm$ 16.16	0.009
Amount of Monoclinic (%)		2.4 $\pm$ 0.6	21.0 $\pm$ 2.0	<0.001
Hardness (GPa)		16.56 $\pm$ 0.81	15.14 $\pm$ 1.83	<0.001
Young's Modulus (GPa)		275.68 $\pm$ 12.26	256.56 $\pm$ 21.56	<0.001
Elemental Analysis (wt %)	Zr	80.73 $\pm$ 3.18	80.68 $\pm$ 2.51	0.966
	O	11.41 $\pm$ 3.50	11.45 $\pm$ 2.47	0.974
	Y	4.43 $\pm$ 0.32	4.46 $\pm$ 0.43	0.848
	H <sub>f</sub>	3.09 $\pm$ 0.27	3.13 $\pm$ 0.31	0.739
	Al	0.305 $\pm$ 0.158	0.305 $\pm$ 0.239	0.999
Flexural Strength (MPa)		586.86 $\pm$ 71.47	578.31 $\pm$ 75.25	0.678

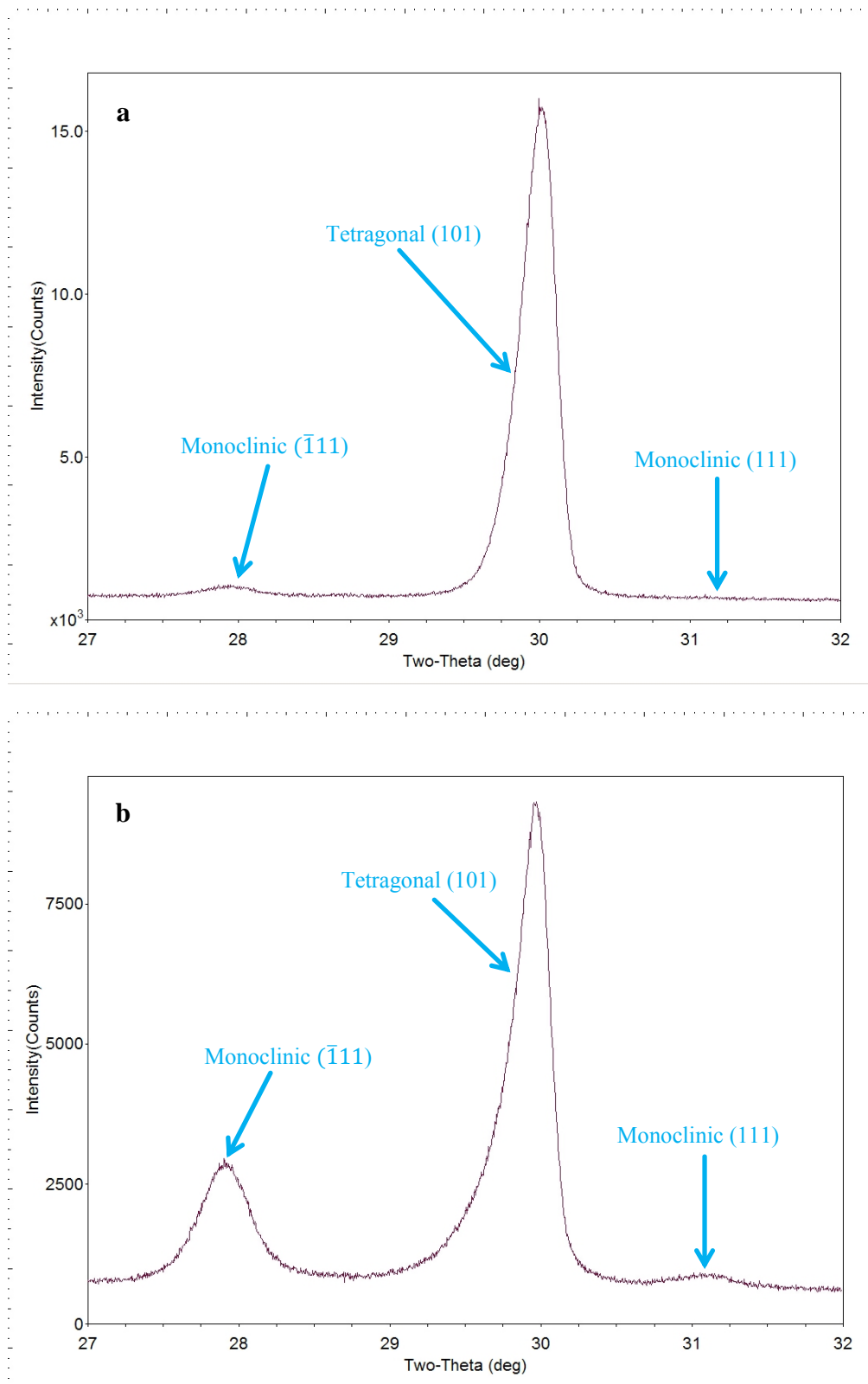


Figure 1. XRD analysis for the control (a) and aged (b) samples. Note a substantial increase of monoclinic phase ( $\bar{1}11$ ) for the aged samples compared with the control.

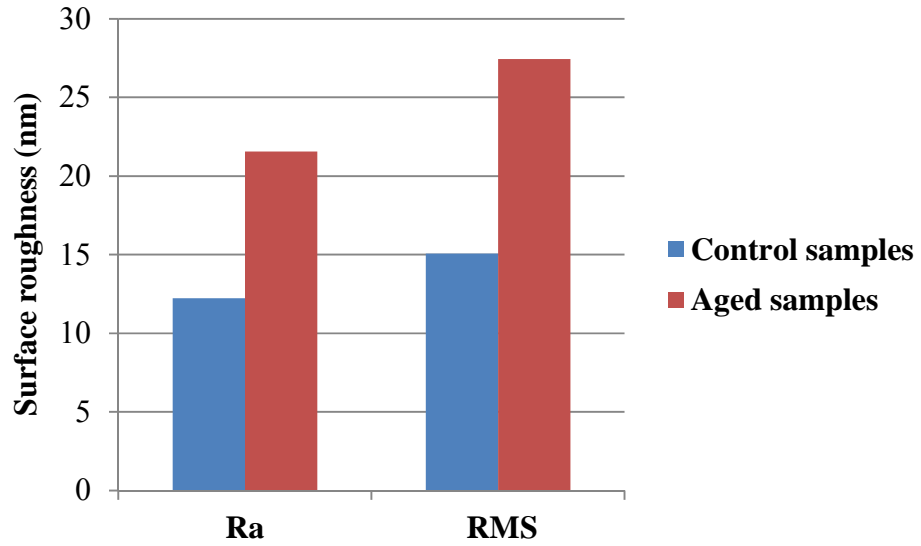


Figure 2. The surface roughness values for control and aged samples.

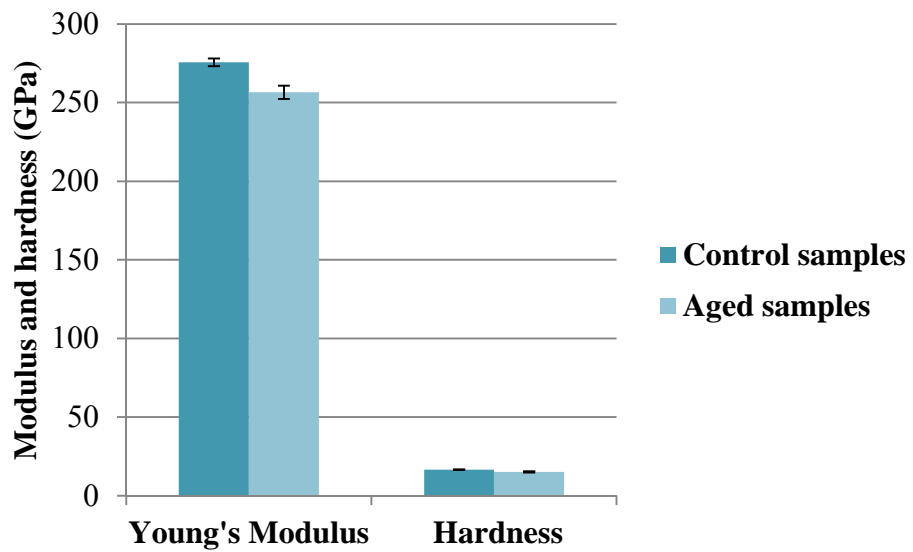


Figure 3. The surface hardness and modulus of elasticity values for control and aged samples.



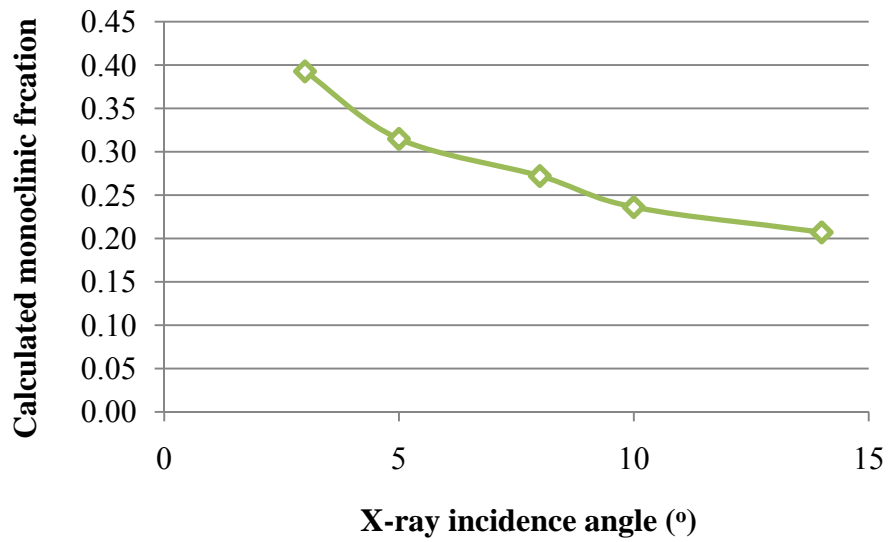


Figure 4. The fraction of monoclinic phase for different incident angles (14, 10, 8, 5, 3 degrees). The 3° incident angle had the highest monoclinic fraction while the 14° angle had the lowest monoclinic fraction.

4. EVALUATION OF THE OPTICAL PROPERTIES OF CAD-CAM GENERATED  
YTTRIA-STABILIZED ZIRCONIA AND GLASS-CERAMIC LAMINATE  
VENEERS

TARIQ F. ALGHAZZAWI, JACK E. LEMONS, PERNG-RU LIU, MILTON E. ESSIG,  
GREGG M. JANOWSKI

*Submitted to Journal of Prosthetic Dentistry*

Format adapted for dissertation

## Abstract

**Statement of problem.** The presence of undesirable tooth colors such as stains from age and tetracycline which extend into dentin often require significant tooth reduction for feldspathic porcelain (FP) laminate veneers for an opaque layer to mask stains and optimize the bonding of the restoration.

**Objectives.** The objectives were to investigate the effect of try-in paste (TP), composite resin abutment (CRA) colors, and veneer regions on the optical properties of feldspathic porcelain (FP), yttria-stabilized zirconia (Y-TZP), and IPS e.max<sup>®</sup> CAD HT (IEC) veneers.

**Methods.** A melamine tooth was prepared for a restoration, and a master cast was fabricated. The master die was scanned and a restoration designed using TDS. A total of 30 CRA were machined and 10 veneers were fabricated for each veneer material. Different colors of TP were used for optical effects on veneers where the colors of the veneers were measured in three regions for veneer materials, CRA and TP colors using a spectrophotometer. Results were analyzed using RM ANOVA and ANOVA were used to assess differences.

**Results.** The color difference for all the veneers was affected by TP and CRA colors at different regions. The Y-TZP veneer color co-ordinates ( $L^*$ :  $74.00 \pm 0.34$ ,  $a^*$ :  $0.094 \pm 0.203$ , and  $b^*$ :  $17.43 \pm 0.44$ ) were significantly different ( $p < 0.001$ ) from those of IEC veneers ( $L^*$ :  $70.15 \pm 0.23$ ,  $a^*$ :  $-0.694 \pm 0.073$ , and  $b^*$ :  $11.48 \pm 0.30$ ) and FP veneers ( $L^*$ :  $70.00 \pm 0.86$ ,  $a^*$ :  $-0.283 \pm 0.203$ , and  $b^*$ :  $13.86 \pm 1.08$ ). There was no difference between IEC for  $L^*$  and FP. Statistical difference ( $p < 0.001$ ) in color coordinates between three veneer materials for  $a^*$  and  $b^*$ .

Conclusion. The TP color affected the color difference for all veneer materials except the Y-TZP while there was no effect on the CRA color. The magnitude of color coordinates were changed as a function of TP color and veneer material.

Clinical Implications. Experience and available literature shows that when the highest translucency for laminate veneers is required to match adjacent teeth, IPS e.max<sup>®</sup> CAD HT laminate veneers will be the material of choice, and the color of the luting cement must be considered for all regions of the veneer. However, yttria-stabilized zirconia laminate veneers will be indicated for heavily-stained teeth, and the color of the luting cement is not a consideration for any region of the veneer.

### Introduction

When light interacts with a tooth, it may be reflected, scattered, or transmitted concurrent with the scattering of photons. The shade of dentin (the primary source of tooth color),<sup>1</sup> enamel structure (thickness and translucency), tooth dimension, and surface texture influence the optical properties of color, translucency, opalescence, and fluorescence.<sup>2</sup> Tooth color has been described by a combination of hue, chroma, and value. Translucency and intensity vary from the incisal region to the cervical region, with incisal, body, and cervical regions becoming progressively darker. This phenomenon is due to the decreasing thickness of the enamel from the incisal to the cervical regions as influenced by the underlying dentin.

The perceived color of an all-ceramic restoration is known to be affected by the shade of the restoring ceramic material, its thickness, and, if it is not significantly opaque, the color of the underlying material. The restoration's color is known to be affected by ceramic firing temperature,<sup>3</sup> the color of the prepared tooth,<sup>4</sup> translucency and thickness

of veneering porcelain,<sup>5-8</sup> luting agent,<sup>3,7</sup> surface glaze,<sup>7</sup> layering technique,<sup>8</sup> firing (temperature/time cycle),<sup>5,8,9</sup> extrinsic colorants, and type of all-ceramic substructure.<sup>10-12</sup>

Zirconia is often considered the material of choice in restorative dentistry because of its superior mechanical properties, but it is opaque due to density, elemental chemistry, high crystallinity<sup>13</sup> which results in a relatively high refractive index (2.1-2.2).<sup>14</sup> The esthetics of dental zirconia have been improved through the following procedures: infiltration (infiltration of machined restorations at the pre-sintered stage with chloride solutions of rare earth elements to produce cores of various shades),<sup>14</sup> pre-colored blocks (pre-colored at the microcrystalline powder state),<sup>14</sup> thinner coping thickness,<sup>15</sup> different colors for the liners,<sup>14</sup> choice of zirconia material,<sup>15,16</sup> and veneering technique.<sup>17,18</sup> If the zirconia restoration is extremely thin, then translucency and the final color might be a concern.<sup>15</sup> In this case, the color selection of luting cement (which is evaluated with pre-cementation try-in paste) as well as the region (cervical-body-incisal) will be more important. Therefore, zirconia laminate veneers have the potential to match the color of adjacent crowns and fixed partial dentures by using appropriate adjunctive procedures.

Laminate veneers have been shown to provide greater clinical longevities and enhanced esthetics as well as being more conservative compared to all-ceramic crowns. Minimal tooth preparation is required for these restorations, thus it is a challenge to achieve the optical properties of natural teeth with laminate veneers.<sup>19</sup> The laminate veneers are relatively weak and fragile, but their fracture resistance can be enhanced through CAD/CAM generated zirconia which has been shown to have greater strength than comparable feldspathic porcelain and glass-ceramic materials. Zirconia may offer more resistance to traumatic parafunctional occlusal forces and undesirable occlusal

schemes where traditional feldspathic laminate veneers cannot be used. The fragile nature of feldspathic porcelain laminate veneers has been shown to limit pre-cementation adjustment, whereas the strength of zirconia facilitates adjustment of the laminate veneer prior to cementation. The opaque nature of zirconia laminate veneers offers an advantage in masking undesirable tooth colors from age and tetracycline stains with minimal tooth reduction and thickness of restorative material. Research shows that traditional feldspathic porcelain requires more tooth reduction in order to have a thicker opaque layer, with or without intrinsic staining, to mask stains. Furthermore, increasing the thickness of traditional feldspathic porcelain veneers may impede photo-polymerization of the luting cement and compromise bonding to dentin.

The objectives of this study were to investigate the effect of try-in paste, composite resin abutment colors, and different veneer regions on the optical properties of feldspathic porcelain, CAD/CAM generated yttria-stabilized zirconia, and IPS e.max<sup>®</sup> CAD laminate veneers. The hypotheses were: (1) a significant color difference between the three regions for the three laminate veneer materials where yttria-stabilized zirconia laminate veneer would show a color difference at the cervical region, whereas IPS e.max<sup>®</sup> CAD would be affected in the body and cervical regions only, and feldspathic porcelain in all three regions; (2) a yttria-stabilized zirconia laminate veneer would mask a dark composite resin abutment; (3) opaque white try-in paste masks a dark composite resin abutment compared to other try-in paste colors; and (4) the color coordinates would be different for the veneer material and the value magnitude of the try-in paste.

## Materials and Methods

### *Fabrication of Master Cast*

A maxillary left lateral incisor (Model #R861, Columbia Dentoform Corporation, Long Island City, NY) was used for the veneer preparations and an index was fabricated prior to preparation to standardize the thickness of the laminate veneers. The incisal overlapped preparation (IOP) was defined as 0.5-mm facial reduction, and 1.5-mm incisal edge reduction. An impression of the prepared tooth with adjacent teeth was made with polyvinyl-siloxane impression material (Aquasil Ultra digit<sup>TM</sup> XLV Regular Set; Aquasil Monophase, DENSPLY International, York, PA). Type IV die stone (Jade Stone, Whip Mix Corp, Louisville, KY) was used to pour the impression in order to fabricate the master cast.

### *Fabrication of Composite Resin Abutments*

The master die was scanned and a restoration site designed using the TurboDent system (TDS) CAD/CAM technology (Pou-Yuen Technology Co., Ltd. No. 6, Fugong Rd., Fusing Township, Changhua County 506, Taiwan). A total of 30 composite resin abutments were machined using Paradigm MZ 100 blocks (3M ESPE, St. Paul, MN) with three different colors: A<sub>1</sub> (light color), A<sub>2</sub> (medium color), A<sub>3</sub> (dark color). Ten composite resin abutments were fabricated for each color.

### *Fabrication of Ceramic Laminate Veneers*

Ten (10) yttria-stabilized zirconia (Y-TZP) laminate veneers were fabricated using the TDS technique as described: an optical impression of the master die was taken with a laser scanner, and a restoration designed, and milled from partially sintered zirconia blocks, colored, sintered to have an overall 0.3 mm thickness. The Y-TZP was cov-

ered with the appropriate veneer porcelain (VITA VM9) according to the manufacturer's instructions.

Ten (10) glass-ceramic laminate veneers were machined from IPS e.max<sup>®</sup> CAD HT blocks (Ivoclar Vivadent Inc, Amherst, N.Y) using CEREC 3D CAD/CAM technology (Sirona Dental Systems LLC, Charlotte, NC). The CEREC powder (IPS Contrast Spray; Ivoclar Vivadent AG, Amherst, NY) was sprayed with opaquing powder to obtain a uniform layer, with an optimal thickness of 32  $\mu\text{m}$  to visualize both the internal line angles of the preparation and define the cavosurface margin.<sup>20</sup> An optical impression of the sprayed master die was made with a laser scanner and then designed according to the manufacturer's instructions with the veneers being milled from partially crystallized blocks, and then fully crystallized according to the manufacturer's instructions. Another ten (10) glass-ceramic laminate veneers were fabricated manually using feldspathic porcelain (Noritake Super Ex 3, Noritake Kizai Co., LTD., Nagoya, Japan) using conventional refractory techniques.

#### *Veneer Thickness*

Each veneer was measured at pre-designated regions using a precision caliper with an accuracy of 0.001 mm. The average thickness, composition, and grain size for each laminate veneer material are provided in Table 1.

#### *Color of Try-in Paste*

Four (4) different colors of try-in pastes: bleach XL, opaque white, transparent, and yellow were utilized for the assessment of the optical effects of the luting cement (Variolink<sup>®</sup> II, Ivoclar Vivadent, Schaan, Liechtstein) on the visual appearance and favorable color coordinates of all the laminate veneers.



A spectrophotometer (Crystaleye, Model CE 100-DC/US, Ver.1.3.1.0 Olympus, Japan) was used in this study to measure CIELAB color coordinates ( $L^*$ ,  $a^*$ ,  $b^*$ ). This device uses seven light emitting diodes (LEDs) as an illumination source with  $45/0^\circ$  geometry. The image-capture time was 0.2 s. The spectral data were acquired from the captured image of the laminate veneers. The reflectance magnitudes were measured from 400 to 700 nm wavelength with 1 nm intervals for pixel regions.

Color coordinates were measured in the incisal, body, and cervical regions of all laminate veneers with different combinations of laminate veneer material, composite resin abutment color, and try-in paste color along with three repeated readings for each combination. The color changes ( $\Delta E$ ) were calculated between the control laminate veneers (using composite resin abutment color ( $A_2$ ) with glycerin) and the experimental laminate veneers (using a combination of three composite resin abutment colors and four try-in paste colors) in the three tooth regions using the following equations:<sup>21</sup>

$$\Delta L = L_{\text{control}} - L_{\text{experiment}}$$

$$\Delta a = a_{\text{control}} - a_{\text{experiment}}$$

$$\Delta b = b_{\text{control}} - b_{\text{experiment}}$$

$$\Delta E = [(\Delta L)^2 + (\Delta a)^2 + (\Delta b)^2]^{1/2}$$

and  $\Delta E = 3.7$  was considered as the perceptibility threshold.<sup>22</sup>

The effect on the colors from the composite resin abutment and try-in paste on the color of the laminate veneer were interpreted in four different cases as shown in Table 2. Case (1): the color of veneers was not changed by the composite resin abutment color nor by the try-in paste color. Case (2): the color of the laminate veneers was changed by the try-in paste color only. Case (3): the color of the veneers was changed by both the com-

posite resin abutment and the try-in paste colors. Case (4): the color of veneers was changed by the composite resin abutment color, but the change was improved by the try-in paste color.

### *Statistical Analysis*

The mean and standard deviation ( $\pm$ SD) of  $\Delta E$  for each veneer material was calculated and averaged for the combinations of the composite resin abutment and try-in paste colors at each veneer region. Comparisons between tooth regions were made using repeated measures of the analysis of variance (RM ANOVA). When the RM ANOVA was significant, the Neuman-Keuls test was used to determine which comparisons were significantly different.

The color coordinates were measured and averaged for each try-in paste color (except transparent) for all laminate veneer materials at the body region of the composite resin abutment color ( $A_2$ ). Color coordinates were measured for the composite resin abutment color ( $A_2$ ) with glycerin at the body region of all laminate veneer materials in order to compare the color coordinates for each veneer material. The effects of try-in paste color and laminate veneer material on color coordinates were assessed using ANOVA. When the ANOVA was significant, Tukey's HSD test was used to determine which comparisons were significantly different. A  $p$ -value of  $<0.05$  was considered significant.

### Results

The data for color differences of all veneer materials is shown in Figure 1. These results combine different try-in paste colors (transparent, bleach XL, opaque, yellow), with different colors of composite resin abutment ( $A_1, A_2, A_3$ ) for different veneer regions

(cervical region, body region, incisal region) which is compared with the control color (composite resin abutment color (A<sub>2</sub>) with glycerin). Each variable will be addressed separately in the following paragraphs.

#### *Yttria-Stabilized Zirconia Laminate Veneers*

The different colors of the composite resin abutments did not cause any color change ( $\Delta E < 3.7$ ) for the yttria-stabilized zirconia laminate veneers when compared at any region. Furthermore, try-in paste color did not result in a color change for any region, when they were placed with different composite resin abutment colors (Figure 1a).

#### *IPS e.max<sup>®</sup> CAD Laminate Veneers*

There was no color change ( $\Delta E < 3.7$ ) for any region of the IPS e.max<sup>®</sup> CAD laminate veneers when they were seated on different colors of the composite resin abutment (Figure 1b). However, the opaque white try-in paste caused a substantial color change ( $\Delta E > 3.7$ ) when the laminate veneers were placed on the different composite resin abutment colors and compared at the three regions. Furthermore, bleach XL try-in paste caused a color change ( $\Delta E > 3.7$ ) when the laminate veneers were placed on the composite resin abutments with A<sub>1</sub> color only when comparing the three regions. However, yellow try-in paste did not cause any color change ( $\Delta E < 3.7$ ) when the laminate veneers were placed on different composite resin abutment colors at the three regions. There was a higher effect of opaque white try-in paste on the color change of IPS e.max<sup>®</sup> CAD laminate veneers when compared to feldspathic porcelain at the body and incisal regions.

### *Feldspathic Porcelain Laminate Veneers*

There was a color change ( $\Delta E > 3.7$ ) at the cervical region of the feldspathic porcelain laminate veneers when they were placed on the composite resin abutments with A<sub>1</sub> color (Figure 1c), but the color change was decreased by the use of yellow try-in paste ( $\Delta E < 3.7$ ). A large color change occurred at each region when the laminate veneers were seated on different colors of composite resin abutment using the opaque white try-in paste. There was a color change at the cervical region only when the laminate veneers were seated with bleach XL try-in paste on the composite resin abutment with A<sub>1</sub> color, but there was no color change at any region when the yellow try-in paste was used with the different composite resin abutment colors.

### *Relationship Between Color Change and Ceramic Thickness (Different Regions)*

The color change magnitudes ( $\Delta E$ ) were averaged for combinations of different composite resin abutment and try-in paste colors for each laminate veneer material as shown in Figure 2. It should be noted that the feldspathic porcelain veneers were significantly thinner than IPS e.max<sup>®</sup> CAD and yttria-stabilized zirconia laminate veneers. There was a statistical difference ( $p < 0.001$ ) in the value magnitude of  $\Delta E$  between the three regions for each laminate veneer material with an increase of color change from the incisal region to the cervical region except between the cervical region ( $\Delta E = 4.053 \pm 2.862$ ) and the incisal region ( $\Delta E = 4.153 \pm 2.642$ ) for IPS e.max<sup>®</sup> CAD laminate veneers. There was a higher magnitude of  $\Delta E$  at each region of the IPS e.max<sup>®</sup> CAD veneers compared with yttria-stabilized zirconia and feldspathic porcelain veneers except at the cervical region ( $\Delta E = 4.053 \pm 2.862$ ) of IPS e.max<sup>®</sup> CAD veneers compared with feldspathic porcelain veneers ( $\Delta E = 4.640 \pm 3.388$ ).

### *Effect of Different Try-in Paste Colors on the Color Coordinates*

As the color of the try-in paste color changed from yellow to bleach XL to opaque white, a significant reduction ( $p < 0.001$ ) in the value  $L^*$  (yellow < bleach < white) as obtained for all laminate veneer materials, as illustrated in Table 3. However, the values of  $a^*$  varied for different veneer materials (yttria-stabilized zirconia: white < bleach = yellow, IPS e.max<sup>®</sup> CAD: white < bleach < yellow, feldspathic porcelain: white < bleach = yellow) as well as  $b^*$  values (yttria-stabilized zirconia: yellow = bleach < white, IPS e.max<sup>®</sup> CAD: white = bleach < yellow, feldspathic porcelain: white < yellow).

### *Effect of Different Laminate Veneer Materials on the Color Coordinates*

The color coordinates were measured at composite resin abutment color ( $A_2$ ) at the body region for all veneer materials as shown in Table 4. Yttria-stabilized zirconia laminate veneers were the highest ( $L^* = 74.00 \pm 0.34$ ), but there was no significant difference ( $p > 0.05$ ) in the  $L^*$  value between IPS e.max<sup>®</sup> CAD ( $70.15 \pm 0.23$ ) and feldspathic porcelain ( $70.00 \pm 0.86$ ) laminate veneers. IPS e.max<sup>®</sup> CAD laminate veneers had the lowest value of  $a^*$  ( $-0.694 \pm 0.073$ ) while it was larger for yttria-stabilized zirconia ( $0.094 \pm 0.203$ ) compared with feldspathic porcelain ( $-0.283 \pm 0.203$ ) laminate veneers. Yttria-stabilized zirconia laminate veneers had the highest  $b^*$  coordinate ( $b^* = 17.43 \pm 0.44$ ) while IPS e.max<sup>®</sup> CAD showed the lowest  $b^*$  coordinate ( $11.48 \pm 0.30$ ) for laminate veneers.

## Discussion

### *Effect of Composite Resin Abutment Color on the Color Difference of Laminate Veneers*

There was no measured effect from the composite resin abutment color on the final color of the laminate veneers using transparent try-in pastes for any region except for

feldspathic laminate veneers at the cervical region which were affected by the composite resin abutment color ( $A_1$ ). Thus, the hypothesis that the opaque white would be the best material to mask dark composite resin abutment is generally rejected. The color shifted using yellow try-in paste, which was the result of the thin ceramic (0.45 mm) at the cervical region. The composite resin abutment color ( $A_3$ ) in the present study was not dark enough to cause a color shift on the overall color of all laminate veneers.

*Effect of Veneer Region (Ceramic Thickness) on the Color Difference of Laminate Veneer*

As the ceramic thickness was increased from the cervical region to the incisal region for feldspathic porcelain and yttria-stabilized zirconia laminate veneers, the color difference decreased except for the cervical and body regions of the yttria-stabilized zirconia veneers. This phenomenon can be explained by an increase of incident light absorption at a thicker region that reflects a reduced quantity of light reflected. These results were in agreement with Chaiyabutr et al.<sup>23</sup> who reported that as the ceramic thickness is increased (from 1.0 to 2.5 mm), the color difference was decreased for IPS e.max<sup>®</sup> CAD LT. However, for IPS e.max<sup>®</sup> CAD veneers, the body region was more affected than other regions, and the incisal region was more affected more than the cervical region. This result was due to the different ceramic thicknesses which were caused by over-milling on the intaglio surface of the IPS e.max<sup>®</sup> CAD veneers more on the body region than other regions. They were fabricated through machining and no layering of veneering porcelain was involved when compared to yttria-stabilized zirconia laminate veneers. There was no consistent relationship between the color difference and ceramic thickness so the null hypothesis was rejected.

The color difference of the body and incisal regions of IPS e.max<sup>®</sup> CAD veneers were more affected than feldspathic porcelain even though the feldspathic porcelain veneers were thinner (0.54 mm) than the IPS e.max<sup>®</sup> CAD veneers (0.85 mm). IPS e.max<sup>®</sup> CAD veneers had a higher magnitude of color change than yttria-stabilized zirconia veneers with similar thickness associated with presence of a glassy phase. However, difference in the thickness between feldspathic porcelain and yttria-stabilized zirconia veneers (Figure 2) creates an ambiguity related to interpretation in the color difference or might be due to opacity of yttria-stabilized zirconia itself. It was difficult to standardize the thicknesses of the laminate veneers when they were fabricated with different techniques and the interpretation of color difference of different materials cannot be tested with standardized flat specimens. Thus testing must be done on restorations not only for simulation of the clinical situation, and it is known that also the optical properties are affected by surface texture.<sup>24</sup>

#### *Effect of Try-in Paste Color on the Color Difference of Laminate Veneer*

The color differences for the yttria-stabilized zirconia laminate veneers were low (0.7-1.5) and were lower than the 3.7 perceptible threshold. These results were not affected by any color of the try-in paste at any region, which supports that the yttria-stabilized zirconia veneers were completely opaque at this thickness so the null hypothesis was rejected. Other studies have shown that there was a higher color difference obtained for different types of zirconia such as 1.99-2.89 for DC-Zirkon,<sup>11</sup> 1.8-3.6 for Digident Digizon,<sup>18</sup> 2.1-3.6 for Vita 2000 YZ cubes,<sup>18</sup> 0.9-2.1 for Katana.<sup>25</sup> This difference was attributed to different brands of zirconia with minor structural and dimensional dif-

ferences in the grains and grain boundaries, which yield higher levels of light absorption and scattering, rather than a direct effect from the grain size.<sup>26</sup>

Dozic et al.<sup>27</sup> reported that the overall color of 0.6 mm Empress laminate veneers was not influenced by different shades of resin cement which was not effective in creating color shifts. This was explained by the limited cement thickness (30  $\mu\text{m}$ ). In the present study, the final color of the IPS e.max<sup>®</sup> CAD and feldspathic porcelain veneers was affected more by opaque white than bleach try-in paste in comparable thicknesses (30-50  $\mu\text{m}$ ) so the null hypothesis was accepted.

#### *Effect of Color Coordinates ( $L^*$ $a^*$ $b^*$ ) on the Color of Try-in Paste*

The color coordinates of the laminate veneers were affected by a different value of try-in paste color so the null hypothesis was accepted. The color coordinates were higher (higher  $L^*$ ), but  $a^*$  and  $b^*$  varied (Table 3). This result indicated that the  $L^*$  of the try-in paste overcame the optical properties imparted by different veneer materials to cause constant  $L^*$  changes and that they have a direct influence on the overall color of the laminate veneers. Therefore, the overall color of the laminate veneer can be changed with different colors of try-in paste in order to have a minimal  $\Delta E$  with adjacent natural teeth, and thereby have the best color match. This finding was not in agreement with Azer et al.<sup>28</sup> who reported that when comparing different shades of composite resin core material or resin luting agents, there was no statistically significant difference found for CIE  $L^*a^*b^*$  color parameters between the various all-ceramic specimen combinations regarding color change. This can be explained by the magnitude of thick specimens (1 mm). Shokry et al.<sup>29</sup> demonstrated that increasing the ceramic thickness reduced the brightness and increased the red and yellowish appearance of ceramic specimens.



### *Clinical Significance*

The results in this study showed different color coordinates (Table 4) for different veneer materials, so the null hypothesis was accepted. The IPS e.max<sup>®</sup> CAD was the most translucent material because it showed the highest color difference even though the veneers were thicker than feldspathic porcelain, it was more blue color ( $b^* = 11.48 \pm 0.30$ ) compared with feldspathic porcelain ( $b^* = 13.86 \pm 1.08$ ). The color coordinates of the teeth should be measured before preparation, and the appropriate material selected in order to match the color coordinates of natural teeth. Furthermore, the shade of the prepared tooth (dentin) should be selected and replicated as closely as possible, using a tooth colored master die when the final restoration is fabricated. The color difference between the abutment and prepared tooth should be corrected by the color of the luting cement for feldspathic porcelain and IPS e.max<sup>®</sup> CAD veneers. The opacity of yttria-stabilized zirconia veneers, as shown in the present study, is advantageous for masking dark substrates. The color difference between the yttria-stabilized zirconia core and the adjacent natural tooth should be reduced through layering techniques for the veneering porcelain. The use of a spectrophotometer to measure color coordinates and calculating the color difference to determine the magnitude of value decrease showed that a modification of the veneering porcelain can be done in order to produce minimum color difference with adjacent teeth and therefore to have an overall esthetic restoration that matches any adjacent natural teeth.<sup>27,30</sup>

## Conclusions

Recognizing some limitations of this study design, this study leads to following conclusions:

1. The underlying color of the tested try-in pastes affected the color difference ( $\Delta E > 3.7$ ) for different regions for IPS e.max<sup>®</sup> CAD (three regions) and feldspathic laminate veneers (cervical and body region).
2. The IPS e.max<sup>®</sup> CAD laminate veneers were affected more by try-in paste color than feldspathic porcelain laminate veneers which was associated with higher glass content.
3. The yttria-stabilized zirconia laminate veneers were not affected by the color of the try-in paste, or the composite resin abutment color which was associated with relative opaqueness.
4. There was no effect of the color of the composite resin abutment on the overall color of all laminate veneers, except at the cervical region for feldspathic porcelain laminate veneers
5. There was an effect of different colors of try-in paste on the color coordinates of the overall color for all the laminate veneers in which  $L^*$  was increased while  $a^*$  and  $b^*$  varied.
6. The yttria-stabilized zirconia laminate veneers were brighter (higher  $L^*$ ), yellowish (higher  $b^*$ ), and reddish (higher  $a^*$ ) compared to the IPS e.max<sup>®</sup> CAD and feldspathic porcelain laminate veneers.

7. The IPS e.max<sup>®</sup> CAD laminate veneers showed the same brightness as feldspathic porcelain laminate veneers, but was more greenish (lower a\*) and bluish (lower b\*) than the feldspathic porcelain laminate veneers.

## References

1. Joiner A. Tooth colour: A review of the literature. *J Dent* 2004;32:3-12.
2. Yu B, Ahn JS, Lee YK. Measurement of translucency of tooth enamel and dentin. *Acta Odontol Scand* 2009;67:57-64.
3. Li Q, Yu H, Wang YN. Spectrophotometric evaluation of the optical influence of core build-up composites on all-ceramic materials. *Dent Mater* 2009;25:158-65.
4. Li Q, Yu H, Wang YN. Spectrophotometric evaluation of the optical influence of core build-up composites on all-ceramic materials. *Dent mater* 2009;25:158-165.
5. Ozturk O, Uludag B, Usumez A, Sahin V, Celik G. The effect of ceramic thickness and number of firings on the color of two all-ceramic systems. *J Prosthet Dent* 2008;100:99-106.
6. Chen YM, Smales RJ, Yip K, Sung WJ. Translucency and biaxial flexural strength of four ceramic core materials. *Dent mater* 2008;24:1506-1511.
7. Denissen H, Dozic A, Waas M, Feilzer A. Effects of 5 manipulative variables on the color of ceramics used for computer-generated restorations. *Quintessence Int* 2007;38:401-408.
8. Sailer I, Holderegger C, Jung RE, Suter A, Thievent B, Pietrobon N, Gebhard W, Hammerle CH. Clinical study of the color stability of veneering ceramics for zirconia frameworks. *Int J Prosthodont* 2007;20:263-269.
9. Souza FC, Casemiro LA, Garcia LF, Cruvinel DR. Color stability of dental ceramics submitted to artificial accelerated aging after repeated firings. *J Prosthet Dent* 2009;101:13-18.
10. Lee YK, Cha HS, Ahn JS. Layered color of all-ceramic core and veneer ceramics. *J Prosthet Dent* 2007;97:279-86.
11. Ozturk O, Uludag B, Usumez A, Sahin V, Celik G. The effect of ceramic thickness and number of firings on the color of two all-ceramic systems. *J Prosthet Dent* 2008;100:99-106.
12. Uludag B, Usumez A, Sahin V, Eser K, Ercoban E. The effect of ceramic thickness and number of firings on the color of ceramic systems: an in vitro study. *J Prosthet Dent* 2007;97:25-31.
13. Heffernan MJ, Aquilino SA, Diaz-Arnold AM, Haselton DR, Stanford CM, Vargas MA. Relative translucency of six all-ceramic systems. Part II: core and veneer materials. *J Prosthet Dent* 2002;88:10-5.

14. Shah K, Holloway JA, Denry IL. Effect of coloring with various metal oxides on the microstructure, color, and flexural strength of 3Y-TZP. *J Biomed Mater Res B Appl Biomater* 2008;87:329-37.
15. Baldissara P, Llukacej A, Ciocca L, Valandro FL, Scotti R. Translucency of zirconia copings made with different CAD/CAM systems. *J Prosthet Dent* 2010;104:6-12.
16. Chen YM, Smales RJ, Yip KH, Sung WJ. Translucency and biaxial flexural strength of four ceramic core materials. *Dent Mater* 2008;24:1506-11.
17. Luo XP, Zhang L. Effect of Veneering Techniques on Color and Translucency of Y-TZP. *J Prosthodont* 2010;19:465-470.
18. Lim HN, Yu B, Lee YK. Spectroradiometric and spectrophotometric translucency of ceramic materials. *J Prosthet Dent* 2010;104:239-246.
19. Vichi A, Ferrari M, Davidson CL. Color and opacity variations in three different resin-based composite products after water aging. *Dent Mater* 2004;20:530-4.
20. Mormann WH. International symposium on computer restorations. Quintessence Publishing Co, Inc. 1991.
21. Knispel G. Factors affecting the process of color matching restorative materials to natural teeth. *Quintessence Int* 1991;22:525-31.
22. Johnston WM, Kao EC: Assessment of appearance matches by visual observation and clinical colorimetry. *J Dent Res* 1989;68:819-822.
23. Chaiyabutr Y, Kois JC, LeBeau D, Nunokawa G. Effect of abutment tooth color, cement color, and ceramic thickness on the resulting optical color of a CAD/CAM glass-ceramic lithium disilicate reinforced crown. *J Prosthet Dent* 2011;105:83-90.
24. Wang H, Xiong F, Zhenhua L. Influence of varied surface texture of dentin porcelain on optical properties of porcelain specimens. *J Prosthet Dent* 2011;105:242-248.
25. Chang J, Silva JD, Sakai M, Kristiansen J, Nagai SI. The optical effect of composite luting cement on all ceramic crowns. *J Dent* 2009;37:937-943.
26. Casolco SR Jr, Xu J, Garay JE. Transparent/translucent polycrystalline nanostructured yttria stabilized zirconia with varying colors. *Scr Mater* 2008;58:516-9.

27. Dozic A, Tsagkari M, Khashayar G, Aboushelib M. Color management of porcelain veneers: Influence of dentin and resin cement colors. *Quintessence Int* 2010;41:567-573.
28. Azer SS, Ayash GM, Johnston WM, Khalil MF, Rosenstiel SF. Effect of esthetic core shades on the final color of IPS Empress all-ceramic crowns. *J Prosthet Dent* 2006;96:397-401.
29. Shokry TS, Shen C, Elhosary MM, Elkhodary AM. Effect of core and veneer thicknesses on the color parameters of two all-ceramic systems. *J Prosthet Dent* 2006;95:124-9.
30. Yoshida A, Miller L, Silva JD, Nagai SI. S Spectrophotometric Analysis of Tooth Color Reproduction on Anterior All-Ceramic Crowns: Part 2: Color Reproduction and Its Transfer from In Vitro to In Vivo. *J Esthet Restor Dent* 2010;22:53-65.

Table 1. The characteristics and the average thickness at each region of laminate veneer materials.

	Average veneer mean thickness in mm ( $\pm$ SD)			Composition	Grain size
	Cervical region	Body region	Incisal region		
Ytria-stabilized zirconia	0.87 $\pm$ 0.06	0.88 $\pm$ 0.09	0.94 $\pm$ 0.08	ZrO <sub>2</sub> (92.6 mol%), Y <sub>2</sub> O <sub>3</sub> (5.3 mol%), HfO <sub>2</sub> (1.78 mol%), Al <sub>2</sub> O <sub>3</sub> (0.25 mol%), others (0.025 mol%)	0.35 $\mu$ m
IPS e.max <sup>®</sup> CAD HT	0.84 $\pm$ 0.08	0.95 $\pm$ 0.07	0.76 $\pm$ 0.05	SiO <sub>2</sub> (57-80 wt%), Li <sub>2</sub> O (11-19 wt%), K <sub>2</sub> O (0-13 wt%), P <sub>2</sub> O <sub>5</sub> (0-11 wt%), ZrO <sub>2</sub> (0-8 wt%), ZnO (0-8 wt%), other and coloring oxides (0-12 wt%)	Platelet-shaped crystals is in the range of 0.2 to 1.0 $\mu$ m
Feldspathic porcelain	0.45 $\pm$ 0.05	0.54 $\pm$ 0.08	0.63 $\pm$ 0.09	SiO <sub>2</sub> (64.5%), Al <sub>2</sub> O <sub>3</sub> (14.4%), CaO (<1%), MgO (<1%), K <sub>2</sub> O (8.7%), Na <sub>2</sub> O (9.2%), Li <sub>2</sub> O (<1%)	26.4 $\mu$ m

Table 2. Interpretation of color change on the laminate veneers according to composite resin abutment color or try-in paste color.

Case	Color of try-in paste	$\Delta E$	The effect of color change on the laminate veneer
1	Transparent Yellow or bleach XL or opaque white	$\Delta E < 3.7$ $\Delta E < 3.7$	The color of laminate veneers was neither changed by composite resin abutment color nor by try-in paste color
2	Transparent Yellow or bleach XL or opaque white	$\Delta E < 3.7$ $\Delta E > 3.7$	The color of laminate veneers was changed by yellow or bleach XL or opaque white try-in paste colors (the higher value of $\Delta E$ , the higher color change)
3	Transparent Yellow or bleach XL or opaque white	$\Delta E > 3.7$ $\Delta E > 3.7$	The color of laminate veneers was changed by both composite resin abutment color and any color of yellow or bleach XL or opaque white try-in paste colors (the higher value of $\Delta E$ , the higher the color change)
4	Transparent Yellow or bleach XL or opaque white	$\Delta E > 3.7$ $\Delta E < 3.7$	The color of laminate veneers was changed by composite resin abutment color (the higher value of $\Delta E$ , the higher color change), but its change was decreased by any color of yellow or bleach XL or opaque white try-in paste colors (the lower value of $\Delta E$ , the better the improvement of color change)



Table 3. The effect of color coordinates (L\* a\* b\*) on increasing value of try-in paste (from yellow to opaque white) for the body region and composite resin abutment color (A<sub>2</sub>) of different laminate veneer materials.

Laminate veneer	Color coordinate	Yellow	Bleach XL	Opaque white	F- test	p -value	Color changes
Yttria-stabilized zirconia	L*	74.8±0.3	74.6±0.4	75.9±0.6	40.3	<0.001	yellow < bleach < white
	a*	0.108±0.190	0.024±0.199	-0.259±0.282	7.2	0.003	white < bleach = yellow
	b*	17.4±0.4	17.6±0.5	18.5±0.7	11.4	<0.001	yellow = bleach < white
IPS e.max <sup>®</sup> CAD HT	L*	70.9±0.2	73.8±0.5	79.8±0.8	695	<0.001	yellow < bleach < white
	a*	-0.529±0.084	-0.946±0.081	-1.180±0.096	144	<0.001	white < bleach < yellow
	b*	13.5±0.3	11.6±0.4	11.4±0.3	117	<0.001	white = bleach < yellow
Feldspathic porcelain	L*	70.5±0.7	72.1±0.8	77.6±1.7	106	<0.001	yellow < bleach < white
	a*	-0.180±0.226	-0.345±0.205	-0.714±0.226	15.5	<0.001	white < bleach = yellow
	b*	14.8±1.3	13.5±1.5	12.3±2.2	5.2	0.012	white < yellow

Table 4. The effect of color coordinates (L\* a\* b\*) on laminate veneer material for the body region and composite resin abutment color (A<sub>2</sub>) with glycerin.

	L*	a*	b*
Yttria-stabilized zirconia	74.00±0.34	0.094±0.203	17.43±0.44
IPS e.max <sup>®</sup> CAD HT	70.15±0.23	-0.694±0.073	11.48±0.30
Feldspathic porcelain	70.00±0.86	-0.283±0.203	13.86±1.08
F test	170	53.1	184
<i>p</i> -value	<0.001	<0.001	<0.001
Comment	Feldspathic porcelain = IPS e.max <sup>®</sup> CAD HT < yttria-stabilized zirconia	IPS e.max <sup>®</sup> CAD HT < Feldspathic porcelain < yttria-stabilized zirconia	IPS e.max <sup>®</sup> CAD HT < Feldspathic porcelain < yttria-stabilized zirconia

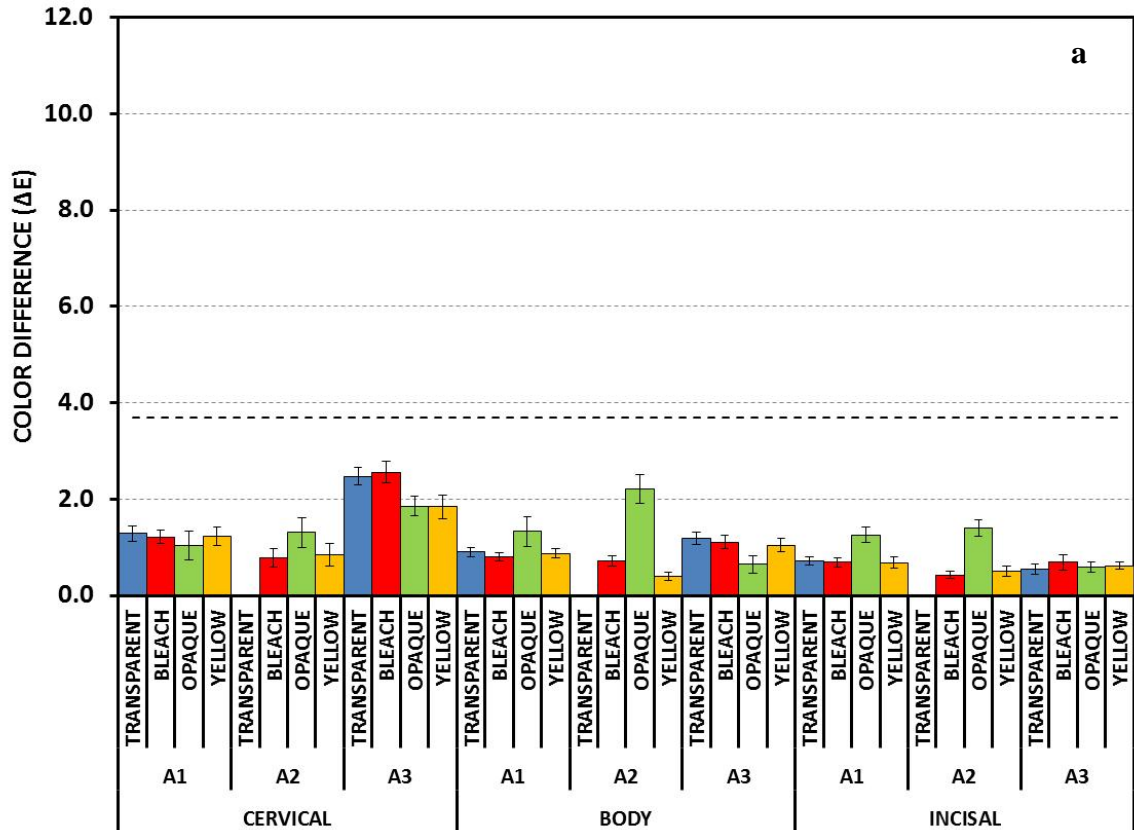
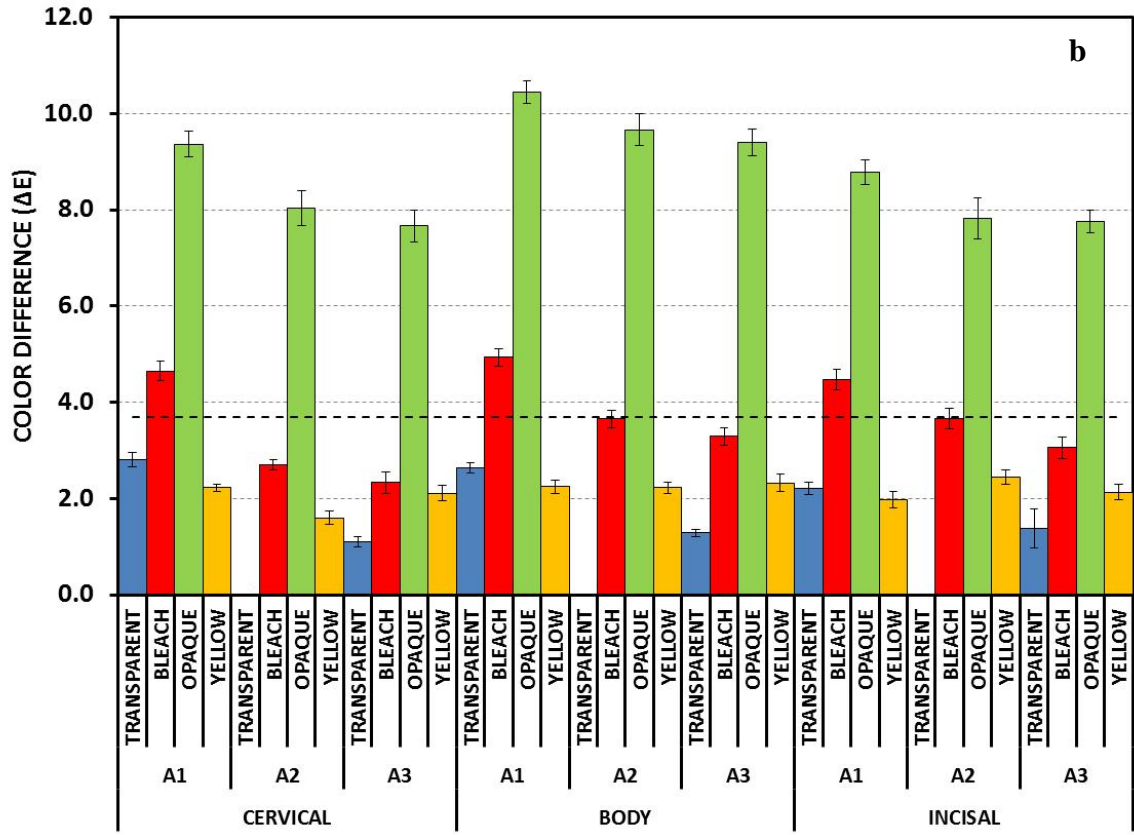
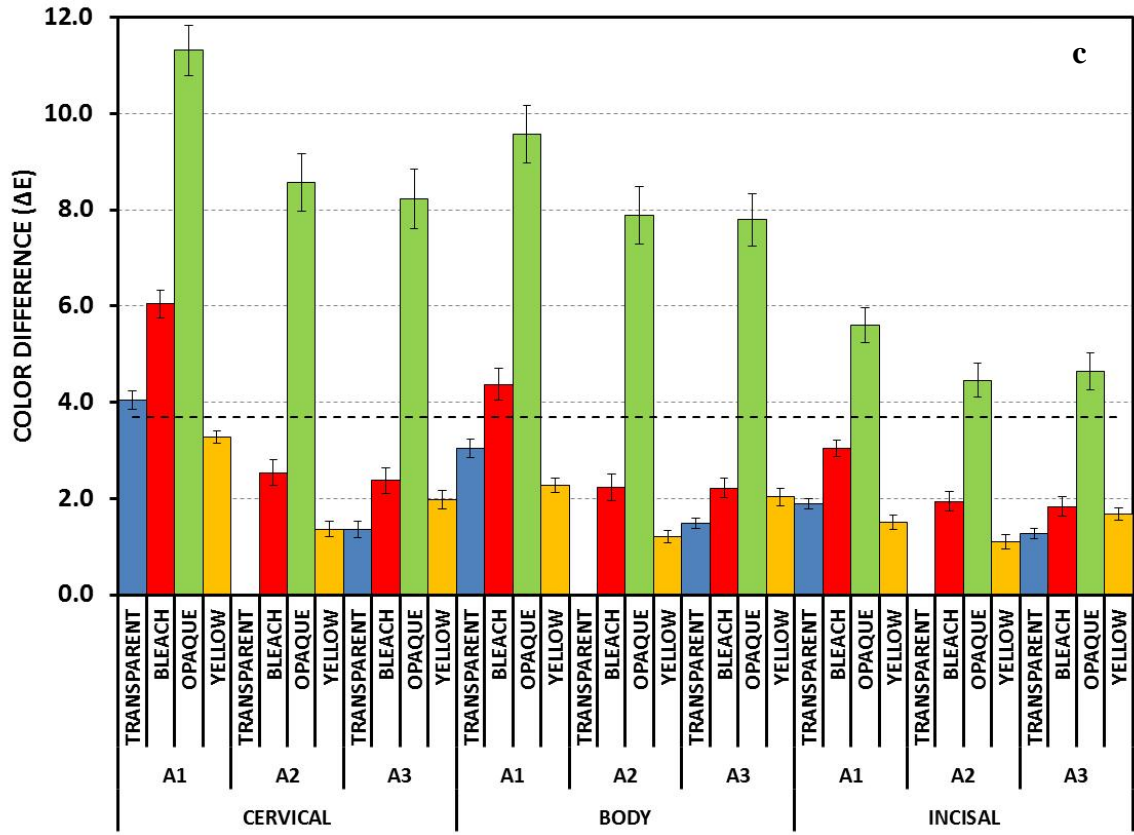


Figure 1. (a) Yttria-stabilized zirconia laminate veneers. (b) IPS e.max<sup>®</sup> CAD HT laminate veneers. (c) Feldspathic porcelain laminate veneers. The color change ( $\Delta E$ ) at the three veneer regions (cervical, body, incisal) with different composite resin abutments (A<sub>1</sub>, A<sub>2</sub>, A<sub>3</sub>) and try-in paste colors (transparent, bleach XL, opaque, yellow) compared to the control color (composite resin abutment color (A<sub>2</sub>) and glycerin). The perceptibility threshold ( $\Delta E$ ) is illustrated by a horizontal dotted line at 3.7.





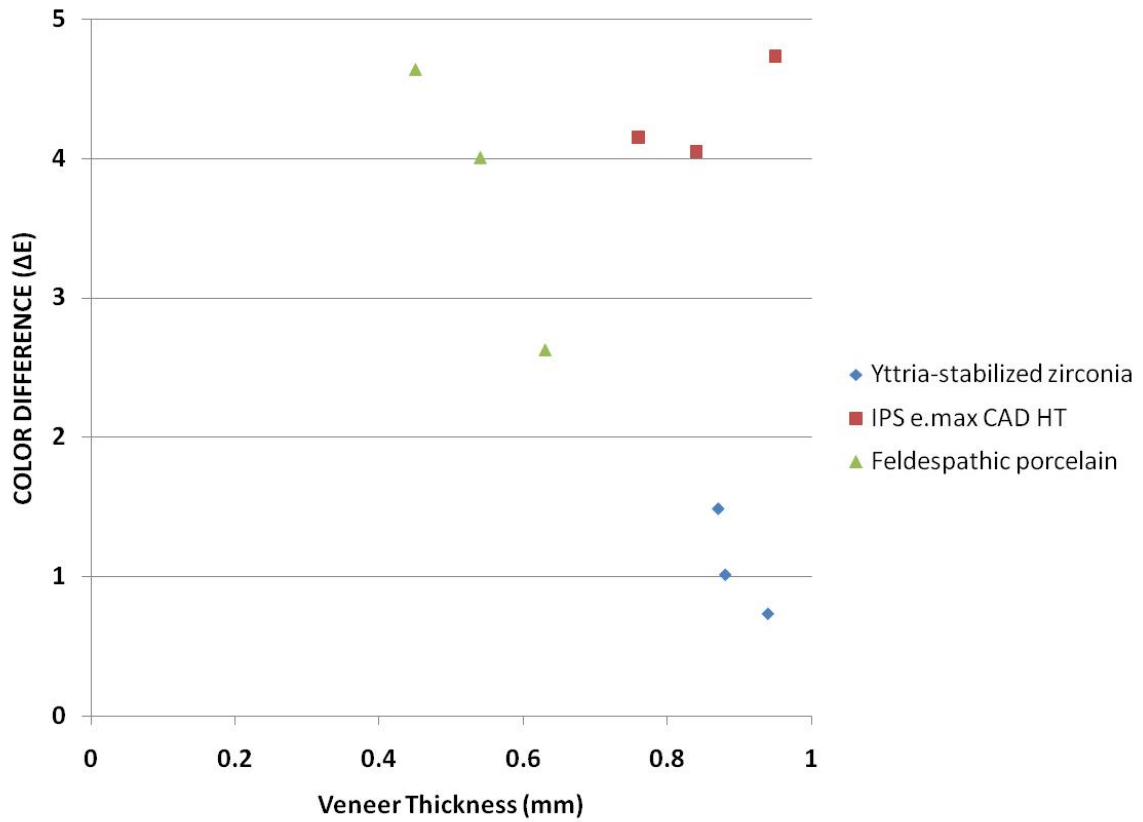


Figure 2. The effect of laminate veneer thickness from cervical region to incisal region on the color difference for yttria-stabilized zirconia, IPS e. max<sup>®</sup> CAD HT, and feldspathic porcelain materials.

5. THE FAILURE LOAD OF CAD-CAM GENERATED ZIRCONIA AND GLASS-  
CERAMIC LAMINATE VENEERS WITH DIFFERENT PREPARATION  
DESIGNS

TARIQ F. ALGHAZZAWI, JACK E. LEMONS, PERNG-RU LIU, MILTON E. ESSIG,  
GREGG M. JANOWSKI

*Submitted to Journal of Prosthetic Dentistry*

Format adapted for dissertation

## Abstract

**Objectives.** The effects of material (yttria stabilized zirconia, TZP, IPS e.max<sup>®</sup> CAD, IEC, and feldspathic porcelain, FP), design (incisal overlapped preparation, IOP, and three-quarter preparation, TQP), and fracture mode was correlated to failure load without thermocycling for laminate veneers supported by composite resin abutments.

**Methods.** A typodont tooth was prepared with two different preparation designs (IOP, TQP). Two master casts were fabricated and the master dies were scanned and designed to fabricate the composite resin abutments (30 for IOP and 30 for TQP). The Y-TZP, IEC and FP veneers were fabricated with 10 veneers for each preparation design. All the veneers were cemented, invested with auto-polymerizing resin, and tested in compression until failure. The t-test and one way ANOVA were used to assess differences.

**Results.** There was no statistical difference ( $p > 0.05$ ) in the preparation design on load for Y-TZP (IOP: 244 vs. TQP: 224 N) and IEC (IOP: 306 vs. TQP: 263 N) veneers.

However, there was a statistical difference in the load ( $p = 0.0177$ ) for FP veneers (IOP: 161 vs. TQP: 246 N) between IOP and TQP. There was no statistical difference in the load between the three veneer materials for each preparation design except between IEC (306 N) and FP (161 N) veneers for TQP.

**Conclusions.** Preparation design showed an influence on the failure load of FP veneers only. Yttria-stabilized zirconia laminate veneers were least likely to fracture but most likely to completely debond; feldspathic porcelain veneers exhibited the opposite characteristics.



## Introduction

Crown preparation involves major tooth structure removal (63-73%)<sup>1</sup> and may cause pulpal irritation, which may lead to irreversible pulpitis.<sup>2</sup> Laminate veneers are more conservative than crowns<sup>3</sup> and maintain the biomechanics of the original tooth with a stress distribution similar to a sound tooth with a success rate of approximately 93% over 15 years of clinical use.<sup>4</sup>

The most frequent failure modes associated with laminate veneers are fracture or debonding,<sup>4</sup> although the magnitude and angle of the load greatly influences the long-term success of laminate veneers.<sup>5</sup> Several studies indicate that stress concentrates at the adhesive interface between the luting cement and enamel.<sup>6,7</sup> The shear stress causes the veneer displace, causing a compressive stress in the weakest areas (incisal or gingival margin).<sup>8</sup> This occurrence can create microcracks which propagate and influence fracture or detachment of veneers.<sup>9</sup> Most fractures are caused by adhesive failure at the porcelain/cement interface by complete debonding or fracture of the veneer.<sup>5</sup> The porcelain is rigid and does not deform significantly during polymerization shrinkage of the composite resin cement, thereby creating residual stress at the interface.<sup>10</sup>

Fractures of laminate veneers represented 67% of total failures over a period of 15 years of clinical performance of such restorations.<sup>4,11</sup> Clinical observations of ceramic veneers showed that cohesive fracture of porcelain mainly occurred on the incisal edge because of a greater stress concentration in this area during function,<sup>12</sup> where compressive stresses are concentrated along the buccal side of the veneer close to the incisal margin.<sup>12,13</sup> Also fracture of laminate veneers has been shown to be affected by angle of load-

ing,<sup>14</sup> preparation design,<sup>14,15</sup> laminate veneer material,<sup>16</sup> mechanical thermal cycling,<sup>17</sup> and tooth location.<sup>18</sup>

Alumina laminate veneers with a 0.25 mm thickness (Procera AllCeram Nobel Biocare) were developed as an alternative to traditional porcelain laminate veneers to improve fracture strength and mask the discolored teeth.<sup>16</sup> However, a main drawback of alumina was stiffness ( $E = 418$  GPa) compared with enamel ( $E = 84.1$  GPa) and dentin ( $E = 18.6$  GPa) which was shown to affect the long-term clinical success of bonded laminate veneers.<sup>14</sup> When a shearing load was applied to an incisor, most of the deformation is distributed in the root structure on both the buccal and palatal side. Sorrentino et al.<sup>13</sup> reported that natural teeth restored with alumina laminate veneers ( $E = 418$  GPa) deformed like a rigid body with a higher strain in the cervical region and a lower strain in the body region. In contrast, feldspathic laminate veneers ( $E = 82$  GPa) resulted in a higher strain with lower stress in the crown body so the crown deformed under the applied load and transferred lower strains to the cervical area of root dentin. This behavior can be explained by the differences in stiffness between alumina and feldspathic porcelain materials.

Yttria-stabilized zirconia has a lower modulus ( $E = 210$  GPa), higher flexural strength (1200 MPa), and higher fracture toughness ( $8 \text{ MPa}\sqrt{\text{m}}$ ) than alumina. Zirconia laminate veneers can be milled very thin (0.2 to 0.3 mm) using CAD/CAM technology and offer several advantages in clinical cases such as a wide diastema or fractured teeth resulting from trauma or decay in which the lingual surface remains intact. When the lost tooth structure is large, a zirconia core can be used to support the veneering porcelain if over 2 mm thickness is required. Otherwise, the traditional feldspathic porcelain is con-

traindicated, and a crown restoration is the only option for treatment. Additionally, feldspathic laminate veneers have been reported to be contraindicated if traumatic para-functional occlusal forces occur or in clinical situations that develop loading stress during function such as cross bite and edge-to-edge occlusal relationships.<sup>19</sup> Zirconia laminate veneers may be a good substitute material because of superior mechanical properties. Traditional porcelain laminate veneers are fragile and, therefore, difficult to adjust and contour before cementation. The strength of zirconia allows for better handling capabilities that facilitate adjustment of the laminate veneer prior to cementation.

The opaque nature of zirconia laminate veneers has an advantage for masking undesirable tooth colors such as age-related discoloration and tetracycline stains with minimal tooth reduction and reduced thickness of restorative material. Traditional feldspathic porcelain often requires more tooth reduction for a sufficiently thick layer to mask stains which may also compromise bonding to dentin.<sup>20</sup> Furthermore, increasing the thickness of traditional feldspathic porcelain veneers may impede any photopolymerization of luting cements.

The objectives of this study were to: (1) compare the failure load without thermocycling of yttria stabilized zirconia, and IPS e.max<sup>®</sup> CAD veneers with feldspathic porcelain veneers supported by composite resin abutments with an elastic modulus close to tooth dentin; (2) evaluate the effect of incisal overlapped preparations and three quarter preparations relative to the failure load of different laminate veneer materials; and (3) determine the failure mode of all laminate veneers. The hypotheses were: (1) yttria-stabilized zirconia laminate veneers would have higher failure load than IPS e.max<sup>®</sup> CAD and feldspathic porcelain laminate veneers for the same preparation design; (2)

three quarter veneer preparations would have higher failure load than incisal overlapped preparations for the same laminate veneer material; and (3) yttria stabilized zirconia laminate veneers would fail by complete debonding while the IPS e.max<sup>®</sup> and feldspathic porcelain laminate veneers would fail by fracture rather than debonding.

## Materials and Methods

### *Fabrication of Master Cast*

A maxillary left lateral incisor (Model #R861, Columbia Dentoform Corporation, Long Island City, NY) was selected as a typical tooth to be restored using a veneer design. An impression was taken of the model tooth using a high precision condensation silicone (Zhermack, Marl, Germany) to obtain a mold for creating laminate veneers of the original form and shape. The tooth was prepared with an incisal overlapped preparation (IOP) with a 0.5 mm facial reduction and 1.5 mm incisal edge reduction. The first impression of the prepared tooth with adjacent teeth was made with polyvinyl-siloxane impression material (Aquasil Ultra digit<sup>TM</sup> XLV Regular Set; Aquasil Monophase, DENSPLY International, York, PA). The IOP was extended to break both the mesial and distal contacts and thereby develop a three quarter preparation (TQP). A second polyvinyl-siloxane impression was taken with the adjacent teeth, and both impressions were poured with type IV die stone (Jade Stone, Whip Mix Corp, Louisville, KY) to fabricate the first and second master casts.

### *Fabrication of Composite Resin Dies and Ceramic Laminate Veneers*

The first and second master dies were scanned and designed using the TurboDent system (TDS) CAD/CAM technology (Pou-Yuen Technology Co., Ltd. No. 6, Fugong Rd., Fusing Township, Changhua County 506, Taiwan). A total of 60 composite resin

abutments (30 abutments for IOP and 30 abutments for TQP) were machined using Paradigm MZ 100 blocks (3M ESPE, St. Paul, MN).

#### *Fabrication of Ceramic Laminate Veneers*

Twenty yttria-stabilized zirconia laminate veneers (10 veneers for IOP and 10 veneers for TQP) were fabricated using TDS. An optical impression of the master die was taken with a laser scanner and the restorations designed according to the manufacturer's instructions with the veneers being milled to a 0.3 mm thickness from partially sintered yttria-stabilized zirconia blocks, then sintered, and covered with the appropriate veneer porcelain (VITA VM9) according to manufacturer protocols. Twenty lithium disilicate glass-ceramic (IPS e.max<sup>®</sup> CAD, Ivoclar Vivadent Inc, Amherst, N.Y) laminate veneers were fabricated (10 veneers for IOP and 10 veneers for TQP) using CEREC 3D CAD/CAM technology (Sirona Dental Systems LLC, Charlotte, NC) with software version 3.10. An optical impression of the master die was taken and the restorations designed using the Biogeneric technique; the veneers were milled from partially crystallized blocks, and then fully crystallized according to the manufacturer instructions. Twenty feldspathic porcelain laminate veneers (Super Porcelain Ex-3, Noritake Kizai Co., LTD., Nagoya, Japan) were fabricated (10 veneers for IOP and 10 veneers for TQP) using a conventional laboratory refractory technique. All the veneers were measured using a caliper after fabrication of the IOP and TQP designs (Table 1). The composition, stiffness and flexural strength of yttria-stabilized zirconia,<sup>21</sup> IPS e.max<sup>®</sup> CAD,<sup>22</sup> and feldspathic porcelain<sup>23</sup> laminate veneers are provided in Table 2.

### *Fabrication of Specimens*

All the composite resin abutments were fixed in a buccal-lingual inclination angle of 135° between the long axis of the abutment and the horizontal plane of the abutment holder using a surveyor, and fixed in place by self-curing acrylic resin (Ortho-Jet, Lang) in the abutment holders. The abutments were embedded 2 mm below the cemento-enamel junction (CEJ) to simulate the clinical bone level, cleaned with 35% phosphoric acid (Ultra-Etch, Ultradent Products, Inc., South Jordan, UT) for 30 s, rinsed, and dried. Subsequently, the laminate veneers were cemented on the composite resin abutments to fabricate the test specimens (Table 3). Feldspathic porcelain and IPS e.max® CAD laminate veneers were bonded with the same procedure and luting agent (Variolink II; Ivoclar Vivadent, Amherst, NY) except for the etching time of hydrofluoric acid (60 s for feldspathic porcelain veneers and 20 s for e.max® CAD veneers). Yttria-stabilized zirconia laminate veneers do not have glass in their microstructure, so RelyX™ Unicem 2 with tribochemical silica-coating was selected for bonding the yttria-stabilized zirconia material as recommended in the literature.<sup>24</sup>

### *Loading to Failure*

Each specimen was mounted in the universal testing machine (Instron, model Apex T5000, Satec Systems Inc., Grove, PA). A polymeric material (0.2 mm thick) was placed between the flat punch (diameter of 4 mm) and the center of the incisal edge of the cemented laminate veneers to facilitate more even load distribution. The specimens were loaded at a crosshead speed of 0.5 mm/min until a sudden drop of the load was recorded.

### *Statistical Analysis*

The failure loads of 10 samples were averaged for each veneer material/preparation design, and mean and standard deviations calculated. The t-test was used to compare the failure load between the two preparation designs (IOP and TQP) for each veneer material, and one way ANOVA was used to compare the failure load between the three veneer materials. If the ANOVA test was significant ( $p < 0.05$ ), Tukey's HSD test was used to determine if veneer materials were significantly different.

### Results

#### *Effect of Preparation Design (IOP vs. TQP) on the Failure Load*

There was no statistical difference of the failure load ( $p > 0.05$ ) for the preparation design of yttria-stabilized zirconia (IOP: 244 vs. TQP: 224 N) and IPS e.max<sup>®</sup> CAD (IOP: 306 vs. TQP: 263 N) laminate veneers (Table 4). However, there was a statistical difference for the failure load ( $p = 0.0177$ ) of feldspathic porcelain veneers (IOP: 161 vs. TQP: 246 N) between the IOP and TQP designs. There was no statistical difference ( $p > 0.05$ ) for the failure load between the three veneer materials of each preparation design except between IPS e.max<sup>®</sup> CAD (306 N) and feldspathic porcelain (161 N) laminate veneers for TQP ( $p = 0.0058$ ).

#### *Failure Mode vs. Load of Laminate Veneers*

The laminate veneers failed in different modes involving fracture of the laminate veneer or complete debonding, chipping of porcelain and fracture of the composite resin abutment (Appendix). There was a correlation between failure load and fracture mode with different laminate veneer materials and preparation designs (IOP vs. TQP) as illustrated in Table 4.

*IPS e.max<sup>®</sup> CAD Laminate Veneers.* Fracture of the composite resin abutments were the main failure mode for IPS e.max<sup>®</sup> CAD veneers with an IOP design at a load of 369±73 N and TQP at a mean load of 280±96 N. Two laminate veneers with the IOP were fractured at the incisal region with a mean load of 259±9 N.

*Feldspathic Porcelain Laminate Veneers.* One veneer completely debonded at a lower load (77 N) for IOP compared with IPS e.max<sup>®</sup> CAD veneers (325±72 N). There were a greater number of fractures of the composite resin abutments with TQP (242±46 N) than with IOP (46±47 N). Feldspathic laminate veneers had the highest fractures (at the incisal region: 206±68 N for IOP and 261±53 N for TQP) as compared with IPS e.max<sup>®</sup> CAD (at the incisal region: 259±9 N for IOP). However, it was surprising that there were two fractures of composite resin abutments with the IOP at a very low load (46±47 N). The mode of failure for the veneers was fracture at the incisal region for IOP with a mean load of 206±68 N and fracture of the composite resin abutments for TQP at a mean load of 261±53 N.

*Yttria-Stabilized Zirconia Laminate Veneers.* The main failure mode of yttria-stabilized zirconia laminate veneers for the IOP design was fracture of the composite resin abutments at a mean load of 230±124 N while the failure mode of TQP was due to complete debonding at a mean load of 196±53 N. There was chipping of the veneering porcelain for two laminate veneers at a mean load of 276±20 N. An equal number of composite resin abutments fractured for the IOP and TQP designs, but there was a higher fraction of complete debonding for the TQP design. Yttria-stabilized zirconia laminate veneers showed the highest incidence of complete debonding when compared with IPS e.max<sup>®</sup> CAD and feldspathic porcelain materials (yttria-stabilized zirconia: 203±137 N



vs. e.max<sup>®</sup> CAD: 325±72 N for IOP, yttria-stabilized zirconia: 196±53 N vs. e.max<sup>®</sup> CAD: 236±33 N for TQP). There were no fracture failures of the laminate veneers with the TQP design as compared with the IOP design. The yttria-stabilized zirconia laminate veneers showed one fracture at the body region (a load of 163 N) as compared with e.max<sup>®</sup> CAD (two veneers fractured at a mean load of 259±9 N for IOP) and feldspathic porcelain veneers (seven veneers fractured at a mean load of 206±68 N for IOP and two veneers at a mean load of 261±53 for TQP).

## Discussion

### *Substrate Material*

The literature shows that use of extracted natural teeth as specimens more closely simulates clinical conditions than resin abutments. However, standardization of natural teeth is difficult because of age, anatomy, size, shape, storage time after extraction, and tooth fracture during loading due to differences in the elastic modulus that occur following extraction and storage in a thymol solution.<sup>17</sup> Tooth preparation along with variances in veneer dimensions that occur with free-hand preparation may result in variable depths of preparation and dentin exposure that can alter restoration bonding. Therefore, synthetic artificial abutments can be more accurately standardized. In the present study, composite resin abutments (Paradigm MZ 100) were used instead of extracted human teeth as a substrate for loading the laminate veneers because of having a closer elastic modulus (E = 12 GPa) to dentin (E = 18.6 GPa) than steel (E = 200 GPa).

### *Challenge of Veneer and Bonding to Resin Cement*

Retention of laminate veneers depends mainly on bonding, whereas tooth preparation design controls the retention of crowns and fixed partial dentures. Since zirconia has

no glass in its microstructure, the material cannot be appropriately etched by hydrofluoric acid, and thereby it does not produce micro-mechanical retention which affects the bond strength to resin cement.<sup>25</sup> Because of this, yttria-stabilized zirconia laminate veneers showed the highest incidence of complete debonding. In comparison, IPS e.max<sup>®</sup> CAD and feldspathic porcelain laminate veneers showed higher bond strength to resin cement because of the glass phase that was etched. However, there was a higher incidence of complete debonding for IPS e.max<sup>®</sup> CAD laminate veneers compared with feldspathic porcelain laminate veneers. This observation could be a result of a difference in the material particle size between IPS e.max<sup>®</sup> CAD (0.2 to 1.0  $\mu\text{m}$ ) and feldspathic porcelain (26.4  $\mu\text{m}$ ), also, the larger grain size results in a different surface roughness which contributes to the micro-mechanical retention.<sup>26, 27</sup> The composite resin abutment and luting agent (Variolink II bleach base) were the same for IPS e.max<sup>®</sup> CAD and feldspathic porcelain laminate veneers, but there were a greater number of complete debonding occurrences with IPS e.max<sup>®</sup> CAD laminate veneers. This observation was associated with a compromised adhesion between the luting agent and the intaglio surface of IPS e.max<sup>®</sup> CAD laminate veneers.

The TQP design resulted in more tooth preparation with a larger adhesive contact surface area between the veneer and the composite resin abutment. This resulted in a higher retention for TQP than IOP.<sup>28</sup> Furthermore, there were more instances of complete debonding for yttria-stabilized zirconia and IPS e.max<sup>®</sup> CAD for the TQP design than the IOP design. This observation could be due to the strength of the laminate veneers with the TQP design and the distribution of the applied load to the weak interface between the

luting cement and yttria-stabilized zirconia and IPS e.max<sup>®</sup> CAD as compared with feldspathic porcelain.

*Effect of Preparation Design within Laminate Veneer Material*

There was no effect of preparation design on the failure load for zirconia laminate veneers (even through there is difference in the veneer thickness: IOP = 0.9 mm and TQP = 1.1 mm). The null hypothesis that the three quarter veneer preparations would have a higher failure load than the incisal overlapped preparation. This hypothesis was rejected because of the higher flexural strength (1200 MPa) and poor bonding to the resin cement. There were no veneer fractures with the TQP design which was associated with reduced stress on the material relative to the IOP design, whereas the veneers failed by complete debonding.<sup>28</sup>

There was no effect of preparation design (IOP vs. TQP) on the failure load for IPS e.max<sup>®</sup> CAD laminate veneers, so the null hypothesis that the three quarter veneer preparations would have a higher failure load than the incisal overlapped preparation was rejected because e.max<sup>®</sup> CAD laminate veneers would have a medium-high flexural strength (360 MPa). There were no veneer fractures with the TQP which for this design was associated with a higher fracture strength than IOP. Furthermore, the cemented veneer-resin cement-composite resin abutment acts as a monoblock, which would influence the veneers to fail due to fracture of the composite resin abutments for the TQP and IOP designs. Therefore, the null hypothesis that IPS e.max<sup>®</sup> laminate veneers would fail and fracture within the veneer itself was rejected.

There was an effect of preparation design (IOP vs. TQP) on the failure load for feldspathic porcelain laminate veneers so the null hypothesis that feldspathic porcelain

laminate veneers would fail in veneer fracture was accepted. This was because of lower flexural strength (111 MPa) and bonding to resin cement. This resulted in more incisal edge fractures for the IOP design as compared with the TQP design. This can be attributed to the difference in the veneer thickness (IOP = 0.54 mm vs. TQP = 0.85 mm). Furthermore, feldspathic porcelain veneers are fabricated manually and the nature of the laboratory technique may result in thickness variations.

There were more fractures of the composite resin abutments with feldspathic porcelain and IPS e.max<sup>®</sup> CAD laminate veneers for TQP compared with IOP. This can be attributed to more coverage on both sides (TQP), and the veneer can distribute more of the load and have increased resistance to fracture. When a load is applied, a higher stress would be generated and distributed through the cemented veneer-resin cement-composite resin abutment monoblock resulting in the fracture of the composite resin abutment. Two composite resin abutments for the feldspathic porcelain laminate veneers with the IOP design fractured at a lower average load (46 N). This observation can be attributed to the shorter supporting platforms for these composite resin abutments. This occurred with immersion in the acrylic resin during specimen preparation and could have resulted in a lower resistance to fracture. There was no difference in the fracture of the composite resin abutments between IOP and TQP for yttria-stabilized zirconia laminate veneers attributed to the higher flexural strength and compromised bonding between the resin cement, and the intaglio surface of the veneers.<sup>25</sup>

#### *Effect of Laminate Veneer Material within Preparation Design*

There was no statistical difference on the failure load between the three laminate veneer materials for the TQP design (even though yttria-stabilized zirconia had a thicker

veneer = 1.1 mm than IPS e.max<sup>®</sup> CAD = 0.84 mm and feldspathic porcelain = 0.85 mm) so the null hypothesis that yttria-stabilized zirconia laminate veneers would have higher failure load than IPS e.max<sup>®</sup> CAD and feldspathic porcelain laminate veneers of the same preparation design was rejected. This type of preparation design provided higher fracture strength for the laminate veneer and was not influenced by the flexural strength of each material separately when compared with the IOP design. However, there was a statistical difference in the failure load between feldspathic porcelain and IPS e.max<sup>®</sup> CAD materials for IOP. This was associated with the preparation design which provided a weaker veneer than the TQP, and the flexural strength of IPS e.max<sup>®</sup> CAD (360 MPa) dominated over the feldspathic porcelain (111 MPa) due to a thicker veneer for the IPS e.max<sup>®</sup> CAD (0.85 mm) vs. the feldspathic porcelain (0.54 mm). Thus the feldspathic porcelain showed more fractures than IPS e.max<sup>®</sup> CAD at the incisal region for both IOP and TQP designs.

#### *Chipping of Veneering Porcelain*

The yttria-stabilized zirconia copings of the laminate veneers were milled from a monolithic blocks and the veneering porcelain was fired onto these copings to mask the yttria-stabilized zirconia. There was an incidence of chipping with yttria-stabilized zirconia laminate veneers during testing, attributed to the bonding between the yttria-stabilized zirconia coping and veneering porcelain which may be compromised as indicated in the literature.<sup>29</sup> There was no chipping of IPS e.max<sup>®</sup> CAD and feldspathic porcelain laminate veneers versus IPS e.max<sup>®</sup> CAD veneers which was attributed to completely milling from a monolithic block without overlying porcelain. Additionally, the feldspathic porcelain veneers were fabricated by a layering technique with no core and veneering porcelain

involved with the fabrication. Yttria-stabilized zirconia laminate veneers contained two different layers, core and veneering porcelain, with different coefficients of thermal expansion (CTE) which may have contributed to the incidence of chipping in the present study. However, the chipping was not the main failure observation for yttria-stabilized zirconia laminate veneers, as documented in the literature for crowns and fixed partial dentures.<sup>29</sup>

Further in vivo studies should be conducted to determine how long the yttria-stabilized zirconia laminate veneers would survive in the oral environment along with the mode of failure.

### Conclusions

Within the limitations of this study design, the following conclusions can be drawn:

1. There was no effect of preparation design on the mean failure load of yttria-stabilized zirconia and IPS e.max<sup>®</sup> CAD laminate veneers except for feldspathic porcelain laminate veneers.
2. All the laminate veneer materials showed the same failure load within the specified preparation design except for IPS e.max<sup>®</sup> CAD laminate veneers which had a higher failure load than feldspathic porcelain for the IOP design.
3. The IOP design, yttria-stabilized zirconia and IPS e.max<sup>®</sup> CAD laminate veneers showed more fractures of the composite resin abutment, while feldspathic porcelain laminate veneers fractured at the incisal region.
4. The TQP design, yttria-stabilized zirconia laminate veneers should failure by complete debonding, while IPS e.max<sup>®</sup> CAD, feldspathic porcelain laminate veneers failed by fracture of the composite resin abutment.

5. Yttria-stabilized zirconia laminate veneers showed the least fractures and highest number of complete debonding, while the feldspathic porcelain laminate veneers showed the highest fracture and lowest occurrence of complete debonding.

## References

1. Edelhoff D, Sorensen JA. Tooth structure removal associated with various preparation designs for anterior teeth. *The Journal of Prosthetic Dentistry* 2002;87:503-9.
2. Bergenholtz G, Nyman S. Endodontic complications following periodontal and prosthetic treatment of patients with advanced periodontal disease. *Journal of Periodontology* 1984;55:64-8.
3. Radz G. Minimum Thickness Anterior Porcelain Restorations. *Dent Clin N Am* 2011;55:353-370.
4. Friedman MJ. A 15-year review of porcelain veneer failure—a clinician's observations. *Compend Contin Educ Dent* 1998;19(6):625–8, 30, 32 passim; quiz 38.
5. Christensen GJ, Christensen RP. Clinical observations of porcelain veneers: a three-year report. *J Esthet Dent* 1991;3:174-9.
6. Tam LE, Pilliar RM. Fracture toughness of dentin/resin-composite adhesive interfaces. *J Dent Res* 1993;72:953-9.
7. Lin CP, Douglas WH. Failure mechanisms at the human dentin-resin interface: a fracture mechanics approach. *J Biomech* 1994;27:1037-47.
8. Troedson M, Derand T. Shear stresses in the adhesive layer under porcelain veneers. A finite element method study. *Acta Odontol Scand* 1998;56:257-62.
9. Yoshikawa T, Sano H, Burrow MF, Tagami J, Pashley DH. Effects of dentin depth and cavity configuration on bond strength. *J Dent Res* 1999;78:898-905.
10. Peumans M, Van Meerbeek B, Yoshida Y, Lambrechts P, Vanherle G. Porcelain veneers bonded to tooth structure: an ultra-morphological FE-SEM examination of the adhesive interface. *Dent Mater* 1999;15:105-19.
11. Barghi N, Berry TG. Post-bonding crack formation in porcelain veneers. *J Esthet Dent* 1997;9:51-4.
12. Friedman M. Multiple potential of etched porcelain laminate veneers. *J Am Dent Assoc* 1987;115(Spec Iss):83E-87.
13. Sorrentino R, Apicella D, Riccio C, Gherlone E, Zarone F, Aversa R, Garcia-Godoy F, Ferrari M, Apicella A. Nonlinear Visco-Elastic Finite Element Analysis of Different Porcelain Veneers Configuration. *J Biomed Mater Res Part B: Appl Biomater* 2009;91B:727-736.



14. Zarone F, Epifania E, Leone G, Sorrentino R, Ferrari M. Dynamometric assessment of the mechanical resistance of porcelain veneers related to tooth preparation: A comparison between two techniques. *J Prosthet Dent* 2006;95:354-63.
15. Schmidt K, Chiayabutr Y, Phillips K, Kois J. Influence of preparation design and existing condition of tooth structure on load to failure of ceramic laminate veneers *J Prosthet Dent* 2011;105:374-382.
16. Chu FC, Chow TW, Chai J. Contrast ratios and masking ability of three types of ceramic veneers. *J Prosthet Dent* 2007;98(5):359-364.
17. Stappert C, Ozden U, Gerds T, Strub JR. Longevity and failure load of ceramic veneers with different preparation designs after exposure to masticatory simulation. *J Prosthet Dent* 2005;94:132-9.
18. Peumans M, Van Meerbeek B, Lambrechts P, Vanherle G. Porcelain veneers: a review of the literature. *J Dent* 2000;28:163-77.
19. Weinberg LA. Tooth preparation for porcelain laminates. *NY State Dent J* 1989;55:25-8.
20. Chu F. Clinical considerations in managing severe tooth discoloration with porcelain veneers. *J Am Dent Assoc* 2009;140:442-446.
21. Personal communication from Pou-Yuen Technology Co., Ltd. No. 6, Fugong Rd., Fusing Township, Changhua County 506, Taiwan.
22. Personal communication from Ivoclar Vivadent Inc, Amherst, N.Y.
23. Personal communication from Noritake Kizai Co., LTD., Nagoya, Japan.
24. Blatz M, Chiche G, Holst S, Sadan A. Influence of surface treatment and simulated aging on bond strengths of luting agents to zirconia. *Quintessence Int* 2007;38:745-753.
25. Thompson J, Stoner B, Piascik J, Smith R. Adhesion/cementation to zirconia and other non-silicate ceramics: Where are we now? *Dental materials* 2011;27:71-82.
26. Denry IL, Peacock JJ, Holloway JA. Effect of heat treatment after accelerated aging on phase transformation in 3Y-TZP. *J Biomed Mater Res Part B: Appl Biomater* 2010;93B: 236-243.
27. Wang H, Aboushelib MN, Feilzer AJ. Strength influencing variables on CAD/CAM zirconia frameworks. *Dental materials* 2008;24:633-638.

28. Abou Tara M, Eschbach S, Wolfart S, Kern M. Zirconia ceramic inlay-retained fixed dental prostheses – first clinical results with a new design. *J Dent* 2011;39:208-211.
29. Al-Amleh B, K Lyons, Swain M Clinical trials in zirconia: a systematic review. *J Oral Rehabil* 2010 37; 641-652.

Table 1. The average veneer means thickness of laminate veneer materials for different preparation designs.

Veneer material	Average veneer mean thickness in mm ( $\pm$ SD)	
	IOP (n= 10 per each design)	TQP (n= 10 per each design)
Yttria-stabilized zirconia	0.90 ( $\pm$ 0.08)	1.10 ( $\pm$ 0.14)
IPS e.max <sup>®</sup> CAD	0.85 ( $\pm$ 0.10)	0.84 ( $\pm$ 0.10)
Feldspathic porcelain	0.54 ( $\pm$ 0.11)	0.85 ( $\pm$ 0.20)

Table 2. The chemical composition and mechanical properties for yttria-stabilized zirconia, IPS e.max<sup>®</sup> CAD, and feldspathic porcelain laminate veneers.

	Composition	Modulus of elasticity (GPa)	Flexural Strength (MPa)
Yttria-stabilized zirconia	ZrO <sub>2</sub> (92.642 mol%), Y <sub>2</sub> O <sub>3</sub> (5.3 mol%), HfO <sub>2</sub> (1.78 mol%), Al <sub>2</sub> O <sub>3</sub> (0.253 mol%), others (0.025 mol%)	210	1200
IPS e.max <sup>®</sup> CAD	SiO <sub>2</sub> (57-80 wt%), Li <sub>2</sub> O (11-19 wt%), K <sub>2</sub> O (0-13 wt%), P <sub>2</sub> O <sub>5</sub> (0-11 wt%), ZrO <sub>2</sub> (0-8 wt%), ZnO (0-8 wt%), other and coloring oxides (0-12 wt%)	95	360
Feldspathic porcelain	SiO <sub>2</sub> (64.5%), Al <sub>2</sub> O <sub>3</sub> (14.4%), CaO (<1%), MgO (<1%), K <sub>2</sub> O (8.7%), Na <sub>2</sub> O (9.2%), Li <sub>2</sub> O (<1%)	82	111

Table 3. The Cementation procedures for yttria-stabilized zirconia, IPS e.max<sup>®</sup> CAD, and feldspathic porcelain laminate veneers.

Step number	Step-by-step procedure	Feldspathic porcelain and IPS e.max <sup>®</sup> CAD	Yttria-stabilized zirconia
1	Surface treatment for the intaglio surface	Etching with 5% hydrofluoric (acid ceramic etching gel; Ivoclar Vivadent, Amherst, NY) for 60 seconds in case of feldspathic porcelain veneers and 20 seconds for IPS e.max <sup>®</sup> CAD veneers, then rinsed with water, dried with air	Tribochemical silica-coating using sandblaster unit (Renfert, basic classic, 2945-4025, Hilzingen/Germany) filled with CoJet-Sand (30- $\mu$ m silica-modified Al <sub>2</sub> O <sub>3</sub> particles, CoJet <sup>™</sup> system; 3M ESPE, St. Paul, Minn): perpendicular to the surface from a distance of approximately 10 mm for a period of 15 s at 2.8 bar pressure, then air blasted
2	Apply silane coupling agent	VersaLink Porcelain Bonding for 5 minutes (Sultan-Healthcare, Hackensack, NJ)	ESPE-Sil for 5 minutes (3M ESPE)
3	Luting cement	Variolink II with light cure bleach base (Variolink II; Ivoclar Vivadent, Amherst, NY)	A self-adhesive universal resin cement (RelyX <sup>™</sup> Unicem 2, 3M ESPE)
4	Cure* for initial fixation from facial side	5 seconds	2 seconds
5	Cure* for final fixation from facial, mesial, distal and palatal sides	40 seconds	20 seconds
6	Finishing	Hand instruments (#15c scalpel, #371716, Bard- Parker; Becton Dickinson, Franklin Lakes, NJ), and Dialite Ultra Polishers (Brasseler USA <sup>®</sup> Dental Rotary Instruments, Savannah, GA.)	
7	Polishing	The margins were polished with a diamond polishing paste (Henry Schein Inc., Melville, NY) and a rubber cup (#9631.204.030; Komet Dental, Rock Hill, SC).	

\* The laminate veneers were light polymerized with at least a 600 mW/cm<sup>2</sup> light intensity (Demetron<sup>®</sup> LC<sup>™</sup> Kerr Corporation, Orange, CA).

Table 4. The location with number of failures at the bonded composite resin abutment-laminate veneer specimen, and mean failure load (N) of different preparation designs for different laminate veneer materials.

Laminate veneer material	Preparation design (n= 10 per each design)	Location with number of failures (mean failure load (N) ±SD)		Laminate veneer				Complete veneer debonding	Mean failure load (N) ± SD at each preparation design
		Fracture of composite resin abutment	Fracture			Chipping			
			C	B	I	C	B		
Yttria-stabilized zirconia	IOP	4 (230±124)	1 (163)				2 (276±20)	3 (203±137)	244±81
	TQP	4 (267±37)						6 (196±53)	224±58
IPS e.max® CAD	IOP	5 (369±73)		2 (259±9)				3 (325±72)	306±101
	TQP	6 (280±96)						4 (236±33)	263±77
Feldspathic porcelain	IOP	2 (46±47)		7 (206±68)				1 (77)	161±93
	TQP	8 (242±46)		2 (261±53)					246±45

C = cervical region, B = body region, I = incisal region.

## 6. CONCLUSIONS

To simulate the long-term exposure of yttria stabilized zirconia to the oral environment, changes in mechanical properties and surface roughness were evaluated after aging to induce low temperature degradation (LTD). The amount of tetragonal to monoclinic transformation was determined and related to surface roughness, modulus, hardness, and flexural strength. The preparation simulating dental practice did not induce transformations (2%) for non-aged samples. However, the amount of transformation was substantially raised (2 vs. 21%) and the surface roughness increased (Ra: 12 to 22 nm,  $p = 0.017$ ) for aged samples. There was a reduction in the modulus of elasticity (17 to 15 GPa,  $p = < 0.001$ ) and the hardness (276 to 257 GPa,  $p = < 0.001$ ). The reduction in elastic modulus may result in increased flexibility for fixed partial dentures during function and thereby lead to fracture.

The fracture strength of yttria-stabilized zirconia was evaluated as a laminate veneer restoration. There was no statistical difference in the failure load within preparation design compared with feldspathic porcelain and IPS e.max<sup>®</sup> CAD materials, but it had the lowest fraction of fractures and highest fraction of debonding. Chipping was not a prevalent mode of fracture for yttria-stabilized zirconia laminate veneers compared with crowns and fixed partial dentures as also documented in the literature. Yttria-stabilized zirconia and IPS e.max<sup>®</sup> CAD laminate veneers of three-quarter preparations showed more failures by complete debonding while feldspathic porcelain laminate veneers fracture at the incisal region. The yttria-stabilized zirconia laminate veneers with incisal over-

lapped preparation showed more failures as complete debonding and chipping, while IPS e.max<sup>®</sup> CAD laminate veneers showed failures by complete debonding, and feldspathic porcelain laminate veneers fractured at the incisal region. Feldspathic porcelain laminate veneers had the highest number of fractures and lowest complete debonding.

The optical properties of yttria-stabilized zirconia were investigated through reduction in thickness (up to 0.3 mm) as a laminate veneer and there was no change in the color difference ( $\Delta E < 3.7$ ) using different colors of try-in paste for composite resin abutments. The yttria-stabilized zirconia was totally opaque when compared with feldspathic porcelain and IPS e.max<sup>®</sup> CAD materials. This finding was confirmed with the measurement of L\* which was the brightest. IPS e.max<sup>®</sup> CAD had the lowest b\* value (more bluish) and the highest color difference ( $\Delta E > 3.7$ ). This confirms that IPS e.max<sup>®</sup> CAD was the most sensitive material to color changes, and its color difference was irrelevant to ceramic thicknesses at different regions. However, feldspathic porcelain and yttria-stabilized zirconia laminate veneers were affected by the thickness, i.e., the color difference decreased as the veneer thickness increased from the cervical to incisal regions.

The results from this project have shown that yttria-stabilized zirconia's strength offers an ability to resist the intense occlusal and parafunctional forces of the masticatory system. Furthermore, one of the most significant potential findings will be whether LTD affects the biomechanical properties of yttria-stabilized zirconia for utilization in restorative dentistry. The major concern for the use of yttria-stabilized zirconia laminate veneers in dentistry has been related to the opacity of the material. However, this study demonstrated that the shading can be modified to replicate the most common dental shades, thus showing that opaqueness can be modified to an acceptable esthetic result. Hence, yttria-



stabilized zirconia should offer the advantages of minimal tooth reduction, strength of ceramic material and acceptable esthetic shading, if modified appropriately.

## 7. GENERAL REFERENCES

1. Piconi C, Maccauro G. Zirconia as a ceramic biomaterial. *Biomaterials* 1999;20:1-25.
2. Denry I, Kelly R. State of the art of zirconia for dental applications. *Dent Mater* 2008;24:299-307.
3. Ferraris M, Verne E, Appendino P, Moisescu C, Krajewski A, Ravaglioli A, et al. Coatings on zirconia for medical applications. *Biomaterials* 2000;21:765-73.
4. Helmer JD, Driskell TD. Research on bioceramics. Symposium on use of ceramics as surgical implants. Clemson, South Carolina: Clemson University; 1969.
5. Christel P, Meunier A, Dorlot J-M, Crolet J-M, Witvoet J, Sedel L, et al. Biomechanical compatibility and design of ceramic implants for orthopaedic surgery. Bioceramics: material characteristics versus in vivo behavior. *Ann NY Acad Sci* 1988;523:234-56.
6. Cales B, Stefani Y, Lilley E. Long-term in vivo and in vitro aging of a zirconia ceramic used in orthopaedy. *J Biomed Mater Res B Appl Biomater* 1994;28:619-24.
7. Prestipino V, Ingber A. Esthetic high-strength implant abutments: Part 1. *J Esthet Dent* 1993;5:29-36.
8. Yildirim M, Edelhoff D, Hanisch O, Spiekermann H. Ceramic abutments—a new era in achieving optimal esthetics in implant dentistry. *Int J Periodontics Restorative Dent* 2000;20:81-91.
9. Potiket N, Chiche G, Finger IM. In vitro fracture strength of teeth restored with different all-ceramic crown systems. *J Prosthet Dent* 2004;92:491-5.
10. Vult von Steyern P, Ebbesson S, Holmgren J, Haag P, Nilner K. Fracture strength of two oxide ceramic crown systems after cyclic pre-loading and thermocycling. *J Oral Rehabil* 2006;33:682-9.
11. Sturzenegger B, Feher A, Luthy I-I, Schumacher M, Loeffel O, Filser F, et al. Clinical study of zirconium oxide bridges in the posterior segments fabricated with the dcm system. *Schweizer Monatsschrift für Zahnmedizin* 2000;110: 131-9.

12. Tinschert J, Natt G, Mautsch W, Augthun M, Spiekermann H. Fracture resistance of lithium disilicate-, alumina-, and zirconia-based three-unit fixed partial dentures: a laboratory study. *Int J Prosthodont* 2001;14:231-8.
13. Keith O, Kusy RP, Whitley JQ. Zirconia brackets: an evaluation of morphology and coefficients of friction. *Am J Orthod Dentofacial Orthop* 1991;106:605-11.
14. Koutayas SO, Kern M. All-ceramic posts and cores: the state of the art. *Quintessence Int* 1999;30:383-92.
15. Ahmad I. Zirconium oxide post and core system for the restoration of an endodontically treated incisor. *Pract Periodontics Aesthet Dent* 1999;11:197-204.
16. Meyenberg KH, Luthy H, Scharer P. Zirconia posts: a new all-ceramic concept for nonvital abutment teeth. *J Esthet Dent* 1995;7:73-80.
17. Piconi C, Maccauro G, Muratori F. Alumina matrix composites in arthroplasty. *Key Eng Mater* 2005;284-286:979-82.
18. Kohorst P, Herzog TJ, Borchers L, Stiesch-Scholz M. Load-bearing capacity of allceramic posterior four-unit fixed partial dentures with different zirconia frameworks. *Eur J Oral Sci* 2007;115:161-166.
19. Al-Amleh B, Lyons K, Swain M. Clinical trials in zirconia: a systematic review. *J Oral Rehabil* 2010 37; 641-652.
20. Wang H, Aboushelib MN, Feilzer AJ. Strength influencing variables on CAD/CAM zirconia frameworks. *Dental materials* 2008;24:633-638.
21. Blatz MB, Sadan A, Arch GH, Lang BR. In vitro evaluation of long-term bonding of porcelana allceram alumina restorations with modified resin luting cement. *J Prosthet Dent* 2003;89:381-7.
22. Valandro LF, Ozcan M, Bottino MA, Bottina MC, Scotti R, Della Bona A. Bond strength of a resin cement to high-alumina and zirconia-reinforced ceramics: the effect of surface conditioning. *J Adhes Dent* 2006;8:175-81.
23. Aboushelib MN, Dozic A, Liem JK. Influence of framework color and layering technique on the final color of zirconia veneered restorations. *Quintessence Int* 2010;41:e84-9.
24. Swab JJ. Low temperature degradation of Y-TZP materials. *J Mater Sci* 1991;26:6706-14.
25. Lugh V, Sergio V. Low temperature degradation—aging— of zirconia: a critical review of the relevant aspects in dentistry. *Dent Mater* 2010;26:807-20.

26. Haraguchi K, Sugano N, Nishii T, Sakai T, Yoshikawa H, Ohzono K. Phase transformation of a zirconia ceramic head after total hip arthroplasty. *J Bone Joint Surg B* 2001;83:996-1000.
27. Roy ME, Whiteside LA, Katerberg BJ, Steiger JA. Phase transformation, roughness, and microhardness of artificially aged yttria- and magnesia-stabilized zirconia femoral heads. *J Biomed Mater Res* 2007;21:1096-1102.
28. Roy ME, Whiteside LA, Steiger JA, Nayfeh TA. Comparison of retrieved yttria- and magnesia-stabilized zirconia femoral heads. *Trans 52nd Orthop Res Soc* 2006;936.
29. Kosmac T, Oblak C, Marion L. The effects of dental grinding and sandblasting on ageing and fatigue behavior of dental zirconia (Y-TZP) ceramics. *J Eur Ceram Soc* 2008;28:1085-1090.
30. Chevalier J, Olagnon C, Fantozzi G. Subcritical crack propagation in 3Y-TZP ceramics: static and cycling fatigue. *J Am Ceram Soc* 1999;82:3129-3138.
31. Lilley E. Review of low temperature degradation in Y-TZPs. In; Tressler RE, McNallan M, editors. *Ceramic transaction: corrosion and corrosive degradation of ceramics*. Westerville; American Ceramics Society 1990;387-407.
32. Papanagiotou HP, Morgano SM, Giordano RA, Pober R. In vitro evaluation of low-temperature aging effects and finishing procedures on the flexural strength and structural stability of Y-TZP dental ceramics. *J Prosthet Dent* 2006;96:154-64.
33. Ardlin BI. Transformation-toughened zirconia for dental inlays, crowns and bridges: chemical stability and effect of low-temperature aging on flexural strength and surface texture. *Dent Mater* 2002;18:590-5.
34. Hjerpe J, Narhi T, Froberg K, Vallittu PK, Lassila LV. Effect of shading the zirconia framework on biaxial strength and surface microhardness. *Acta Odontol Scand* 2008;66:262-7.
35. Stevenson B, Ibbetson R. The effect of the substructure on the colour of samples/restorations veneered with ceramic: a literature review. *J Dent* 2010;38:361-8.
36. Ho-Jung S, Woong-Chul K, Sang-Ho J, Young-Su K, Sung-Won J, Jin-Soo A. Influence of dentin porcelain thickness on layered all-ceramic restoration color. *J Dent* 2010, doi:10.106/j.dent.2010.08.007.
37. Lee YK, Cha HS, Ahn JS. Layered color of all-ceramic core and veneers. *J Prosthet Dent* 2007;97:279-86

38. Dozic 2003 Dozic A, Kleverlaan CJ, Meegdes M, van der Zel J, Feilzer AJ. The influence of porcelain layer thickness on the final shade of ceramic restorations. *J Prosthet Dent* 2003;90:563-70.
39. Heffernan MJ, Aquilino SA, Diaz-Arnold AM, Haselton DR, Stamford CM, Vargas MA. Relative translucency of six all-ceramic systems. II. Core and veneer materials. *J Prosthet Dent* 2002;88:10-5.
40. Celik G, Uludag B, Usumez A, Sahin V, Ozturk O, Goktug G. The effect of repeated firings on the color of an all-ceramic system with two different veneering porcelain shades. *J Prosthet Dent* 2008;99:203-8.
41. Ozturk O, Uludag B, Usumez A, Sahin V, Celik G. The effect of ceramic thickness and number of firings on the color of two all-ceramic systems. *J Prosthet Dent* 2008;100:99-106.
42. Chen YM, Smales RJ, Yip KH, Sung WJ. Translucency and biaxial flexural strength of four ceramic core materials. *Dent Mater* 2008;24:1506-11.
43. Baldissara P, Llukacej A, Ciocca L, Valandro FL, Scotti R. Translucency of zirconia copings made with different CAD/CAM systems. *J Prosthet Dent* 2010;104:6-12.
44. Kramer N, Lohbauer U, Frankenberger R. Adhesive luting of indirect restorations. *Am J Dent* 2000;13:60D-76D.
45. Uo M, Sjoren G, Sundh A, Watari F, Bergman M, Lerner U. Cytotoxicity and bonding property of dental ceramics. *Dent Mater* 2003;19:487-92.
46. Kern M, Wegner SM. Bonding to zirconia ceramic: adhesion methods and their durability. *Dent Mater* 1998;14:64-71.
47. Wegner SM, Kern M. Long-term resin bond strength to zirconia ceramic. *J Adhes Dent* 2000;2:139-47.
48. Derand P, Derand T. Bond strength of luting cements to zirconium oxide ceramics. *Int J Prosthodont* 2000;13:131-5.
49. Lee HJ, Ryu JJ, Shin SW, Suh KW. Effect of surface treatment methods on the shear bond strength of resin cement to zirconia ceramic. *J Korean Acad Prosthodont* 2007;45:743-52.
50. Ernst CP, Cohnen U, Stender E, Willershausen B. In vitro retentive strength of zirconium oxide ceramic crowns using different luting agents. *J Prosthet Dent* 2005;93:551-8.

51. Blatz MB, Chiche G, Holst S, Sadan A. Influence of surface treatment and simulated aging on bond strengths of luting agents to zirconia. *Quintessence Int* 2007;38:745-53.
52. Sahafi A, Peutzfeldt A, Asmussen E, Gotfredsen K. Bond strength of resin cement to dentin and to surface-treated posts of titanium alloy, glass fiber, and zirconia. *J Adhes Dent* 2003;5:153-62.
53. Blatz MB, Richter C, Sadan A, Chiche GJ. Resin bond to dental ceramics, part ii: high-strength ceramics. *J Esthetic Rest Dent* 2004;16:324-8.
54. Luthy J, Loeffel O, Hammerle CHF. Effect of thermocycling on bond strength of luting cements to zirconia ceramic. *Dent Mater* 2006;22:195–200.
55. Wolfart M, Lehmann F, Wolfart S, Kern M. Durability of the resin bond strength to zirconia ceramic after using different surface conditioning methods. *Dent Mater* 2007;23:45-50.
56. Piwowarczyk A, Lauer HC, Sorensen JA. The shear bond strength between luting cements and zirconia ceramics after two pre-treatments. *Oper Dent* 2005;30:382-8.
57. Kumbuloglu O, Lassila LVJ, User A, Vallittu PK. Bonding of resin composite luting cements to zirconium oxide by two air-particle abrasion methods. *Oper Dent* 2006;31:248-55.
58. Palacios RP, Johnson GH, Phillips KM, Raigrodski AJ. Retention of zirconium oxide ceramic crowns with three types of cement. *J Prosthet Dent* 2006;96:104-14.
59. Senyilmaz DP, Palin WM, Shortall ACC, Burke FJT. The effect of surface preparation and luting agent on bond strength to a zirconium-based ceramic. *Oper Dent* 2007;32:623-30.
60. Atsu SS, Lilicarlan MA, Kucukesmen HC, Aka PS. Effect of zirconium-oxide ceramic surface treatments on the bond strength to adhesive resin. *J Prosthet Dent* 2006;95:430-6.
61. Tanaka R, Fujishima A, Shibata Y, Manabe A, Miyazaki T. Cooperation of phosphate monomer and silica modification on zirconia. *J Dent Res* 2008;87:666-70.
62. Miller JD, Hoh K-P, Ishida H. Studies of the simulation of silane coupling agent structures on particulate fillers; the ph effect. *Polym Compos* 1984;5:18-28.

63. Nothdurft FP, Motter PJ, Pospiech PR. Effect of surface treatment on the initial bond strength of different luting cements to zirconium oxide ceramic. *Clin Oral Invest* 2009;13:229-35.
64. Glauser R, Sailer I, Wohlwend A, Studer S, Schibli M, Scharer P. Experimental zirconia abutments for implant-supported single-tooth restorations in esthetically demanding regions: 4-year results of a prospective clinical study. *Int J Prosthodont* 2004;17:285-90.
65. Komine F, Tomic M. A single-retainer zirconium dioxide ceramic resin-bonded fixed partial denture for single tooth replacement: a clinical report. *J Oral Sci* 2005;47:139-42.
66. Ortorp A, Kihl ML, Carlsson GE. A 3-year retrospective and clinical follow-up study of zirconia single crowns performed in a private practice. *J Dent* 2009;37:731-6.
67. Sailer I, Feher A, Filser F, Gauckler LJ, Luthy H, Hammerle CHF. Five-year clinical results of zirconia frameworks for posterior fixed partial dentures. *Int J Prosthodont* 2007;20:383-8.
68. Sailer I, Feher A, Filser F, Luthy H, Gauckler LJ, Scharer P, et al. Prospective clinical study of zirconia posterior fixed partial dentures: 3-year follow-up. *Quintessence Int* 2006;37:685-93.
69. Raigrodski AJ. Contemporary all-ceramic fixed partial dentures: a review. *Dent Clin North Am.* 2004;48:531-544.
70. Personal communication from Pou-Yuen Technology Co., Ltd. No. 6, Fugong Rd., Fusing Township, Changhua County 506, Taiwan.
71. Mormann WH. International symposium on computer restorations. Quintessence Publishing Co, Inc. 1991.
72. Blatz M, Chiche G, Holst S, Sadan A. Influence of surface treatment and simulated aging on bond strengths of luting agents to zirconia. *Quintessence Int* 2007;38:745-753.
73. Personal communication from Firoz Rahemtulla, PhD. The University of Alabama at Birmingham, School of Dentistry Department of Prosthodontics.
74. BS EN ISO 4287: 2000 Geometrical product specification (GPS). Surface texture: profile method-terms, definitions and surface texture parameters.
75. Garvie RC, Nicholson PS. Phase analysis in zirconia systems. *J Am Ceram Soc* 1972;55:303-5.

76. International Standard ISO 6872:2008 Dental ceramics. International Organization for Standardization, Geneva, Switzerland.
77. Burkinshaw SM. Colour in relation to dentistry. *Fundamentals of colour science. British Dental Journal* 2004;196(1):33-41.
78. Knispel G. Factors affecting the process of color matching restorative materials to natural teeth. *Quintessence Int* 1991;22:525-31.
79. Johnston WM, Kao EC: Assessment of appearance matches by visual observation and clinical colorimetry. *J Dent Res* 1989;68:819-822.
80. Norman GR, Streiner DL. *Biostatistics, The Bare Essentials 3<sup>rd</sup> Edition*, People's Medical Publishing House, Shelton, CT 2008:70-76.
81. Norman GR, Streiner DL. *Biostatistics, The Bare Essentials 3<sup>rd</sup> Edition*, People's Medical Publishing House, Shelton, CT 2008:107-116.
82. Norman GR, Streiner DL. *Biostatistics, The Bare Essentials 3<sup>rd</sup> Edition*, People's Medical Publishing House, Shelton, CT 2008:81-84.



APPENDIX: DIFFERENT FAILURE MODES AFTER LOADING OF CEMENTED  
LAMINATE VENEERS ON COMPOSITE RESIN ABUTMENTS

APPENDIX: DIFFERENT FAILURE MODES AFTER LOADING OF CEMENTED LAMINATE VENEERS ON COMPOSITE RESIN ABUTMENTS

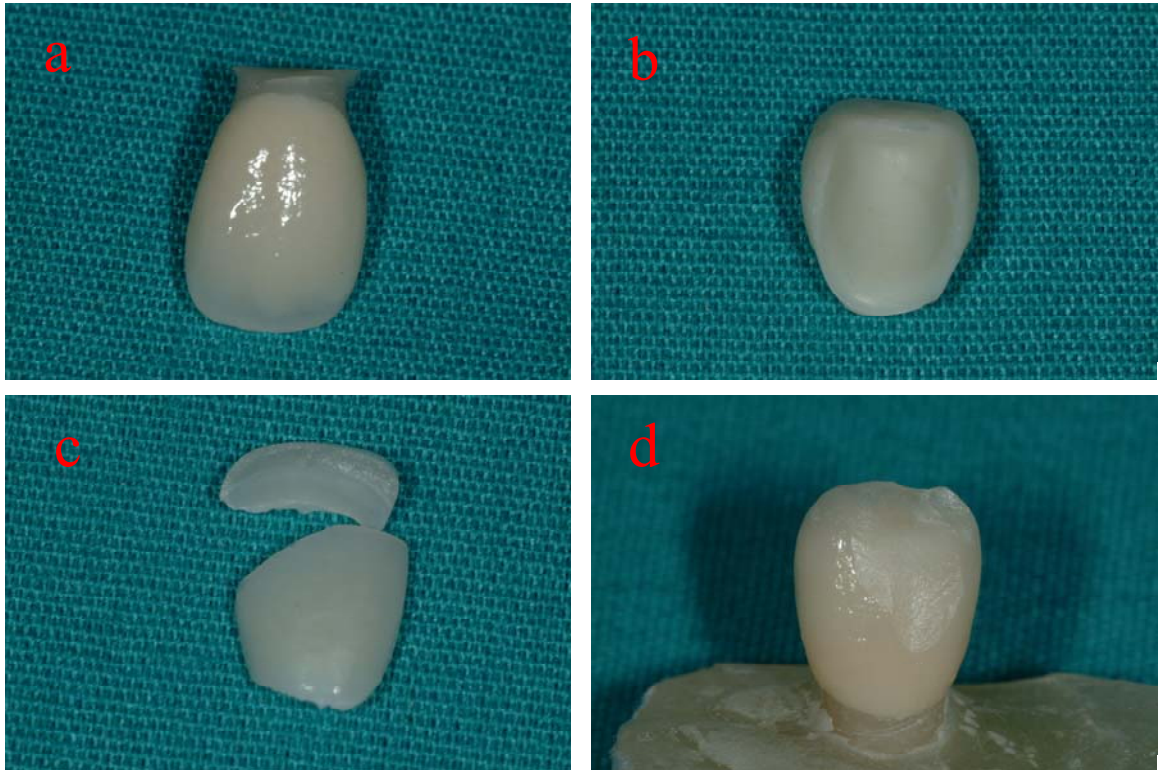


Figure 1. Different failure modes after loading of cemented laminate veneers on composite resin abutments: (a) Fracture of composite resin abutment, (b) complete laminate veneer debonding, (c) fracture of laminate veneer (incisal edge), and (d) chipping of porcelain.